UNIVERSITY OF CALIFORNIA SAN DIEGO

Genetically Engineered Cell Membrane–Coated Nanoparticles for Enhanced Drug Delivery

A dissertation submitted in partial satisfaction of the
requirements for the degree Doctor of Philosophy

in

Chemical Engineering

by

Joon Ho Park

Committee in charge:

Professor Liangfang Zhang, Chair
Professor Jesse Jokerst
Professor Nisarg Shah
Professor Peter Yingxiao Wang
Professor Wei Wang

2021

The dissertation of Joon Ho Park is approved, and it is acceptable in quality and form for publication on microfilm and electronically.

University of California San Diego

2021

DEDICATION

This dissertation is dedicated to my wife, Jei Yoon Park, who has been my side in my lowest of lows and highest of highs. I could not have done it without her.

This dissertation is also dedicated to my mother, Young Ae Choi, who has been my spiritual mentor through my entire life, my father, Tai Hyun Park, who has been my life mentor through my entire life, and my brother, Joon Mo Park, who has been my best friend through my entire life.

Last but not least, I dedicate my dissertation to my daughter, Hailey Park, and my son, Hayden Park. You have blessed me with the Joy like the feeling of warm Summer breeze.

EPIGRAPH

But we gon' be alright.

Kendrick Lamar

TABLE OF CONTENTS

LIST OF FIGURES

ACKNOWLEDGEMENTS

First and foremost, I would like to thank my PhD advisor, Professor Liangfang Zhang for his mentorship and all the support he has given my throughout my PhD program. As an aspiring independent research myself, he is the one who I can look up to and take inspirations from. I have learned so much not only about research, but also about life in general, and I am forever grateful for all the wisdom and opportunity he gave me.

I would also like to thank my mentor, Ronnie Fang, who helped me achieve this milestone. He is not only my mentor, but also a friend and a lab mate who I can discuss anything about without hesitation. He has taught me how to think and to do research when I was struggling to get my thesis off the ground. He is the best mentor I could have ever asked for. I thank him for being patient with me when I was slow and celebrating with me when I have achieved something. He made my journey through PhD a lot more enjoyable when it could have been a painful rocky road.

I would also like to thank my current and past lab mates, Weiwei Gao, Hua Gong, Xiangzhao Ai, Diana Dehaini, Yue Zhang, Xiaoli Wei, Pavimol Angsantikul, Qiangzhe Zhang, Jia Zhuang, Yaou Duan, Yao Jiang, Jiarong Zhou, Maya Holay, Shuyan Wang, Dan Wang, Zhongyuan Guo, Ashley Kroll, Ilkoo Noh, Nishta Krishnan, Luke Kubiatowicz, and Animesh Mohapatra. All of you and my interactions with you have made who I am today. I feel so lucky to have been a part of such an amazing and supportive lab. I would like to especially thank Yao Jiang for teaching me basically all the technique I use in the lab and also being an awesome friend, and Animehs Mohapatra for sticking with me in all of my fails and successes.

Last but not least, I would like to thank UC San Diego which is an amazing school in an amazing location with competent and friendly staffs and faculties. Especially the

NanoEngineering department faculties and staffs who I constantly interacted with were always helpful and friendly.

The first portion of chapter 1, in part, contains the material in *Nanoscale Horizons*, 2020, Joon Ho Park*, Diana Dehaini*, Jiarong Zhou, Maya Holay, Ronnie H. Fang and Liangfang Zhang. The dissertation author was a primary author (equally contributing with Diana Dehaini) of this paper.

The second portion of chapter 1, in part, contains the material in *Theranostics*, 2019, Jia Zhuang, Maya Holay, Joon Ho Park, Ronnie H. Fang, Jie Zhang and Liangfang Zhang. The dissertation author was a major contributor and co-author of this paper.

Chapter 2, in full, is a reprint of the material as it appears in *Science Advances,* 2021, Joon Ho Park, Yao Jiang, Jiarong Zhou, Hua Gong, Animesh Mohapatra, Jiyoung Heo, Weiwei Gao, Ronnie H. Fang and Liangfang Zhang. The dissertation author was a primary author of this paper.

Chapter 3, in full, is a reprint of the material being submitted. Joon Ho Park, Animesh Mohapatra, Jiarong Zhou, Maya Holay, Nishta Krishnan, Weiwei Gao, Ronnie H. Fang and Liangfang Zhang. The dissertation author was a primary author of this paper.

VITA

2010	B.S. in Chemical and Biological Engineering, Seoul National University, Korea
2012	M.S. in Chemical and Biological Engineering, Seoul National University, Korea
2012-2015	Assoicate Researcher, AmorePacific corp. R&D Center, Korea
2021	Ph.D. in Chemical Engineering, University of California San Diego, USA

PUBLICATIONS

1. Park JH, Mohapatra A, Zhou J, Holay M, Krishnan N, Gao W, Fang RH, Zhang L. Virus-Mimicking Cell Membrane-Coated Nanoparticles for Cytosolic Delivery of mRNA. *Angewandte Chemie* 2021, under revision.

2. Park JH, Jiang Y, Zhou J, Gong H, Mohapatra A, Heo J, Gao W, Fang RH, Zhang L. Genetically engineered cell membrane–coated nanoparticles for targeted delivery of dexamethasone to inflamed lungs. *Science Advances* 2021, 7(25):eabf7820.

3. Park JH, Dehaini D, Zhou J, Holay M, Fang RH, Zhang L. Biomimetic nanoparticle technology for cardiovascular disease detection and treatment. *Nanoscale horizons* 2020, 5(1):25-42.

4. Holay M, Guo Z, Pihl J, Heo J, Park JH, Fang RH, Zhang L. Bacteria-inspired nanomedicine. *ACS Applied Bio Materials* 2020, 4(5):3830-48.

5. Zhuang J, Holay M, Park JH, Fang RH, Zhang J, Zhang L. Nanoparticle delivery of immunostimulatory agents for cancer immunotherapy. *Theranostics* 2019, 9(25):7826.

6. Yang L, Mih N, Anand A, Park JH, Tan J, Yurkovich JT, Monk JM, Lloyd CJ, Sandberg TE, Seo SW, Kim D. Cellular responses to reactive oxygen species are predicted from molecular mechanisms. *Proceedings of the National Academy of Sciences* 2019, 116(28):14368-73.

7. Kim EM, Park JH, Kim BG, Seo JH. Identification of (R)-selective ω-aminotransferases by exploring evolutionary sequence space. *Enzyme and microbial technology* 2018, 110:46-52.

8. Choi YH, Kim JH, Park JH, Lee N, Kim DH, Jang KS, Park IH, Kim BG. Protein engineering of α2, 3/2, 6-sialyltransferase to improve the yield and productivity of in vitro sialyllactose synthesis. *Glycobiology* 2014, 24(2):159-69.

9. Kim BJ, Park JH, Park TH, Bronstein PA, Schneider DJ, Cartinhour SW, Shuler ML. Effect of iron concentration on the growth rate of Pseudomonas syringae and the expression of virulence factors in hrp-inducing minimal medium. *Applied and environmental microbiology* 2009, 75(9):2720-6.

ABSTRACT OF THE DISSERTATION

Genetically Engineered Cell Membrane–Coated Nanoparticles for Enhanced Drug Delivery

by

Joon Ho Park

Doctor of Philosophy in Chemical Engineering

University of California San Diego, 2021

Professor Liangfang Zhang, Chair

Drug delivery field has benefitted greatly from the advancements in nanoparticle technology. Nanoparticles have been developed to protect the payload, improve targeted delivery, control the release profile, and enhance solubility and bioavailability of drugs. In recent years,

cell membrane-coated nanoparticle technology which is a biomimetic platform that utilizes cell membranes has revolutionized the drug delivery field by utilizing the natural characteristics and advantages cell membranes inherently possess. In order to further improve upon the cell membrane-coated nanoparticle technology, genetic engineering can be applied to the membranes thus granting the resulting nanoparticles with enhanced abilities depending on the type of proteins that are being engineered. In this dissertation, the ways in which genetic engineering can enhance the drug delivery capability of cell membrane-coated nanoparticle will be discussed.

Herein, the first chapter will discuss the development and the current status of the biomimetic delivery strategies. The following two chapters will discuss the strategies using genetic engineering that can enhance two key aspects of drug delivery: cytosolic delivery and targeted delivery. The second chapter will focus on endosome escaping nanoparticles that enhance the cytosolic delivery of mRNA. The nanoparticle coated with membrane that was genetically engineered to mimic the influenza virus, once taken up by a host cell, is able to escape endosome and deliver mRNA to the cytosol which then can be translated into proteins. Model mRNA was successfully delivered to the cytosol using this platform when injected locally or systemically in a mouse model. The third chapter will focus on nanoparticles coated with membrane that was genetically engineered to target inflammation. The inflammation targeting nanoparticles, when loaded with an anti-inflammatory drug, was able to target and treat lung inflammation in a mouse model.

This dissertation aims to demonstrate the versatility of the genetically engineered cell membrane-coated nanoparticle technology that can be applied to many facets of drug delivery. Customizability of its synthetic core, payload, membrane source and engineered membrane protein will allow this platform to suit the needs of vastly different application.

Chapter 1

Introduction

1.1 Introduction

Nanotechnology has been widely applied to the medical field, enabling researchers to design novel diagnostic and therapeutic platforms that can outperform traditional modalities [1-4]. In particular, nanoparticle-based delivery systems have had a major impact on the clinical management of cancer, with a number of nanoformulations having been approved for use in human patients [5]. Their advantages include the ability to enhance bioavailability by prolonging blood residence, deliver a wide range of payloads, and sustain release of therapeutic agents over time. Significant efforts have also been placed on developing actively targeted formulations, which can more accurately localize to disease sites [6-8]. Many of these design principles are now being leveraged by researchers working in other fields where they also have the potential to bring about significant improvements [9, 10]. More recently, the application of biomimetic nanotechnology has become increasingly popular as a means of streamlining the creation of highly functional nanoparticle platforms [11, 12]. In particular, these nanoparticles excel at performing in complex biological environments [13].

1.2 Biomimetic Delivery Strategies

1.2.1 Introduction to Biomimetic Delivery

Particulate delivery systems have demonstrated the ability to enhance the bioavailability of immunostimulants and can promote increased immune activation; however, conventional platforms can still be limited by certain pitfalls. For instance, in spite of effective incorporation

into delivery systems, some of these immunostimulatory agents still need to be delivered in large quantities to achieve the desired effects, which necessitate the use of delivery platforms with high loading yields [14]. Finding alternative solutions to achieve better immune stimulation at lower dosages would thus be highly beneficial. Another challenge with many conventional delivery platforms is that they are still regarded as foreign by the immune system, which can lead to rapid immune clearance or unwanted immune responses [15]. Furthermore, delivery of immunostimulant payloads to the appropriate immune cell populations is essential for proper immune activation. As such, targeted delivery approaches could ensure better immune recognition and augment overall immune responses [16].

An ideal immunostimulant delivery platform would interact minimally with irrelevant cells but elicit strong immune stimulation upon reaching target immune cells [17]. As a result, on-demand immune activation could be achieved without compromised safety or tolerability parameters. Recently, biomimetic nanodelivery platforms have been increasingly employed for the delivery of immunostimulatory agents because of their ability to readily fulfill some of these design requirements [11, 12, 18, 19]. Biomimetic modifications or delivery vehicles have the potential to significantly improve upon the overall delivery efficiency and subsequent immune responses associated with current delivery platforms. In this section, three general approaches for achieving biomimetic delivery will be discussed in depth.

1.2.2 Biomimetic Modifications

Biological targeting functionality can be achieved by employing naturally occurring moieties to modify the surface of nanoparticles, thus enhancing uptake efficiency by target

immune cells. These modifications are oftentimes achieved through chemical conjugation or physical incorporation processes that are easy to implement and highly controllable [20]. One representative ligand is mannose, which has affinity to receptors that are abundant on APCs [21]. Mannose receptors on macrophages and DCs enhance affinity towards the cell surface of microorganisms, facilitating their uptake and subsequent presentation to T cells [22]. When mannose is attached as a targeting ligand to immunostimulant delivery platforms, these mannosylated vehicles can be readily recognized and internalized by APCs, resulting in enhanced immune stimulation. In one example, a vaccine delivery system based on mannosylated chitosan microspheres was formulated for intranasal mucosal vaccination [23]. Compared to unmodified particles, the mannosylated microspheres could tightly bind with mannose receptors on murine macrophages and stimulated immunoglobulin production. Similarly, a PEG-sheddable, mannose-modified polymeric nanoparticle platform has been assembled and shown to efficiently target tumor-associated macrophages after PEG shedding in the acidic tumor microenvironment [24]. In a case of DC targeting, mannose was used to modify lipid-calcium phosphate nanoparticles, which contained the Trp2 melanoma self-antigen and CpG ODN as an adjuvant for immunotherapy against melanoma [25, 26].

Mannosylation can help to enhance nanoparticle localization in the lymph nodes, facilitating antigen presentation by DCs. In an example, mannose was selected to decorate chitosan nanoparticles [27]. Due to the innate immunostimulatory effect of chitosan, the nanoparticles were able to elicit strong immune responses without the addition of any other immunostimulants. The mannose-modified chitosan nanoparticles were loaded with whole tumor cell lysate prepared from B16 melanoma cells. Prompt uptake by endogenous DCs within the draining lymph node was observed, which correlated with an elevation in IFNγ and IL4 levels.

The therapeutic effects of this formulation were remarkable and resulted in a significant delay of tumor growth in an animal model of melanoma.

DC targeting can also be achieved using other sugar monomers, and galactose modification is another example of biomimetic targeting using simple sugar ligands. Galactosylation was performed on dextran-retinal nanogels for cancer vaccine delivery [28]. The formulation exhibited improved cell targeting, which translated to significantly improved DC maturation. With its inherent adjuvancy, this immunostimulatory nanogel platform represented a potent delivery system for anticancer vaccination. Additionally, more complex carbohydrates have been studied for their natural binding interactions with immune cells. Among these, glycans have been employed as biomimetic targeting moieties. Lewis-type (Le) glycan structures can be grafted to delivery vehicles for specific binding to DC-specific intercellular adhesion molecule-3-grabbing nonintegrin (DC-SIGN) expressed on DCs [29]. In one example, liposomes were modified with targeting glycans Le^B or Le^X, which result in increased binding and internalization by bone marrow-derived DCs expressing DC-SIGN [30]. This glycoliposome-based vaccine could boost $CD4^+$ and $CD8^+$ T cell responses when the melanoma antigen MART1 was co-delivered.

1.2.3 Natural Carriers

Leveraging natural constructs for biomolecule transportation is another strategy for delivering immunostimulatory agents. By deriving nanovehicles from biological systems and loading them with immunostimulants, these delivery platforms can induce potent immune responses by targeting and interacting with specific immune cell subtypes. Additionally, because

many of these carriers are either naturally occurring or easily self-assembled, their production can be readily streamlined, which enhances their translational potential.

1.2.3.1 Virus Nanoparticles

Among the naturally occurring nanocarriers, virus-like particles (VLPs) have attracted significant attention, as they can be readily used to induce immune responses. VLPs are protein structures isolated from viruses that can inherit viral targeting capabilities and lack the presence of potentially dangerous genetic material [31]. Viruses can inherently activate immune responses through repetitive surface structures and pathogen-associated molecular patterns, which often carry over to VLPs [32]. Identified as exogenous, VLPs can trigger potent immunity on their own, which can greatly reduce the need for incorporating other immunostimulants. Thus, owing to their intrinsic targeting and immunogenicity, VLPs can promote better antigen delivery, boost immune responses, and enhance antigen presentation to the adaptive immune system [33].

A notable example of a VLP platform for immunomodulation is one based on the cowpea mosaic virus (CPMV), which has been shown to interact with APCs [34]. In one such work, VLPs made from CPMV (CPMV-VLPs) suppressed established metastatic B16F10 melanoma and generated potent systemic antitumor immunity against the poorly immunogenic cancer cells [35]. After intratracheal administration, CPMV-VLPs activated neutrophils in the tumor microenvironment and coordinated downstream antitumor immune responses. In combination with an antigenic peptide derived from the human epidermal growth factor receptor 2 (HER2) protein, CPMV-VLPs have also served as a cancer vaccine for the treatment of $HER2^+$ tumors

[36]. Upon *in vivo* administration, the CPMV-VLP platform shows significant lymph node accumulation and potently activates APCs [37].

Rod-shaped plant viruses such as the tobacco mosaic virus (TMV) have also been investigated. For example, vaccination using antigen-carrying TMV-VLPs has demonstrated efficacy against various tumor models [38]. TMV-VLPs have been found to participate in specific interactions with DCs and lymphocytes and can effectively stimulate APC activation. VLP systems based on the bacteriophage Qβ have demonstrated the ability to promote DC maturation and CTL stimulation [39]. CpG ODN was loaded into Qβ-VLPs for synergistic immune activation, and the resulting formulation was shown to potently prime CTL responses and maintain memory CTL levels. Additionally, a lentivector has been engineered for specific targeting to DCs [40]. The platform employed a viral glycoprotein from the Sindbis virus, enabling it to avidly bind with the DC surface protein DC-SIGN and induce cell maturation. Using OVA as a model antigen, the engineered lentivector promoted production of a high frequency of OVA-specific $CD8^+$ T cells after subcutaneous administration in a murine model. VLPs derived from other virus sources, such as human papillomavirus [41, 42], enterovirus 71 [43, 44], and hepatitis B [45, 46], have also been evaluated for cancer immunotherapy applications.

1.2.3.2 Protein Nanoparticles

Protein-based nanoparticles can be obtained by the self-assembly of protein structures from sources other than viruses [47]. These particles exhibit highly-ordered surface patterns and geometries, which make them competitive delivery platforms for cancer immunotherapy

applications [48]. Nanoparticles assembled from the E2 component of pyruvate dehydrogenase have become an emerging class of nanocarriers for biomimetic delivery [49]. Because of their small size, E2 nanoparticles are well-suited for lymphatic transport and DC uptake. Systematic work on the utilization of E2 nanoparticles as biomimetic carriers for cancer immunotherapy have been published. In one work, a virus-mimicking DC-targeted vaccine platform was engineered to deliver the DC-activating CpG ODN (Figure 1.1) [50]. By co-delivering a peptide epitope from OVA along with the adjuvant using the E2 nanoparticle, DC maturation and antigen cross-presentation were achieved after particle uptake by DCs. Impressively, CpG ODN in the E2 formulation could activate DCs at a 25-fold lower concentration than free CpG ODN, which highlights the high delivery efficiency of this approach. Ultimately, the formulation was able to increase and prolong antigen-specific $CD8^+$ T cell activation. In subsequent works, a variety of TAAs have been successfully delivered together with CpG ODN using E2 nanoparticles for cancer vaccination [51, 52].

Heat-shock proteins (HSPs) have also been explored for use in nanoformulations for cancer immunotherapy [53]. Protein nanoparticles derived from HSPs can exhibit strong receptor-specific interactions with APCs, which facilitates downstream antigen presentation and immune stimulation [54]. Several *in vivo* studies have been conducted on the use of HSP nanoparticles for immunization applications. For example, antigenic peptides bound to HSP96 have been used as cancer vaccines for patients with recurrent glioblastoma multiforme and colorectal liver metastases [55, 56]. Similarly, immunization with natural HSP110 complexed with the melanoma-associated antigen gp100 protected mice against subsequent challenge with gp100-expressing B16 melanoma by bolstering both $CD4^+$ and $CD8^+$ T cell populations [57].

Other protein nanoparticles that have been used as natural carriers for antigen delivery include ferritin and protein vault nanoparticles. Other than their applications in drug delivery and imaging, ferritin nanoparticles were recently studied for cancer immunotherapy [58]. Antigenic peptides derived from OVA were introduced to ferritin nanoparticles via attachment onto the exterior surface or encapsulation inside the interior cavity [59]. Immunization with the antigen-loaded ferritin nanoparticles could efficiently induce antigen-specific $CD4^+$ and $CD8^+$ T cell proliferation in mice. Similarly, the inner cavity of vault nanoparticles can be used to encapsulate payloads, including immunostimulatory agents [60]. For example, they were used to efficiently deliver CCL21, a lymphoid chemokine predominantly expressed in lymph nodes, in order to promote antitumor activity and inhibit lung cancer growth *in vivo* [61]. Intratumoral administration of the CCL21-complexed formulation enhanced CCL21-associated leukocytic infiltrates and reduced the frequency of immunosuppressive cells.

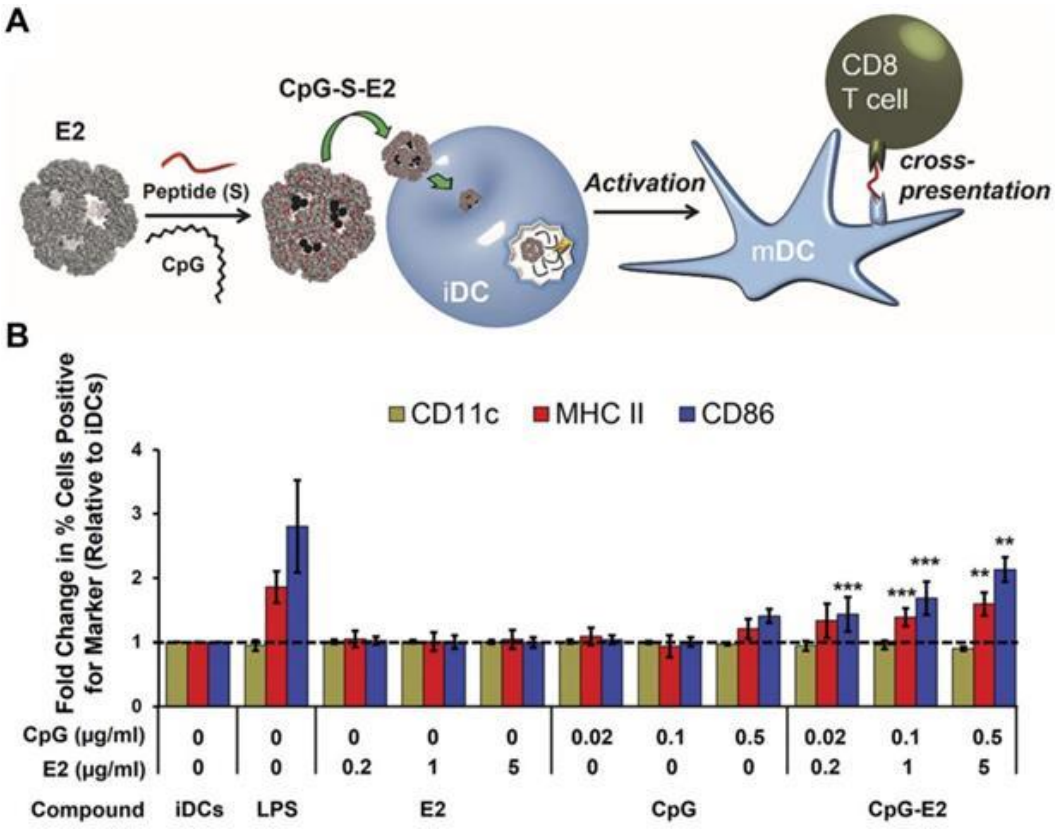

Figure 1.1: Adjuvant and antigen delivery using protein-based nanoparticles. (A) CpG ODN and a peptide antigen can be encapsulated into E2 protein nanoparticles for use as an anticancer vaccine formulation. Upon delivery into immature DCs (iDCs), they can promote transition into a mature phenotype (mDC) and enhance antigen cross-presentation to T cells. (B) The CpG-loaded E2 protein nanoparticles enhance dendritic cell maturation. Adapted with permission from [50]. Copyright 2013 American Chemical Society.

1.2.3.3 Lipoproteins

Another popular type of biomimetic material that can be used for immunotherapeutic applications is lipoproteins, which are endogenous nanocarriers involved in the metabolic transport of fat molecules, as well as biomolecules such proteins, vitamins, hormones, and miRNA [62]. Due to their high biocompatibility and long lifespan, lipoprotein-based nanocarriers have become emerging delivery vehicles for exogenous payload transport [63]. Furthermore, the size of lipoproteins can be tuned for efficient lymph node draining and

promotion of adaptive immune responses [64]. Synthetic high-density lipoprotein (sHDL)-mimicking nanodiscs for personalized neoantigen vaccination and cancer immunotherapy have recently been reported (Figure 1.2) [65]. In the design, cholesterol-modified CpG ODN and identified neoantigen peptides were added to the sHDL nanodiscs to prepare homogeneous ultrasmall cancer nanovaccines. The sHDL nanodiscs improved delivery to lymphoid organs and stimulated antigen presentation by DCs. Remarkably, the nanodiscs elicited a more than 30-fold greater frequency of antigen-specific CTLs compared with a soluble CpG ODN formulation, validating the robustness of using sHDL as an immunostimulant delivery platform. When combined with other immunotherapies such as anti-PD-L1 or anti-CTLA-4 mAbs, the sHDL nanodiscs could eradicate established MC-38 and B16F10 tumors *in vivo*.

Furthermore, other TLR agonists such as MPLA have been successfully incorporated into nanolipoproteins via self-assembly [66]. Compared to administration of the agonist alone, its immunostimulatory profile could be significantly enhanced in the nanoformulation, resulting in elevated cytokine levels and upregulation of immunoregulatory genes. In another work, MPLA and CpG ODN were readily loaded into Ni^{2+}-chelating nanodiscs via insertion into loosely packed lipid bilayers [67]. His-tagged antigens were then loaded into the nanodiscs via binding to Ni^{2+}. It is noteworthy that the adjuvant dosages in the nanodisc formulations were 10-fold lower than what was needed to elicit similar antibody levels and immune responses by independent administration of the components. Overall, lipoprotein-based nanocarriers represent an effective platform for antigen and adjuvant co-delivery. Additionally, it has been shown that co-delivery of chemotherapeutics along with immunostimulatory payloads via these platforms can help to further amplify antitumor efficacy [68, 69].

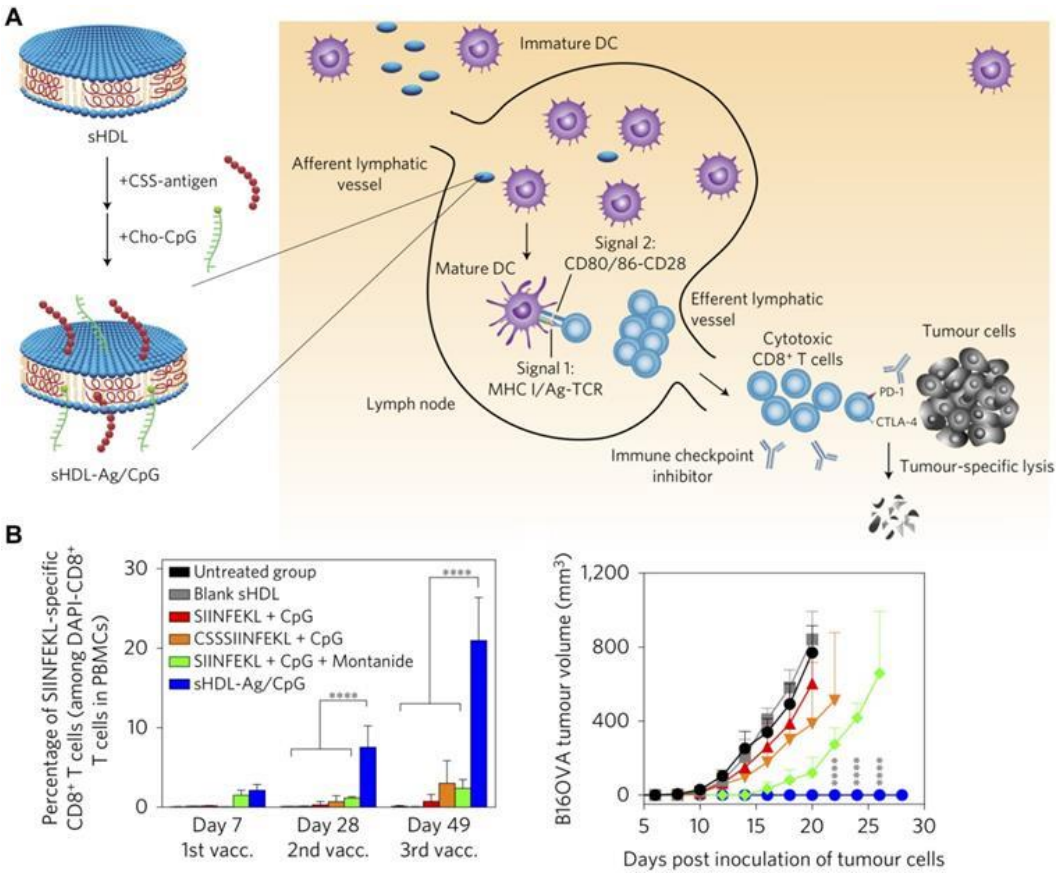

Figure 1.2: Adjuvant and antigen delivery using lipoprotein nanoparticles. (A) Synthetic high-density lipoprotein (sHDL) nanodiscs can be inserted with antigens (Ag) and adjuvants (CpG) using a cysteine-serine-serine (CSS) linker and cholesterol (Cho), respectively. Upon administration, the nanoparticles can drain into nearby lymph nodes, where they are uptaken by DCs that can subsequently activate tumor-specific T cell populations. (B) The dual-loaded nanodisc formulation elicits strong antigen-specific T cell responses and greatly inhibits tumor growth. Adapted with permission from [65]. Copyright 2017 Nature Publishing Group.

1.2.3.4 Oligonucleotides and Polypeptides

Oligonucleotides can be designed to self-assemble into nanoparticles with well-defined structures and uniform sizes, and these particles have been leveraged for the delivery of immunostimulatory agents [70]. In particular, CpG ODNs have been attached to structural oligonucleotides and assembled into multivalent DNA nanostructures [71]. These particles were readily taken up by APCs and engaged TLR9 to activate proinflammatory immune processes. In

another approach, flower-like nanostructures were self-assembled from long nucleotides integrated with tandem CpG ODNs through rolling circle replication [72]. These DNA nanoparticles were able to efficiently deliver the CpG payload while preventing it from nuclease degradation. CpG-containing oligonucleotide nanostructures can also be used for the co-delivery of additional payloads. In one of such example, a programmable DNA nanocomplex was constructed through the self-assembly of a model antigen streptavidin and CpG ODN with precise control over valency and spatial arrangement [73]. The resulting antigen-adjuvant nanocomplex could be used to induce long-lasting antigen-specific immunity. In another work, anti-PD-1 mAbs were loaded into a CpG ODN nanostructure to achieve synergistic action while reducing potential side effects [74]. Similar to oligonucleotide nanoparticles, those based on polypeptides have also been tested for the delivery of immunostimulatory payloads. In one representative work, CpG ODN was conjugated onto polyglutamic acid, and microparticles were obtained through infiltration of the conjugates into porous silica templates, followed by crosslinking of the polypeptide chains and subsequent template removal [75]. The formulation was used to successfully deliver CpG ODN to primary human DCs.

1.2.3.5 Cell Membrane Vesicles

The last major class of naturally occurring delivery vehicles is cell membrane vesicles. Payload delivery using cell-derived membrane vesicles enables concurrent use of multiple membrane biomolecules and biomarkers for functions such as immune cell targeting, cytosolic localization, and elicitation of cytokine production, among others [18]. Exosomes are fragmented vesicles secreted from cells and have essential roles in cellular signaling and metabolic transport

[76]. Depending on their origin, they can exhibit natural affinity towards specific tissues within the body. In the presence of proper immune stimulation, tumor cell-derived exosomes containing TAAs can induce strong adaptive immunity when delivered to APCs [77]. For instance, CpG ODN was incorporated onto exosomes derived from modified B16BL6 cells [78]. The CpG ODN-carrying exosomes were effective at inducing maturation of DCs for enhanced TAA presentation and generation of B16BL6-specific CTLs. Immunization with the modified exosome vaccine resulted in stronger *in vivo* immunotherapeutic efficacy on B16BL6-challenged mice compared with the co-administration of exosomes and CpG ODN. Tumor membrane has also been utilized for antigen inclusion and adjuvant delivery in a different type of approach [79]. In the example, OVA-expressing B16F10 melanoma cells were lysed and vesiculated by sonication. Lipid-conjugated PEG and cholesterol-linked CpG ODN were then loaded onto the nanoparticles via lipid insertion. The resulting tumor membrane vesicle-based formulation exhibited effective lymph node draining and induced the generation of OVA-specific CTLs. When combined with anti-PD-L1 immunotherapy, the treatment mediated complete tumor regression in more than half of the animals that were treated and protected all survivors against a subsequent tumor cell re-challenge. Adjuvant loading can also be achieved by incorporation into tumor membrane particles both before and after vesiculation. In an example, whole B16F10 melanoma cells were broken down into membrane-enclosed vesicular compartments by extrusion or sonication in the presence of CpG ODN, followed by incubation with MPLA [80]. The breadth and diversity of the TAA repertoire was maintained on these membrane particles. The formulation promoted the uptake of the loaded adjuvant payloads and potentiated DC activation. When administered *in vivo*, the adjuvant-loaded particles stimulated antigen-specific cellular and humoral immune responses against B16F10.

Unlike membrane vesicles from tumor origins, those derived from innate immune cells can be directly leveraged for downstream immune stimulation. For instance, membrane vesicles derived from DCs primed with tumor vesicles have been shown to activate T cells and promote robust antitumor immunity [81]. In another example, immature DCs separated from C57BL/6 mice were pretreated and stimulated by the TLR4 agonist MPLA, which led to the elevated expression of costimulatory markers [82]. DC membrane vesicles were then obtained after multiple freeze-thaw cycles. A model antigenic peptide from OVA was loaded into the membrane vesicles, and the resulting formulation was shown to activate immature DCs *in situ* and augment the expansion of antigen-specific $CD8^+$ T cells.

Bacterial outer membrane vesicles (OMVs) have also been explored for cancer immunotherapy applications. OMVs are lipid vesicles released from the outer membrane of Gram-negative bacteria and serve a variety of roles during infection [83]. They contain a number of natural adjuvants such as LPS, flagellin, and peptidoglycan that can be used to trigger strong immune reactions [84]. This intrinsic immunostimulatory property has been tested in different disease applications [85]. The potential of *Escherichia coli* OMVs as an effective anticancer agent has been explored, where they were tested against four different tumor models (CT26, MC38, B16BL6, and 4T1) [86]. Intravenous administration of the OMVs led to accumulation in tumor tissue and induced cytokine production that enabled the growth of established tumors to be controlled.

1.2.3.6 Genetically Modified Membrane Vesicles

In addition to their ability to encapsulate and deliver immunotherapeutic payloads, natural membrane vesicles can be genetically modified to introduce additional functionalities. IL12 plays an important role in the activation of NK cells and CTLs [87]. However, the direct administration of IL12 can cause severe adverse effects, which undermine its benefits in cancer immunotherapy applications [88]. In one work, cells were genetically modified to express functional IL12 using a glycolipid anchor [89]. The anchored IL12 could then be efficiently intercalated and transferred onto membrane vesicles isolated from various tumor cell lines. It was found that the incorporation of IL12 onto the tumor membrane vesicles could significantly induce T cell proliferation and the release of IFNγ. In a subsequent work, together with IL12, glycolipid-anchored HER2 and CD80 were also transferred to plasma membrane vesicles homogenized from tumor tissues [90]. The IL12 and CD80 served to enhance immune stimulation against the HER2 antigen. Immunization with these vesicles induced strong HER2-specific immune responses and resulted in complete protection against $HER2^+$ tumor challenge.

In another type of approach, the engineering of membrane vesicles to express immunoregulatory proteins can be used to achieve a checkpoint blockade effect for antitumor therapy. In one work, PD-1 was stably expressed on the membrane of HEK 293T cells, which were subsequently extruded to form nanovesicles [91]. The resulting PD-1-presenting membrane vesicles could effectively bind to and neutralize the PD-L1 ligand on tumor cells, leading to the reactivation of exhausted antigen-specific $CD8^+$ T cells. Furthermore, using a similar editing process, PD-1 receptors were expressed on megakaryocytes before differentiation into platelets [92]. Taking advantage of the outstanding tumor targeting ability of platelets, the platelet-derived PD-1-containing membrane vesicles could be retained at the tumor site post-resection to enhance the activity of $CD8^+$ T cells against residual disease.

Other protein ligands can be integrated into membrane vesicles using similar genetic modification approaches. A virus-mimetic nanovesicle was produced by expressing viral proteins in mammalian cells, which were then sonicated in the presence of surfactants [93]. This approach enabled the display of functional polypeptides with correct conformations and could aid in future vaccine design. In a different type of example, a hepatitis B virus receptor was engineered into nanovesicles in order to generate nanoscale decoys that could block infection by the virus *in vivo* [94]. Besides viral proteins, tumor-targeting moieties, such as human epidermal growth factor or anti-HER2 affibodies, have been successfully integrated onto nanovesicles [95]. The engineered liposome-like nanovesicles could be used to enhance the delivery of phototheranostic or chemotherapeutic agents to tumor cells.

In terms of bacterial vesicles, OMVs can also be easily modified to introduce additional functional components. As an example, *E. coli* OMVs were genetically decorated with two epitopes present in B16F10 melanoma cells expressing epidermal growth factor receptor variant III, and the resulting formulation was tested for its protective activity against tumor growth [96]. High levels of antigen-specific antibody titers were elicited, and significant amounts of tumor-infiltrating lymphocytes were found at the tumor site. This ultimately led to effective protection of the immunized mice upon tumor challenge.

1.2.4 Engineered Cell Membrane Hybrids

For payload delivery, naturally occurring membrane can be integrated with other synthetic materials in a manner that takes advantage of the distinct strengths of each component. Specifically, for the delivery of immunostimulants, the presence of cell membrane-derived

functionality can facilitate targeting to immune cells and accumulation in immune-rich organs, while other components can be included to augment immune stimulation performance. The membrane component can be further engineered to confer exogenous functional moieties, including cytokines, receptor-binding ligands, targeting antibodies, and immunogenic antigens, among others [97]. Compared with traditional nanoformulations, a major advantage of these hybrid platforms is the ability of the natural component to camouflage artificial materials that would normally be cleared quickly by the immune system [98]. These approaches also enable sophisticated delivery strategies where different payload combinations can be employed in unique ways [99]. Additionally, in these hybrid systems, the intrinsic properties of various synthetic nanomaterials can be readily leveraged to achieve multimodal functionality or to create combinatorial treatments [18].

1.2.4.1 White Blood Cell Membrane Hybrids

Mimicking the function of immune cells can be an effective means for achieving targeted delivery of immunostimulatory agents for cancer therapy. The transfer of bioactive cellular components to synthetic particles is one of the strategies that can bestow the biological functions of immune cells to synthetic hybrids [100]. A bottom-up approach has been proposed based on the extraction of plasma membrane proteins from macrophages and subsequent incorporation of these proteins with synthetic choline-based phospholipids [101]. The assembled hybrid vesicles retained the targeting capability of macrophages and were used for preferential targeting to inflamed vasculature. Similarly, porous silicon particles have been cloaked using membrane derived from leukocytes [102]. The resulting hybrid particles possessed immunological

functionalities similar to the source cells, including protection from opsonization, reduced phagocytic uptake, and binding to tumor endothelium. It has been shown that the source of membrane is critical for improving systemic tolerance and minimizing inflammatory responses [103]. Membrane hybrid particles derived from syngeneic membrane exhibited less uptake by the murine immune system compared with those fabricated from xenogeneic membrane, possibly due to the presence of critical biomarkers and self-recognition receptors preserved after cloaking.

A recent work described the coating of leukocyte membrane onto magnetic nanoclusters for the construction of artificial APCs [104]. Specifically, a macrophage cell line was pre-modified with azide before membrane extraction and uniformly coated onto the nanocluster cores. The nanohybrids were then functionalized with an MHC complex and anti-CD28 for antigen presentation to $CD8^+$ T cells. The resulting artificial APCs could not only stimulate the expansion of antigen-specific CTLs, but also helped to effectively guide reinfused CTLs to tumor tissues through magnetic control. Immunotherapeutic nanoformulations cloaked by membrane from another leukocyte cell type, NK cells, have also been reported [105]. NK cells were selected because of their immunoregulatory roles. By coating polymeric nanoparticles with NK cell membrane, the resulting particles were able to induce M1 macrophage polarization and elicit tumor-specific immune responses. A photosensitizer was loaded into the polymeric cores for photodynamic therapy, which helped to improve immunotherapeutic efficacy of the system by inducing expression of damage-associated molecular patterns on dying tumor cells.

1.2.4.2 Red Blood Cell Membrane Hybrids

Owing to their high blood abundancy, facile processing, and remarkable biocompatibility, red blood cells (RBCs) have used extensively as a source of membrane coating material to construct versatile platforms for nanodelivery applications [106, 107]. The resulting membrane-coated nanoparticles can protect encapsulated payloads from immune clearance and facilitate enhanced delivery. As recently discovered, RBCs can help to mediate certain immune processes [108, 109], which may eventually be leveraged for immunotherapeutic applications. Their ability to interact with certain pathological immune cell subsets has also aided in the design of targeted membrane-coated nanoformulations [110]. In the work, a subpopulation of B cells was positively labelled by RBC membrane-coated nanoparticles based on cognate receptor binding. Additionally, an active particulate vaccine system based on RBC membrane-coated micromotors has recently been reported [111]. Antigen-inserted RBC membrane was integrated with core-shell micromotors that provided propulsion properties for enhanced oral vaccination. The RBC membrane-coated vaccine formulation demonstrated improved retention in the mucosal layer of the small intestine, which led to more robust antibody production.

Specifically in terms of cancer applications, an RBC membrane-based nanovaccine platform for the stimulation of antitumor immunity was recently reported [112]. The platform was constructed by enveloping RBC membrane around a polymeric PLGA core, which was used to load MPLA adjuvant and an antigenic peptide. Additionally, mannose was inserted into the RBC membrane for active APC targeting. Enhanced retention in the draining lymph nodes after intradermal injection was observed, along with elevated IFNγ secretion and $CD8^+$ T cell responses. This nanovaccine effectively inhibited tumor growth and suppressed tumor metastasis in a murine B16F10 melanoma model.

1.2.4.3 Cancer Cell Membrane Hybrids

Cancer cell membrane represents a rich source of functional ligands as well as TAAs [18, 19], and these properties have been leveraged in the design of hybrid nanostructures for cancer imaging [113], photothermal therapy [114], photodynamic therapy [115], virotherapy [116], and immunotherapy [117]. In one such work on cancer immunotherapy, the immunogenic properties of HSP70 was leveraged to enhance immune responses against cancer cell membrane antigens [118]. The protein was incorporated into a membrane structure along with TAAs from B16-OVA cell membrane, which was subsequently coated around a phosphate calcium core encapsulating CpG ODN. The platform effectively delivered the antigen and adjuvant payloads to APCs and NK cells, which led to the expansion of IFNγ-expressing $CD8^+$ T cells and $NKG2D^+$ NK cells. In another approach, the membrane from MDA-MB-231 breast cancer cells was coated around thermally oxidized porous silica, which was used as a novel immunostimulatory agent [119]. The resulting hybrid nanoparticles greatly enhanced IFNγ secretion by peripheral blood monocytes and oriented the polarization of T cells towards a T_h1 phenotype.

Without the assistance of immunostimulatory agents, the immunogenicity of TAAs is generally insufficient to elicit potent antitumor responses [120]. In addition to the above examples, there are many other strategies by which adjuvants can be included in cancer cell membrane-based nanoformulations. In an example, cell membrane from B16F10 melanoma coated onto PLGA nanoparticles was incorporated with the adjuvant MPLA [121]. Besides its ability to homotypically target the source cancer cells, this cell membrane hybrid platform could efficiently induce the maturation of professional APCs and improved downstream T cell stimulation. In a follow-up study, CpG ODN loaded into PLGA cores was used to generate

another anticancer vaccine formulation (Figure 1.3) [122]. The nanoparticulate delivery of the adjuvant significantly enhanced its biological activity compared with CpG ODN in free form. Upon uptake by DCs, the nanovaccine formulation promoted the generation of multiple CTL populations with tumor specificity. When combined with other immunotherapies such as checkpoint blockades, the nanoformulation demonstrated the ability to significantly enhance control of tumor growth in a therapeutic setting. Over time, increasingly sophisticated nanovaccine formulations have been developed using the membrane coating concept. In a recent design, PLGA nanoparticles were loaded with the TLR7 agonist R837 and then coated with membrane from B16-OVA cancer cells (Figure 1.4) [123]. To provide APC targeting functionality, the membrane shell was further modified with a mannose moiety using a lipid anchoring approach. The hybrid nanoformulation not only exhibited efficacy in delaying tumor growth as a preventative vaccine, but also displayed activity against established tumors when co-administered with anti-PD-1 mAbs.

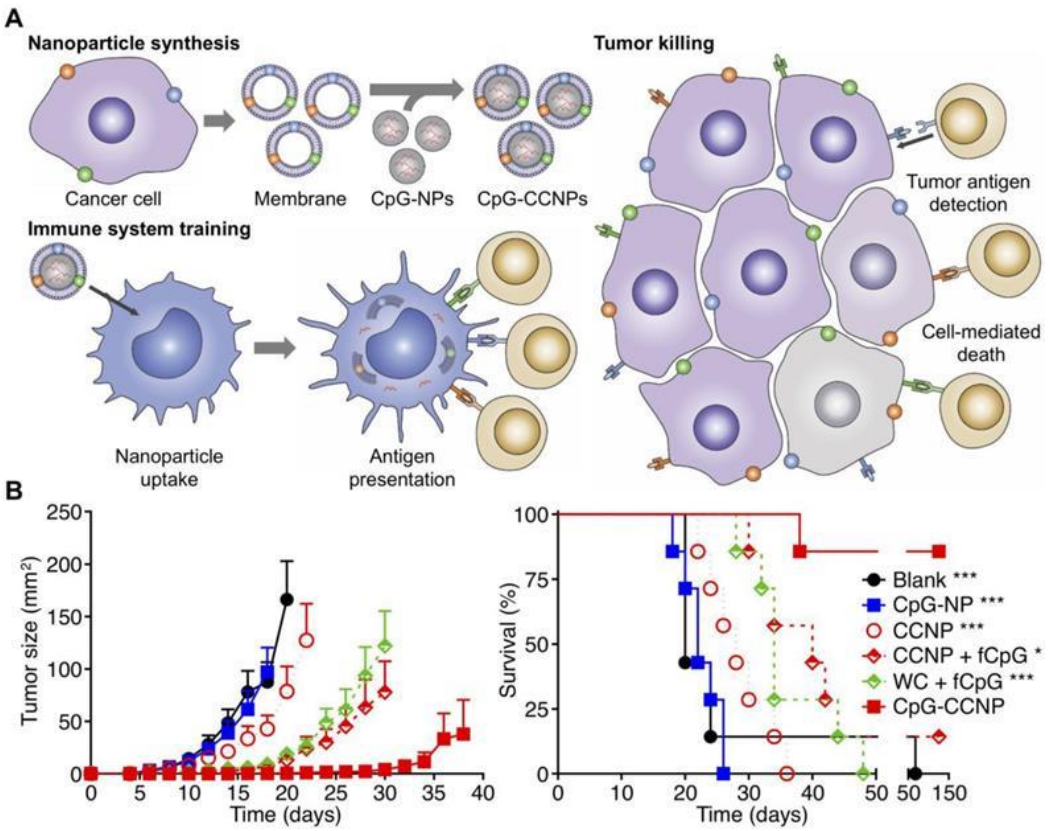

Figure 1.3: Anticancer vaccination using cancer cell membrane-coated nanoparticles (CCNPs). (A) The membrane derived from cancer cells, along with its associated tumor antigens, is coated onto CpG ODN-loaded nanoparticle cores to yield a nanoparticulate anticancer vaccine (CpG-CCNPs). Upon delivery to APCs, the vaccine formulation enables activation of T cells with multiple antitumor specificities. (B) The co-delivery of both tumor antigens and CpG together in CpG-CCNPs greatly protects against tumor growth and enhances survival. Adapted with permission from [122]. Copyright 2017 Wiley-VCH.

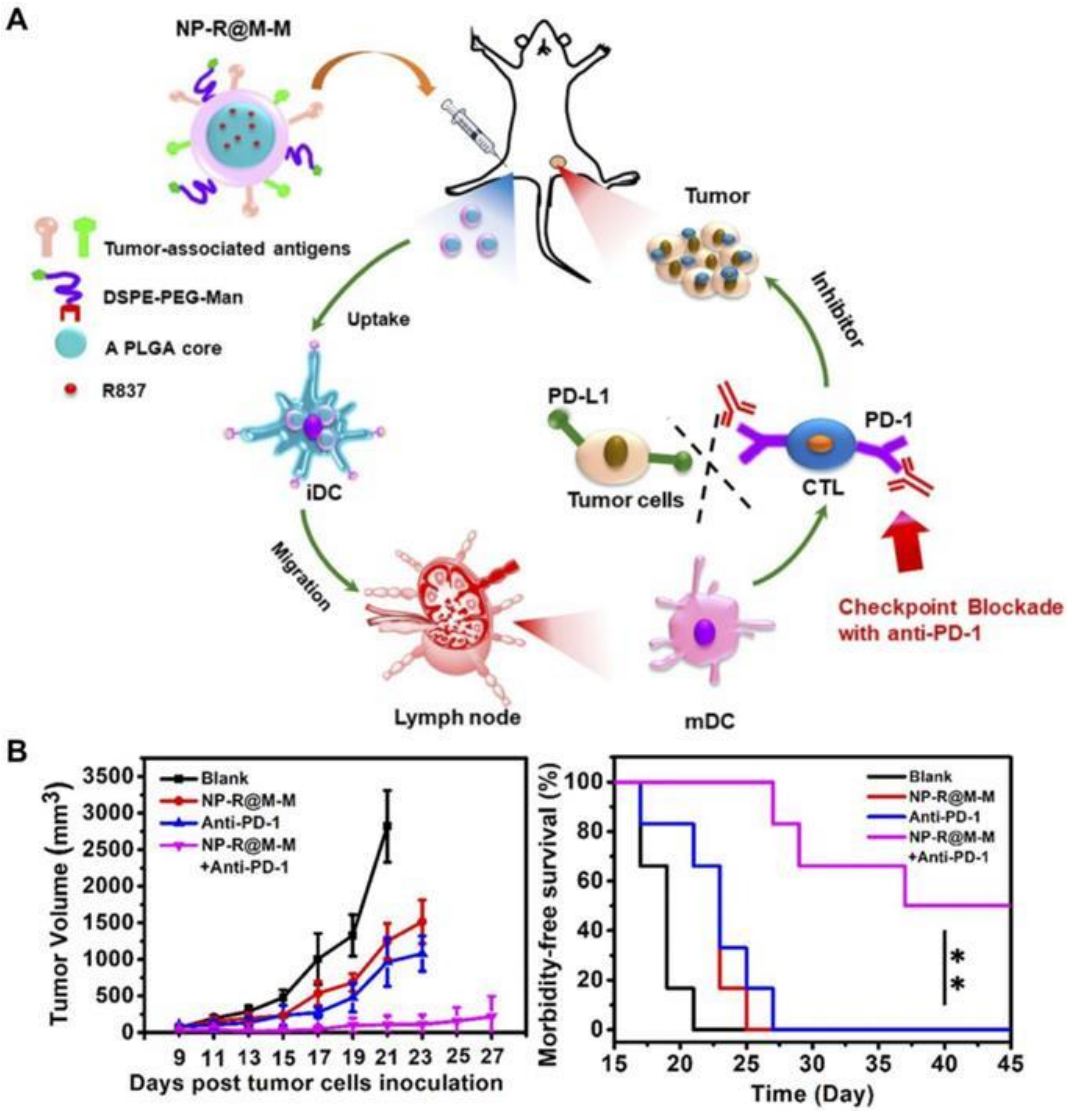

Figure 1.4: Anticancer vaccination using targeted CCNPs. (A) Tumor cell membrane-coated, R837-loaded, and mannose-modified PLGA nanoparticles (NP-R@M-M) can promote transition of DCs from an immature (iDC) to mature (mDC) phenotype. (B) When combined with checkpoint blockade therapy, tumor growth can be effectively inhibited, and survival is enhanced. Adapted with permission from [123]. Copyright 2018 American Chemical Society.

1.3 Conclusion and Perspectives

In this review, we have discussed current progress in the development of nanoscale platforms for the delivery of immunostimulatory agents. Adjuvants, cytokines, and mAbs all

represent immunotherapeutic agents that can benefit from the enhanced transport afforded by nanodelivery. The formulation of these compounds into particulate nanocarriers protects their biological activity and elevates their bioavailability, both of which can contribute to stronger immune stimulation. To address the need for specific delivery to target immune cell subsets and immune-rich tissues, bioinspired platforms and modifications can provide certain advantages over current nanoparticle technologies. Biomimetic delivery approaches generally enable facile immune cell targeting, and the inherent immunogenicity or antigenicity associated with many of these platforms can be directly leveraged for more efficient vaccine design. Furthermore, by integrating immunostimulants with tumor antigens in the same particulate system, significant immunotherapeutic efficacy against established tumors can be achieved.

Although the emerging biomimetic approaches discussed in this review have shown significant potential for cancer immunotherapy, there are still several areas in which improvements can be made. For one, further enhancement of immunostimulatory potency in a safe manner is highly desirable. This can be achieved by improving targeting efficacy or developing new materials with better immunostimulatory characteristics. As tumor immunosuppression occurs by a variety of different mechanisms, it is likely that a large percentage of patients will not respond to mono-immunotherapies. Therefore, effort will need to be placed on the exploration of how to best combine different immunotherapeutic modalities to maximize antitumor responses. For example, agents that affect innate and adaptive immunity can be combined together to provide comprehensive immune activation. Otherwise, immunotherapies can also be combined with other therapeutic modalities, including surgery, radiation, chemotherapy, and targeted therapy, among many others. Finally, as biomimetic technologies mature, more work will need to be done in order to facilitate clinical translation.

Challenges along these lines include the cost-effective sourcing of biological nanomaterials, large-scale production of pharmaceutical grade products, and optimization of long-term storage conditions. As many of these promising new platforms exist at the interface between natural and synthetic, this is a new frontier that will need to be explored in concert with regulatory agencies.

The first portion of chapter 1, in part, contains the material in *Nanoscale Horizons*, 2020, Joon Ho Park*, Diana Dehaini*, Jiarong Zhou, Maya Holay, Ronnie H. Fang and Liangfang Zhang. The dissertation author was a primary author (equally contributing with Diana Dehaini) of this paper.

The second portion of chapter 1, in part, contains the material in *Theranostics*, 2019, Jia Zhuang, Maya Holay, Joon Ho Park, Ronnie H. Fang, Jie Zhang and Liangfang Zhang. The dissertation author was a major contributor and co-author of this paper.

1.4 References

1. Wang, A.Z., R. Langer, and O.C. Farokhzad, *Nanoparticle delivery of cancer drugs.* Annu Rev Med, 2012. **63**: p. 185-98.
2. Farokhzad, O.C. and R. Langer, *Impact of nanotechnology on drug delivery.* ACS Nano, 2009. **3**(1): p. 16-20.
3. Shi, J., P.W. Kantoff, R. Wooster, and O.C. Farokhzad, *Cancer nanomedicine: progress, challenges and opportunities.* Nat Rev Cancer, 2017. **17**(1): p. 20-37.
4. Hosoyama, K., M. Ahumada, K. Goel, M. Ruel, E.J. Suuronen, and E.I. Alarcon, *Electroconductive materials as biomimetic platforms for tissue regeneration.* Biotechnol Adv, 2019. **37**(3): p. 444-458.
5. Zhang, L., F.X. Gu, J.M. Chan, A.Z. Wang, R.S. Langer, and O.C. Farokhzad, *Nanoparticles in medicine: therapeutic applications and developments.* Clin Pharmacol Ther, 2008. **83**(5): p. 761-9.
6. Brannon-Peppas, L. and J.O. Blanchette, *Nanoparticle and targeted systems for cancer therapy.* Adv Drug Deliv Rev, 2004. **56**(11): p. 1649-59.

7. Singh, R. and J.W. Lillard, Jr., *Nanoparticle-based targeted drug delivery.* Exp Mol Pathol, 2009. **86**(3): p. 215-23.

8. Byrne, J.D., T. Betancourt, and L. Brannon-Peppas, *Active targeting schemes for nanoparticle systems in cancer therapeutics.* Adv Drug Deliv Rev, 2008. **60**(15): p. 1615-26.

9. Martin Gimenez, V.M., D.E. Kassuha, and W. Manucha, *Nanomedicine applied to cardiovascular diseases: latest developments.* Ther Adv Cardiovasc Dis, 2017. **11**(4): p. 133-142.

10. Gupta, P., E. Garcia, A. Sarkar, S. Kapoor, K. Rafiq, H.S. Chand, and R.D. Jayant, *Nanoparticle Based Treatment for Cardiovascular Diseases.* Cardiovasc Hematol Disord Drug Targets, 2019. **19**(1): p. 33-44.

11. Fang, R.H., C.M. Hu, and L. Zhang, *Nanoparticles disguised as red blood cells to evade the immune system.* Expert Opin Biol Ther, 2012. **12**(4): p. 385-9.

12. Yoo, J.W., D.J. Irvine, D.E. Discher, and S. Mitragotri, *Bio-inspired, bioengineered and biomimetic drug delivery carriers.* Nat Rev Drug Discov, 2011. **10**(7): p. 521-35.

13. Kroll, A.V., R.H. Fang, and L. Zhang, *Biointerfacing and Applications of Cell Membrane-Coated Nanoparticles.* Bioconjug Chem, 2017. **28**(1): p. 23-32.

14. Mohan, T., P. Verma, and D.N. Rao, *Novel adjuvants & delivery vehicles for vaccines development: a road ahead.* Indian J Med Res, 2013. **138**(5): p. 779-95.

15. Bachmann, M.F. and G.T. Jennings, *Vaccine delivery: a matter of size, geometry, kinetics and molecular patterns.* Nat Rev Immunol, 2010. **10**(11): p. 787-96.

16. Conniot, J., J.M. Silva, J.G. Fernandes, L.C. Silva, R. Gaspar, S. Brocchini, H.F. Florindo, and T.S. Barata, *Cancer immunotherapy: nanodelivery approaches for immune cell targeting and tracking.* Front Chem, 2014. **2**: p. 105.

17. Leleux, J. and K. Roy, *Micro and nanoparticle-based delivery systems for vaccine immunotherapy: an immunological and materials perspective.* Adv Healthc Mater, 2013. **2**(1): p. 72-94.

18. Fang, R.H., A.V. Kroll, W. Gao, and L. Zhang, *Cell Membrane Coating Nanotechnology.* Adv Mater, 2018. **30**(23): p. e1706759.

19. Kroll, A.V., Y. Jiang, J. Zhou, M. Holay, R.H. Fang, and L. Zhang, *Biomimetic Nanoparticle Vaccines for Cancer Therapy.* Adv Biosyst, 2019. **3**(1): p. e1800219.

20. Dehaini, D., R.H. Fang, and L. Zhang, *Biomimetic strategies for targeted nanoparticle delivery.* Bioeng Transl Med, 2016. **1**(1): p. 30-46.

21. Irache, J.M., H.H. Salman, C. Gamazo, and S. Espuelas, *Mannose-targeted systems for the delivery of therapeutics.* Expert Opin Drug Deliv, 2008. **5**(6): p. 703-24.

22. Taylor, P.R., S. Gordon, and L. Martinez-Pomares, *The mannose receptor: linking homeostasis and immunity through sugar recognition.* Trends Immunol, 2005. **26**(2): p. 104-10.

23. Jiang, H.L., M.L. Kang, J.S. Quan, S.G. Kang, T. Akaike, H.S. Yoo, and C.S. Cho, *The potential of mannosylated chitosan microspheres to target macrophage mannose receptors in an adjuvant-delivery system for intranasal immunization.* Biomaterials, 2008. **29**(12): p. 1931-9.

24. Zhu, S., M. Niu, H. O'Mary, and Z. Cui, *Targeting of tumor-associated macrophages made possible by PEG-sheddable, mannose-modified nanoparticles.* Mol Pharm, 2013. **10**(9): p. 3525-30.

25. Xu, Z., S. Ramishetti, Y.C. Tseng, S. Guo, Y. Wang, and L. Huang, *Multifunctional nanoparticles co-delivering Trp2 peptide and CpG adjuvant induce potent cytotoxic T-lymphocyte response against melanoma and its lung metastasis.* J Control Release, 2013. **172**(1): p. 259-265.

26. Xu, Z., Y. Wang, L. Zhang, and L. Huang, *Nanoparticle-delivered transforming growth factor-beta siRNA enhances vaccination against advanced melanoma by modifying tumor microenvironment.* ACS Nano, 2014. **8**(4): p. 3636-45.

27. Shi, G.N., C.N. Zhang, R. Xu, J.F. Niu, H.J. Song, X.Y. Zhang, W.W. Wang, Y.M. Wang, C. Li, X.Q. Wei, and D.L. Kong, *Enhanced antitumor immunity by targeting dendritic cells with tumor cell lysate-loaded chitosan nanoparticles vaccine.* Biomaterials, 2017. **113**: p. 191-202.

28. Wang, C., P. Li, L. Liu, H. Pan, H. Li, L. Cai, and Y. Ma, *Self-adjuvanted nanovaccine for cancer immunotherapy: Role of lysosomal rupture-induced ROS in MHC class I antigen presentation.* Biomaterials, 2016. **79**: p. 88-100.

29. Lepenies, B., J. Lee, and S. Sonkaria, *Targeting C-type lectin receptors with multivalent carbohydrate ligands.* Adv Drug Deliv Rev, 2013. **65**(9): p. 1271-81.

30. Unger, W.W., A.J. van Beelen, S.C. Bruijns, M. Joshi, C.M. Fehres, L. van Bloois, M.I. Verstege, M. Ambrosini, H. Kalay, K. Nazmi, J.G. Bolscher, E. Hooijberg, T.D. de Gruijl, G. Storm, and Y. van Kooyk, *Glycan-modified liposomes boost CD4+ and CD8+ T-cell responses by targeting DC-SIGN on dendritic cells.* J Control Release, 2012. **160**(1): p. 88-95.

31. Roldao, A., M.C. Mellado, L.R. Castilho, M.J. Carrondo, and P.M. Alves, *Virus-like particles in vaccine development.* Expert Rev Vaccines, 2010. **9**(10): p. 1149-76.

32. Yan, D., Y.Q. Wei, H.C. Guo, and S.Q. Sun, *The application of virus-like particles as vaccines and biological vehicles.* Appl Microbiol Biotechnol, 2015. **99**(24): p. 10415-32.

33. Neek, M., T.I. Kim, and S.W. Wang, *Protein-based nanoparticles in cancer vaccine development.* Nanomedicine, 2019. **15**(1): p. 164-174.

34. Gonzalez, M.J., E.M. Plummer, C.S. Rae, and M. Manchester, *Interaction of Cowpea mosaic virus (CPMV) nanoparticles with antigen presenting cells in vitro and in vivo.* PLoS One, 2009. **4**(11): p. e7981.

35. Lizotte, P.H., A.M. Wen, M.R. Sheen, J. Fields, P. Rojanasopondist, N.F. Steinmetz, and S. Fiering, *In situ vaccination with cowpea mosaic virus nanoparticles suppresses metastatic cancer.* Nat Nanotechnol, 2016. **11**(3): p. 295-303.

36. Shukla, S., M. Jandzinski, C. Wang, X. Gong, K.W. Bonk, R.A. Keri, and N.F. Steinmetz, *A Viral Nanoparticle Cancer Vaccine Delays Tumor Progression and Prolongs Survival in a HER2(+) Tumor Mouse Model.* Adv Ther (Weinh), 2019. **2**(4).

37. Shukla, S., J.T. Myers, S.E. Woods, X. Gong, A.E. Czapar, U. Commandeur, A.Y. Huang, A.D. Levine, and N.F. Steinmetz, *Plant viral nanoparticles-based HER2 vaccine: Immune response influenced by differential transport, localization and cellular interactions of particulate carriers.* Biomaterials, 2017. **121**: p. 15-27.

38. McCormick, A.A., T.A. Corbo, S. Wykoff-Clary, L.V. Nguyen, M.L. Smith, K.E. Palmer, and G.P. Pogue, *TMV-peptide fusion vaccines induce cell-mediated immune responses and tumor protection in two murine models.* Vaccine, 2006. **24**(40-41): p. 6414-23.

39. Schwarz, K., E. Meijerink, D.E. Speiser, A.C. Tissot, I. Cielens, R. Renhof, A. Dishlers, P. Pumpens, and M.F. Bachmann, *Efficient homologous prime-boost strategies for T cell vaccination based on virus-like particles.* Eur J Immunol, 2005. **35**(3): p. 816-21.

40. Yang, L., H. Yang, K. Rideout, T. Cho, K.I. Joo, L. Ziegler, A. Elliot, A. Walls, D. Yu, D. Baltimore, and P. Wang, *Engineered lentivector targeting of dendritic cells for in vivo immunization.* Nat Biotechnol, 2008. **26**(3): p. 326-34.

41. Pineo, C.B., Hitzeroth, II, and E.P. Rybicki, *Immunogenic assessment of plant-produced human papillomavirus type 16 L1/L2 chimaeras.* Plant Biotechnol J, 2013. **11**(8): p. 964-75.

42. Huber, B., C. Schellenbacher, C. Jindra, D. Fink, S. Shafti-Keramat, and R. Kirnbauer, *A chimeric 18L1-45RG1 virus-like particle vaccine cross-protects against oncogenic alpha-7 human papillomavirus types.* PLoS One, 2015. **10**(3): p. e0120152.

43. Ng, Q., F. He, and J. Kwang, *Recent Progress towards Novel EV71 Anti-Therapeutics and Vaccines.* Viruses, 2015. **7**(12): p. 6441-57.

44. Lin, Y.L., Y.C. Hu, C.C. Liang, S.Y. Lin, Y.C. Liang, H.P. Yuan, and B.L. Chiang, *Enterovirus-71 virus-like particles induce the activation and maturation of human monocyte-derived dendritic cells through TLR4 signaling.* PLoS One, 2014. **9**(10): p. e111496.

45. Zhang, Y., S. Song, C. Liu, Y. Wang, X. Xian, Y. He, J. Wang, F. Liu, and S. Sun, *Generation of chimeric HBc proteins with epitopes in E.coli: formation of virus-like particles and a potent inducer of antigen-specific cytotoxic immune response and anti-tumor effect in vivo.* Cell Immunol, 2007. **247**(1): p. 18-27.

46. Ding, F.X., F. Wang, Y.M. Lu, K. Li, K.H. Wang, X.W. He, and S.H. Sun, *Multiepitope peptide-loaded virus-like particles as a vaccine against hepatitis B virus-related hepatocellular carcinoma.* Hepatology, 2009. **49**(5): p. 1492-502.

47. Lohcharoenkal, W., L. Wang, Y.C. Chen, and Y. Rojanasakul, *Protein nanoparticles as drug delivery carriers for cancer therapy.* Biomed Res Int, 2014. **2014**: p. 180549.

48. Molino, N.M. and S.W. Wang, *Caged protein nanoparticles for drug delivery.* Curr Opin Biotechnol, 2014. **28**: p. 75-82.

49. Izard, T., A. Aevarsson, M.D. Allen, A.H. Westphal, R.N. Perham, A. de Kok, and W.G. Hol, *Principles of quasi-equivalence and Euclidean geometry govern the assembly of cubic and dodecahedral cores of pyruvate dehydrogenase complexes.* Proc Natl Acad Sci U S A, 1999. **96**(4): p. 1240-5.

50. Molino, N.M., A.K. Anderson, E.L. Nelson, and S.W. Wang, *Biomimetic protein nanoparticles facilitate enhanced dendritic cell activation and cross-presentation.* ACS Nano, 2013. **7**(11): p. 9743-52.

51. Molino, N.M., M. Neek, J.A. Tucker, E.L. Nelson, and S.W. Wang, *Viral-mimicking protein nanoparticle vaccine for eliciting anti-tumor responses.* Biomaterials, 2016. **86**: p. 83-91.

52. Neek, M., J.A. Tucker, T.I. Kim, N.M. Molino, E.L. Nelson, and S.W. Wang, *Co-delivery of human cancer-testis antigens with adjuvant in protein nanoparticles induces higher cell-mediated immune responses.* Biomaterials, 2018. **156**: p. 194-203.

53. Ciocca, D.R. and S.K. Calderwood, *Heat shock proteins in cancer: diagnostic, prognostic, predictive, and treatment implications.* Cell Stress Chaperones, 2005. **10**(2): p. 86-103.

54. Binder, R.J. and P.K. Srivastava, *HSP-APC interactions: Initiation of immune responses.* Heat Shock Proteins: Potent Mediators of Inflammation and Immunity, 2007: p. 131-145.

55. Crane, C.A., S.J. Han, B. Ahn, J. Oehlke, V. Kivett, A. Fedoroff, N. Butowski, S.M. Chang, J. Clarke, M.S. Berger, M.W. McDermott, M.D. Prados, and A.T. Parsa, *Individual patient-specific immunity against high-grade glioma after vaccination with autologous tumor derived peptides bound to the 96 KD chaperone protein.* Clin Cancer Res, 2013. **19**(1): p. 205-14.

56. Mazzaferro, V., J. Coppa, M.G. Carrabba, L. Rivoltini, M. Schiavo, E. Regalia, L. Mariani, T. Camerini, A. Marchiano, S. Andreola, R. Camerini, M. Corsi, J.J. Lewis, P.K. Srivastava, and G. Parmiani, *Vaccination with autologous tumor-derived heat-shock*

protein gp96 after liver resection for metastatic colorectal cancer. Clin Cancer Res, 2003. **9**(9): p. 3235-45.

57. Wang, X.Y., X. Chen, M.H. Manjili, E. Repasky, R. Henderson, and J.R. Subjeck, *Targeted immunotherapy using reconstituted chaperone complexes of heat shock protein 110 and melanoma-associated antigen gp100.* Cancer Res, 2003. **63**(10): p. 2553-60.

58. Wang, Z., H. Gao, Y. Zhang, G. Liu, G. Niu, and X. Chen, *Functional ferritin nanoparticles for biomedical applications.* Front Chem Sci Eng, 2017. **11**(4): p. 633-646.

59. Han, J.A., Y.J. Kang, C. Shin, J.S. Ra, H.H. Shin, S.Y. Hong, Y. Do, and S. Kang, *Ferritin protein cage nanoparticles as versatile antigen delivery nanoplatforms for dendritic cell (DC)-based vaccine development.* Nanomedicine, 2014. **10**(3): p. 561-9.

60. Benner, N.L., X. Zang, D.C. Buehler, V.A. Kickhoefer, M.E. Rome, L.H. Rome, and P.A. Wender, *Vault Nanoparticles: Chemical Modifications for Imaging and Enhanced Delivery.* ACS Nano, 2017. **11**(1): p. 872-881.

61. Kar, U.K., M.K. Srivastava, A. Andersson, F. Baratelli, M. Huang, V.A. Kickhoefer, S.M. Dubinett, L.H. Rome, and S. Sharma, *Novel CCL21-vault nanocapsule intratumoral delivery inhibits lung cancer growth.* PLoS One, 2011. **6**(5): p. e18758.

62. Feingold, K.R., *Introduction to Lipids and Lipoproteins*, in *Endotext*, K.R. Feingold, et al., Editors. 2000: South Dartmouth (MA).

63. Kuai, R., D. Li, Y.E. Chen, J.J. Moon, and A. Schwendeman, *High-Density Lipoproteins: Nature's Multifunctional Nanoparticles.* ACS Nano, 2016. **10**(3): p. 3015-41.

64. Randolph, G.J. and N.E. Miller, *Lymphatic transport of high-density lipoproteins and chylomicrons.* J Clin Invest, 2014. **124**(3): p. 929-35.

65. Kuai, R., L.J. Ochyl, K.S. Bahjat, A. Schwendeman, and J.J. Moon, *Designer vaccine nanodiscs for personalized cancer immunotherapy.* Nat Mater, 2017. **16**(4): p. 489-496.

66. Weilhammer, D.R., C.D. Blanchette, N.O. Fischer, S. Alam, G.G. Loots, M. Corzett, C. Thomas, C. Lychak, A.D. Dunkle, J.J. Ruitenberg, S.A. Ghanekar, A.J. Sant, and A. Rasley, *The use of nanolipoprotein particles to enhance the immunostimulatory properties of innate immune agonists against lethal influenza challenge.* Biomaterials, 2013. **34**(38): p. 10305-18.

67. Fischer, N.O., A. Rasley, M. Corzett, M.H. Hwang, P.D. Hoeprich, and C.D. Blanchette, *Colocalized delivery of adjuvant and antigen using nanolipoprotein particles enhances the immune response to recombinant antigens.* J Am Chem Soc, 2013. **135**(6): p. 2044-7.

68. Han, Y., B. Ding, Z. Zhao, H. Zhang, B. Sun, Y. Zhao, L. Jiang, J. Zhou, and Y. Ding, *Immune lipoprotein nanostructures inspired relay drug delivery for amplifying antitumor efficiency.* Biomaterials, 2018. **185**: p. 205-218.

69. Kadiyala, P., D. Li, F.M. Nunez, D. Altshuler, R. Doherty, R. Kuai, M. Yu, N. Kamran, M. Edwards, J.J. Moon, P.R. Lowenstein, M.G. Castro, and A. Schwendeman, *High-Density Lipoprotein-Mimicking Nanodiscs for Chemo-immunotherapy against Glioblastoma Multiforme.* ACS Nano, 2019. **13**(2): p. 1365-1384.

70. Hu, Q., H. Li, L. Wang, H. Gu, and C. Fan, *DNA Nanotechnology-Enabled Drug Delivery Systems.* Chem Rev, 2019. **119**(10): p. 6459-6506.

71. Li, J., H. Pei, B. Zhu, L. Liang, M. Wei, Y. He, N. Chen, D. Li, Q. Huang, and C. Fan, *Self-assembled multivalent DNA nanostructures for noninvasive intracellular delivery of immunostimulatory CpG oligonucleotides.* ACS Nano, 2011. **5**(11): p. 8783-9.

72. Zhang, L., G. Zhu, L. Mei, C. Wu, L. Qiu, C. Cui, Y. Liu, I.T. Teng, and W. Tan, *Self-Assembled DNA Immunonanoflowers as Multivalent CpG Nanoagents.* ACS Appl Mater Interfaces, 2015. **7**(43): p. 24069-74.

73. Liu, X., Y. Xu, T. Yu, C. Clifford, Y. Liu, H. Yan, and Y. Chang, *A DNA nanostructure platform for directed assembly of synthetic vaccines.* Nano Lett, 2012. **12**(8): p. 4254-9.

74. Wang, C., W. Sun, G. Wright, A.Z. Wang, and Z. Gu, *Inflammation-Triggered Cancer Immunotherapy by Programmed Delivery of CpG and Anti-PD1 Antibody.* Adv Mater, 2016. **28**(40): p. 8912-8920.

75. Cui, J., R. De Rose, J.P. Best, A.P. Johnston, S. Alcantara, K. Liang, G.K. Such, S.J. Kent, and F. Caruso, *Mechanically tunable, self-adjuvanting nanoengineered polypeptide particles.* Adv Mater, 2013. **25**(25): p. 3468-72.

76. Thery, C., L. Zitvogel, and S. Amigorena, *Exosomes: composition, biogenesis and function.* Nat Rev Immunol, 2002. **2**(8): p. 569-79.

77. Gao, L., L. Wang, T. Dai, K. Jin, Z. Zhang, S. Wang, F. Xie, P. Fang, B. Yang, H. Huang, H. van Dam, F. Zhou, and L. Zhang, *Tumor-derived exosomes antagonize innate antiviral immunity.* Nat Immunol, 2018. **19**(3): p. 233-245.

78. Morishita, M., Y. Takahashi, A. Matsumoto, M. Nishikawa, and Y. Takakura, *Exosome-based tumor antigens-adjuvant co-delivery utilizing genetically engineered tumor cell-derived exosomes with immunostimulatory CpG DNA.* Biomaterials, 2016. **111**: p. 55-65.

79. Ochyl, L.J., J.D. Bazzill, C. Park, Y. Xu, R. Kuai, and J.J. Moon, *PEGylated tumor cell membrane vesicles as a new vaccine platform for cancer immunotherapy*. Biomaterials, 2018. **182**: p. 157-166.

80. Cheung, A.S., S.T. Koshy, A.G. Stafford, M.M. Bastings, and D.J. Mooney, *Adjuvant-Loaded Subcellular Vesicles Derived From Disrupted Cancer Cells for Cancer Vaccination.* Small, 2016. **12**(17): p. 2321-33.

81. Wu, J., C. Ji, F. Cao, H. Lui, B. Xia, and L. Wang, *Bone marrow mesenchymal stem cells inhibit dendritic cells differentiation and maturation by microRNA-23b.* Biosci Rep, 2017. **37**(2).

82. Ochyl, L.J. and J.J. Moon, *Dendritic Cell Membrane Vesicles for Activation and Maintenance of Antigen-Specific T Cells.* Adv Healthc Mater, 2019. **8**(4): p. e1801091.

83. Wang, S., J. Gao, and Z. Wang, *Outer membrane vesicles for vaccination and targeted drug delivery.* Wiley Interdiscip Rev Nanomed Nanobiotechnol, 2019. **11**(2): p. e1523.

84. van der Pol, L., M. Stork, and P. van der Ley, *Outer membrane vesicles as platform vaccine technology.* Biotechnol J, 2015. **10**(11): p. 1689-706.

85. Tan, K., R. Li, X. Huang, and Q. Liu, *Outer Membrane Vesicles: Current Status and Future Direction of These Novel Vaccine Adjuvants.* Front Microbiol, 2018. **9**: p. 783.

86. Kim, O.Y., H.T. Park, N.T.H. Dinh, S.J. Choi, J. Lee, J.H. Kim, S.W. Lee, and Y.S. Gho, *Bacterial outer membrane vesicles suppress tumor by interferon-gamma-mediated antitumor response.* Nat Commun, 2017. **8**(1): p. 626.

87. Nastala, C.L., H.D. Edington, T.G. McKinney, H. Tahara, M.A. Nalesnik, M.J. Brunda, M.K. Gately, S.F. Wolf, R.D. Schreiber, W.J. Storkus, and et al., *Recombinant IL-12 administration induces tumor regression in association with IFN-gamma production.* J Immunol, 1994. **153**(4): p. 1697-706.

88. Lasek, W., R. Zagozdzon, and M. Jakobisiak, *Interleukin 12: still a promising candidate for tumor immunotherapy?* Cancer Immunol Immunother, 2014. **63**(5): p. 419-35.

89. Nagarajan, S. and P. Selvaraj, *Human tumor membrane vesicles modified to express glycolipid-anchored IL-12 by protein transfer induce T cell proliferation in vitro: a potential approach for local delivery of cytokines during vaccination.* Vaccine, 2006. **24**(13): p. 2264-74.

90. Patel, J.M., V.F. Vartabedian, E.N. Bozeman, B.E. Caoyonan, S. Srivatsan, C.D. Pack, P. Dey, M.J. D'Souza, L. Yang, and P. Selvaraj, *Plasma membrane vesicles decorated with glycolipid-anchored antigens and adjuvants via protein transfer as an antigen delivery platform for inhibition of tumor growth.* Biomaterials, 2016. **74**: p. 231-44.

91. Zhang, X., C. Wang, J. Wang, Q. Hu, B. Langworthy, Y. Ye, W. Sun, J. Lin, T. Wang, J. Fine, H. Cheng, G. Dotti, P. Huang, and Z. Gu, *PD-1 Blockade Cellular Vesicles for Cancer Immunotherapy.* Adv Mater, 2018. **30**(22): p. e1707112.

92. Zhang, X., J. Wang, Z. Chen, Q. Hu, C. Wang, J. Yan, G. Dotti, P. Huang, and Z. Gu, *Engineering PD-1-Presenting Platelets for Cancer Immunotherapy.* Nano Lett, 2018. **18**(9): p. 5716-5725.

93. Zhang, P., Y. Chen, Y. Zeng, C. Shen, R. Li, Z. Guo, S. Li, Q. Zheng, C. Chu, Z. Wang, Z. Zheng, R. Tian, S. Ge, X. Zhang, N.S. Xia, G. Liu, and X. Chen, *Virus-mimetic*

nanovesicles as a versatile antigen-delivery system. Proc Natl Acad Sci U S A, 2015. **112**(45): p. E6129-38.

94. Liu, X., L. Yuan, L. Zhang, Y. Mu, X. Li, C. Liu, P. Lv, Y. Zhang, T. Cheng, Q. Yuan, N. Xia, X. Chen, and G. Liu, *Bioinspired Artificial Nanodecoys for Hepatitis B Virus.* Angew Chem Int Ed Engl, 2018. **57**(38): p. 12499-12503.

95. Zhang, P., L. Zhang, Z. Qin, S. Hua, Z. Guo, C. Chu, H. Lin, Y. Zhang, W. Li, X. Zhang, X. Chen, and G. Liu, *Genetically Engineered Liposome-like Nanovesicles as Active Targeted Transport Platform.* Adv Mater, 2018. **30**(7).

96. Grandi, A., M. Tomasi, I. Zanella, L. Ganfini, E. Caproni, L. Fantappie, C. Irene, L. Frattini, S.J. Isaac, E. Konig, F. Zerbini, S. Tavarini, C. Sammicheli, F. Giusti, I. Ferlenghi, M. Parri, and G. Grandi, *Synergistic Protective Activity of Tumor-Specific Epitopes Engineered in Bacterial Outer Membrane Vesicles.* Front Oncol, 2017. **7**: p. 253.

97. Saeui, C.T., M.P. Mathew, L. Liu, E. Urias, and K.J. Yarema, *Cell Surface and Membrane Engineering: Emerging Technologies and Applications.* J Funct Biomater, 2015. **6**(2): p. 454-85.

98. Hu, C.M., L. Zhang, S. Aryal, C. Cheung, R.H. Fang, and L. Zhang, *Erythrocyte membrane-camouflaged polymeric nanoparticles as a biomimetic delivery platform.* Proc Natl Acad Sci U S A, 2011. **108**(27): p. 10980-5.

99. Cheng, H., X.Y. Jiang, R.R. Zheng, S.J. Zuo, L.P. Zhao, G.L. Fan, B.R. Xie, X.Y. Yu, S.Y. Li, and X.Z. Zhang, *A biomimetic cascade nanoreactor for tumor targeted starvation therapy-amplified chemotherapy.* Biomaterials, 2019. **195**: p. 75-85.

100. Buddingh, B.C. and J.C.M. van Hest, *Artificial Cells: Synthetic Compartments with Life-like Functionality and Adaptivity.* Acc Chem Res, 2017. **50**(4): p. 769-777.

101. Molinaro, R., C. Corbo, J.O. Martinez, F. Taraballi, M. Evangelopoulos, S. Minardi, I.K. Yazdi, P. Zhao, E. De Rosa, M.B. Sherman, A. De Vita, N.E. Toledano Furman, X. Wang, A. Parodi, and E. Tasciotti, *Biomimetic proteolipid vesicles for targeting inflamed tissues.* Nat Mater, 2016. **15**(9): p. 1037-46.

102. Parodi, A., N. Quattrocchi, A.L. van de Ven, C. Chiappini, M. Evangelopoulos, J.O. Martinez, B.S. Brown, S.Z. Khaled, I.K. Yazdi, M.V. Enzo, L. Isenhart, M. Ferrari, and E. Tasciotti, *Synthetic nanoparticles functionalized with biomimetic leukocyte membranes possess cell-like functions.* Nat Nanotechnol, 2013. **8**(1): p. 61-8.

103. Evangelopoulos, M., A. Parodi, J.O. Martinez, I.K. Yazdi, A. Cevenini, A.L. van de Ven, N. Quattrocchi, C. Boada, N. Taghipour, C. Corbo, B.S. Brown, S. Scaria, X. Liu, M. Ferrari, and E. Tasciotti, *Cell source determines the immunological impact of biomimetic nanoparticles.* Biomaterials, 2016. **82**: p. 168-77.

104. Zhang, Q., W. Wei, P. Wang, L. Zuo, F. Li, J. Xu, X. Xi, X. Gao, G. Ma, and H.Y. Xie, *Biomimetic Magnetosomes as Versatile Artificial Antigen-Presenting Cells to Potentiate T-Cell-Based Anticancer Therapy.* ACS Nano, 2017. **11**(11): p. 10724-10732.

105. Deng, G., Z. Sun, S. Li, X. Peng, W. Li, L. Zhou, Y. Ma, P. Gong, and L. Cai, *Cell-Membrane Immunotherapy Based on Natural Killer Cell Membrane Coated Nanoparticles for the Effective Inhibition of Primary and Abscopal Tumor Growth.* ACS Nano, 2018. **12**(12): p. 12096-12108.

106. Gao, W. and L. Zhang, *Engineering red-blood-cell-membrane-coated nanoparticles for broad biomedical applications.* AIChE J., 2015. **61**: p. 738-746.

107. Zhuang, J., M. Ying, K. Spiekermann, M. Holay, Y. Zhang, F. Chen, H. Gong, J.H. Lee, W. Gao, R.H. Fang, and L. Zhang, *Biomimetic Nanoemulsions for Oxygen Delivery In Vivo.* Adv Mater, 2018. **30**(49): p. e1804693.

108. Karsten, E., E. Breen, and B.R. Herbert, *Red blood cells are dynamic reservoirs of cytokines.* Sci Rep, 2018. **8**(1): p. 3101.

109. Nombela, I. and M.D.M. Ortega-Villaizan, *Nucleated red blood cells: Immune cell mediators of the antiviral response.* PLoS Pathog, 2018. **14**(4): p. e1006910.

110. Luk, B.T., Y. Jiang, J.A. Copp, C.J. Hu, N. Krishnan, W. Gao, S. Li, R.H. Fang, and L. Zhang, *Biomimetic Targeting of Nanoparticles to Immune Cell Subsets via Cognate Antigen Interactions.* Mol Pharm, 2018. **15**(9): p. 3723-3728.

111. Wei, X., M. Beltran-Gastelum, E. Karshalev, B. Esteban-Fernandez de Avila, J. Zhou, D. Ran, P. Angsantikul, R.H. Fang, J. Wang, and L. Zhang, *Biomimetic Micromotor Enables Active Delivery of Antigens for Oral Vaccination.* Nano Lett, 2019. **19**(3): p. 1914-1921.

112. Guo, Y., D. Wang, Q. Song, T. Wu, X. Zhuang, Y. Bao, M. Kong, Y. Qi, S. Tan, and Z. Zhang, *Erythrocyte Membrane-Enveloped Polymeric Nanoparticles as Nanovaccine for Induction of Antitumor Immunity against Melanoma.* ACS Nano, 2015. **9**(7): p. 6918-33.

113. Rao, L., L.L. Bu, B. Cai, J.H. Xu, A. Li, W.F. Zhang, Z.J. Sun, S.S. Guo, W. Liu, T.H. Wang, and X.Z. Zhao, *Cancer Cell Membrane-Coated Upconversion Nanoprobes for Highly Specific Tumor Imaging.* Adv Mater, 2016. **28**(18): p. 3460-6.

114. Chen, Z., P. Zhao, Z. Luo, M. Zheng, H. Tian, P. Gong, G. Gao, H. Pan, L. Liu, A. Ma, H. Cui, Y. Ma, and L. Cai, *Cancer Cell Membrane-Biomimetic Nanoparticles for Homologous-Targeting Dual-Modal Imaging and Photothermal Therapy.* ACS Nano, 2016. **10**(11): p. 10049-10057.

115. Yu, Z., P. Zhou, W. Pan, N. Li, and B. Tang, *A biomimetic nanoreactor for synergistic chemiexcited photodynamic therapy and starvation therapy against tumor metastasis.* Nat Commun, 2018. **9**(1): p. 5044.

116. Lv, P., X. Liu, X. Chen, C. Liu, Y. Zhang, C. Chu, J. Wang, X. Wang, X. Chen, and G. Liu, *Genetically Engineered Cell Membrane Nanovesicles for Oncolytic Adenovirus Delivery: A Versatile Platform for Cancer Virotherapy.* Nano Lett, 2019. **19**(5): p. 2993-3001.

117. Liu, W.L., M.Z. Zou, T. Liu, J.Y. Zeng, X. Li, W.Y. Yu, C.X. Li, J.J. Ye, W. Song, J. Feng, and X.Z. Zhang, *Expandable Immunotherapeutic Nanoplatforms Engineered from Cytomembranes of Hybrid Cells Derived from Cancer and Dendritic Cells.* Adv Mater, 2019. **31**(18): p. e1900499.

118. Kang, T., Y. Huang, Q. Zhu, H. Cheng, Y. Pei, J. Feng, M. Xu, G. Jiang, Q. Song, T. Jiang, H. Chen, X. Gao, and J. Chen, *Necroptotic cancer cells-mimicry nanovaccine boosts anti-tumor immunity with tailored immune-stimulatory modality.* Biomaterials, 2018. **164**: p. 80-97.

119. Fontana, F., M.A. Shahbazi, D. Liu, H. Zhang, E. Makila, J. Salonen, J.T. Hirvonen, and H.A. Santos, *Multistaged Nanovaccines Based on Porous Silicon@Acetalated Dextran@Cancer Cell Membrane for Cancer Immunotherapy.* Adv Mater, 2017. **29**(7).

120. Zalba, S. and T.L. Ten Hagen, *Cell membrane modulation as adjuvant in cancer therapy.* Cancer Treat Rev, 2017. **52**: p. 48-57.

121. Fang, R.H., C.M. Hu, B.T. Luk, W. Gao, J.A. Copp, Y. Tai, D.E. O'Connor, and L. Zhang, *Cancer cell membrane-coated nanoparticles for anticancer vaccination and drug delivery.* Nano Lett, 2014. **14**(4): p. 2181-8.

122. Kroll, A.V., R.H. Fang, Y. Jiang, J. Zhou, X. Wei, C.L. Yu, J. Gao, B.T. Luk, D. Dehaini, W. Gao, and L. Zhang, *Nanoparticulate Delivery of Cancer Cell Membrane Elicits Multiantigenic Antitumor Immunity.* Adv Mater, 2017. **29**(47).

123. Yang, R., J. Xu, L. Xu, X. Sun, Q. Chen, Y. Zhao, R. Peng, and Z. Liu, *Cancer Cell Membrane-Coated Adjuvant Nanoparticles with Mannose Modification for Effective Anticancer Vaccination.* ACS Nano, 2018. **12**(6): p. 5121-5129.

Chapter 2

Engineered Cell Membrane-Coated Nanoparticles for Lung Inflammation Targeted Delivery

2.1 Introduction

The chemical and physiological changes associated with inflammation are an important part of the innate immune system [1]. Proinflammatory processes can lead to the release of cytokines such as interleukin-6 (IL-6) and tumor necrosis factor, which are capable of effecting vascular changes to improve immune responses at a site of stress or injury [2]. These may include vasodilation and an increase in vascular permeability, which can promote more efficient immune cell recruitment [3, 4]. On the cellular level, proinflammatory cytokines cause the upregulation of specific surface markers, including vascular cell adhesion molecule-1 (VCAM-1) or intercellular adhesion molecule-1 (ICAM-1), which allow for immune cell adhesion at the site of inflammation [5, 6]. Although inflammation is an integral process that is required for survival, a dysregulated immune system is implicated in a wide range of disease states [7, 8]. The disease relevance of inflammation is further supported by the fact that inflammatory markers like cellular adhesion molecules are often implicated in pathogenesis [9, 10], and these have been explored as therapeutic and diagnostic targets.

Nanoparticle-based platforms, especially those functionalized with active targeting ligands, have the potential to serve as powerful tools for managing a wide range of diseases associated with inflammation [11]. Along these lines, the targeted delivery of anti-inflammatory agents to the vasculature of affected sites via cell adhesion molecules represents a promising strategy [12-14]. Employing inflammation as the cue, a diverse range of nanodelivery systems have been designed to target upregulated markers such as VCAM-1 and ICAM-1 [15-20], and this approach has been leveraged to treat disease conditions such as cancer and cardiovascular diseases [21-23]. More recently, cell membrane coating technology has garnered significant

attention in the field of nanomedicine [24, 25]. From erythrocytes to cancer cells, virtually any type of cell membrane can be coated onto the surface of nanoparticles, resulting in nanoformulations with enhanced functionality that can be custom-tailored to specific applications [26, 27]. In particular, cell membrane-coated nanoparticles have proven to be effective drug delivery systems due to their extended circulation times and disease-homing capabilities [26-28]. The targeting ability of these biomimetic nanoparticles is often mediated by specific proteins that are expressed on the source cells, and this bestows the nanoparticles with specific interactions with various disease substrates. For example, nanoparticles coated with the membrane derived from platelets were shown to specifically target bacteria as well as the exposed subendothelium in damaged vasculature [29]. A similar platform was shown to target the lungs in a murine model of cancer metastasis [30]. On top of the natural biointerfacing capabilities of cell membrane-coated nanoparticles, their traits can be further enhanced by introducing exogenous moieties onto the membrane surface. One way to achieve this is to tether targeting ligands via a lipid anchor, which can then be inserted into the cell membrane [31, 32]. Red blood cell membrane-coated nanoparticles, which exhibit prolonged blood circulation, have been functionalized in this manner to enhance their cancer targeting ability.

Instead of relying on post-fabrication methods to introduce additional functionality, cell membrane-coated nanoparticles can be developed using the membrane from genetically engineered source cells [33]. A wide range of tools are available to introduce or upregulate the expression of specific surface markers [34, 35], and this approach enables researchers to augment the functionality of cell membrane-based nanodelivery platforms based on application-specific needs [36, 37]. In this study, we genetically engineered cell membrane-coated nanoparticles to specifically target sites of inflammation (Figure 2.1). Inflamed endothelial cells

are known to upregulate the expression of VCAM-1 in order to recruit immune cells such as leukocytes that express its cognate ligand, very late antigen-4 (VLA-4) [38]. In order to exploit this interaction, we genetically modified a source cell line to stably express VLA-4 and harvested the engineered membrane to coat polymeric nanoparticle cores. A potent anti-inflammatory drug dexamethasone (DEX) was used as a model drug to be loaded for the treatment of inflammation. The ability of the final nanoformulation to target inflamed cells without compromising the activity of DEX was first tested *in vitro*. Then, therapeutic efficacy was evaluated *in vivo* using a murine model of endotoxin-induced lung inflammation.

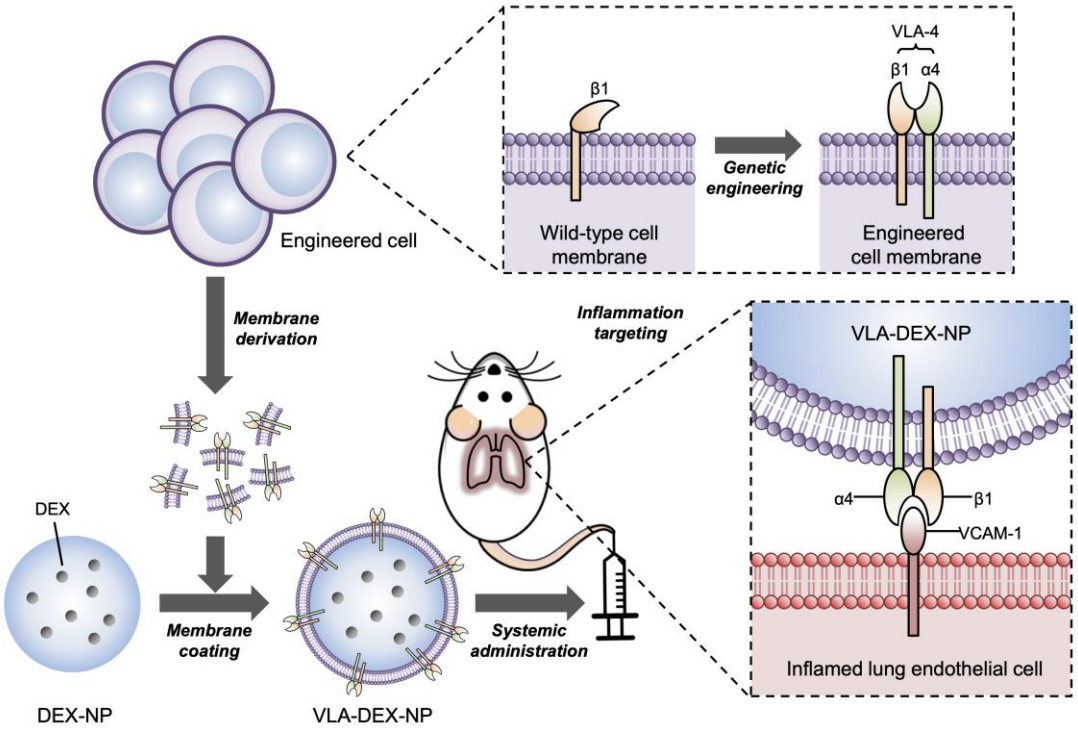

Figure 2.1: Schematic illustration of genetically engineered cell membrane-coated nanoparticles for targeted drug delivery to inflamed lungs. Wild-type cells were genetically engineered to express VLA-4, which is comprised of integrins α4 and β1. Then, the plasma membrane from the genetically engineered cells was collected and coated onto dexamethasone-loaded nanoparticle cores (DEX-NP). The resulting VLA-4-expressing cell membrane-coated DEX-NP (VLA-DEX-NP) can target VCAM-1 on inflamed lung endothelial cells for enhanced drug delivery.

2.2 Experimental Methods

2.2.1 Cell Culture

Wild-type C1498 mouse leukemia cells (TIB-49, American Type Culture Collection) were cultured at 37 ℃ in 5% CO_2 with Dulbecco's modified Eagle medium (w/ L-glutamine, 4.5 g/L glucose, and sodium pyruvate; DMEM; Corning) supplemented with 10% bovine growth serum (BGS; Hyclone) and 1% penicillin-streptomycin (Pen-Strep; Gibco). Engineered C1498-VCAM cells were cultured with DMEM supplemented with 10% USDA fetal bovine serum (FBS; Omega Scientific), 1% Pen-Strep, and 400 μg/mL hygromycin B (Invivogen). Engineered C1498-VLA cells were cultured with DMEM supplemented with 10% USDA FBS, 1% Pen-Strep, and 1 μg/mL puromycin (Invivogen). bEnd.3 mouse brain endothelial cells (CRL-2299, American Type Culture Collection) were cultured with DMEM supplemented with 10% BGS and 1% Pen-Strep. AmphoPhoenix cells (obtained from the National Gene Vector Biorepository) were cultured with DMEM supplemented with 10% BGS and 1% Pen-Strep. DC2.4 mouse dendritic cells (SCC142, Sigma-Aldrich) were cultured with DMEM supplemented with 10% BGS and 1% Pen-Strep.

2.2.2 Genetic Engineering

Engineered C1498-VLA and C1498-VCAM cells were created by transducing C1498-WT. Briefly, the genes for integrin α4 (MG50049-M, Sino Biological) and VCAM-1 (MG50163-

UT, Sino Biological) gene were cloned into pQCXIP and pQCXIH plasmids (Clontech), respectively, using an In-Fusion HD cloning kit (Clontech) following the manufacturer's protocol, yielding pQCXIP-α4 and pQCXIH-VCAM-1. AmphoPhoenix cells were plated onto 100-mm tissue culture dishes containing 10 mL of medium at 3×10^5 cells/mL and cultured overnight. The cells were transfected with pQCXIP-α4 or pQCXIH-VCAM-1 using Lipofectamine 2000 (Invitrogen) following the manufacturer's instructions. The supernatant of the transfected AmphoPhoenix was collected and used to resuspend C1498-WT cells, which were then centrifuged at 800 *g* for 90 min. After the spin, the transduced cells were incubated for 4 h before the media was changed with fresh media. Fluorescently labeled antibodies, including FITC anti-mouse CD49d (R1-2, Biolegend), Alexa647 anti-mouse/rat CD29 (HMβ1-1, Biolegend), or PE anti-mouse CD106 (STA, Biolegend), were used in order to assess the expression levels of VLA-4 or VCAM-1. Data were collected using a Becton Dickinson FACSCanto-II flow cytometer and analyzed using Flowjo software. All of the engineered cells were sorted using a Becton Dickinson FACSAria-II flow cytometer to select for cells expressing high levels of VLA-4 or VCAM-1.

2.2.3 Cell Membrane Derivation

The membranes from C1498-WT and engineered C1498-VLA cells were derived using a previously described method with some modifications [39]. First, the cells were harvested and washed in a starting buffer containing 30 mM Tris-HCl pH 7.0 (Quality Biological) with 0.0759 M sucrose (Sigma-Aldrich) and 0.225 M D-mannitol (Sigma-Aldrich). The washed cells were resuspended in an isolation buffer containing 0.5 mM ethylene glycol-bis(β-aminoethyl ether)-

N,N,N′,N′-tetraacetic acid (Sigma-Aldrich), a phosphatase inhibitor cocktail (Sigma-Aldrich), and a protease inhibitor cocktail (Sigma-Aldrich). Then, the cells were homogenized using a Kinematica Polytron PT 10/35 probe homogenizer at 70% power for 15 passes. The homogenate was first centrifuged at 10,000 *g* in a Beckman Coulter Optima XPN-80 ultracentrifuge for 25 min. The supernatant was then collected and centrifuged at 150,000 *g* for 35 min. The resulting pellet of cell membrane was washed and stored in a solution containing 0.2 mM ethylenediaminetetraacetic acid (USB Corporation) in UltraPure DNase free/RNase-free distilled water (Invitrogen). Total membrane protein content was quantified by a BCA protein assay kit (Pierce).

2.2.4 Synthesis of Membrane-Coated Nanoparticles

Polymeric cores were prepared by a single emulsion process using 0.66 dL/g carboxyl-terminated 50:50 poly(lactic-*co*-glycolic) acid (PLGA; LACTEL Absorbable Polymers). For DEX-loaded PLGA cores, 500 μL of 50 mg/mL PLGA in dichloromethane (DCM; Sigma-Aldrich) was mixed with 500 μL of 10 mg/mL DEX in acetone. This mixture was added to 5 mL of 10 mM Tris-HCl pH 8 and sonicated using a Fisher Scientific 150E Sonic Dismembrator at 70% power for 2 min. The sonicated mixture was added to 10 mL of 10 mM Tris-HCl pH 8 and was magnetically stirred at 700 rpm overnight. For 1,1′-dioctadecyl-3,3,3′,3′-tetramethylindodicarbocyanine (DiD, ex/em = 644/663 nm; Biotium) labeling, 500 μL of 50 mg/mL PLGA in DCM was mixed with 500 μL of 20 μg/mL DiD in DCM. This mixture was added to 5 mL of 10 mM Tris-HCl pH 8 and sonicated using a Fisher Scientific 150E Sonic Dismembrator at 70% power for 2 min. The sonicated mixture was added to 10 mL of 10 mM

Tris-HCl pH 8 and was magnetically stirred at 700 *g* for 3 h. Empty PLGA core preparation followed the same procedure, except substituting the DiD solution for 500 µL of neat DCM. In order to coat the polymeric cores with cell membranes, the nanoparticle cores were first centrifuged at 21,100 *g* for 8 min. The pellets were resuspended in solution containing membranes derived from C1498-WT or C1498-VLA. The mixture was sonicated in a 1.5 mL disposable sizing cuvette (Brandtech) using a Fisher Scientific FS30D bath sonicator at a frequency of 42 kHz and a power of 100 W for 3 min. For the *in vitro* studies, UltraPure water and sucrose were added to adjust the polymer concentration to 1 mg/mL and the sucrose concentration to 10%. For the *in vivo* studies, UltraPure water and sucrose were added to adjust the polymer concentration to 10 mg/mL and the sucrose concentration to 10%.

2.2.5 Nanoparticle Characterization

The size and surface zeta potential of WT-NP and VLA-NP were measured by dynamic light scattering using a Malvern ZEN 3600 Zetasizer. For electron microscopy visualization, a VLA-NP sample was negatively stained with 1 wt % uranyl acetate (Electron Microscopy Sciences) on a carbon-coated 400-mesh copper grid (Electron Microscopy Sciences) and visualized using a JEOL 1200 EX II transmission electron microscope. The presence of VLA-4 on WT-NP and VLA-NP was determined using western blotting. First, the samples were adjusted to 1 mg/mL protein content, followed by the addition of NuPAGE 4× lithium dodecyl sulfate sample loading buffer (Novex) and heating at 70 ℃ for 10 min. Then, 25 µL was loaded into the wells of 12-well Bolt 4–12% Bis-Tris gels (Invitrogen) and ran at 165 V for 45 min in MOPS running buffer (Novex). The proteins were transferred for 60 min at a voltage of 10 V

onto 0.45 µm nitrocellulose membranes (Pierce) in Bolt transfer buffer (Novex). Nonspecific interactions were blocked using 5% milk (Genesee Scientific) in phosphate buffered saline (PBS; Thermo Fisher Scientific) with 0.05% Tween 20 (National Scientific). The blots were probed using anti-integrin α4 antibody (B-2; Santa Cruz Biotechnology) or anti-integrin β1 antibody (E-11; Santa Cruz Biotechnology). The secondary staining was done using the corresponding horseradish peroxidase-conjugated antibodies (Biolegend). Membranes with stained samples were developed in a dark room using ECL western blotting substrate (Pierce) and an ImageWorks Mini-Medical/90 Developer. Long-term stability of WT-NP and VLA-NP in 10% sucrose solution was tested by storing the particles at 4 ℃ for 2 months with weekly size measurements.

2.2.6 Binding Studies

The expression level of VCAM-1 on C1498-WT, C1498-VCAM, untreated bEnd.3 cells, and bEnd.3 cells treated overnight with 1 µg/mL of lipopolysaccharide from *E. coli* K12 (LPS; Invivogen) was evaluated as described above. For the first binding study, 5×10^4 cells, either C1498-WT or C1498-VCAM, were collected and resuspended in 160 µL of DMEM containing 0.5% USDA FBS, 1% bovine serum albumin (BSA; Sigma-Aldrich), and 1 mM $MnCl_2$ (Sigma-Aldrich). For blocking, anti-mouse CD106 antibody was added to the cells, followed by incubation at 4 ℃ for 30 min. Then, 40 µL of 1 mg/mL DiD-labeled WT-NP or VLA-NP was added, and the mixture was incubated at 4 ℃ for another 30 min. After washing the cells twice with PBS, the fluorescent signals from the cells were detected using flow cytometry. For the second study, 5×10^4 bEnd.3 cells were plated and then either left untreated or pretreated with

LPS overnight. The media was then removed and replaced with 160 µL of DMEM containing 0.5% USDA FBS, 0.8% BSA, and 1 mM $MnCl_2$. For blocking, anti-mouse CD106 antibody was added to the cells, followed by incubation at 4 °C for 30 min. Then, 40 µL of 1 mg/mL DiD-labeled WT-NP or VLA-NP was added, and the mixture was incubated at 4 ℃ for another 30 min. After washing the cells twice with PBS, the cells were detached by scraping, and the fluorescent signals from the cells were detected using flow cytometry. All data were collected using a Becton Dickinson FACSCanto-II flow cytometer and analyzed using Flowjo software.

2.2.7 Drug Loading and Release

Drug loading and encapsulation efficiency were measured using by high performance liquid chromatography (HPLC) on an Agilent 1220 Infinity II gradient liquid chromatography system equipped with a C18 analytical column (Brownlee). VLA-DEX-NP samples were dissolved overnight in 80% acetonitrile (ACN; EMD Millipore) and then centrifuged at 21,100 *g* for 8 min to collect the supernatant for analysis. The solutions were run through the column at a flow rate of 0.3 mL/min and DEX was detected at a wavelength of 242 nm. The DEX release profile was obtained by loading 200 µL of 1 mg/mL VLA-DEX-NP into Slide-A-Lyzer MINI dialysis devices (10K MWCO; Thermo Fisher Scientific) and floating them on 1 L of PBS stirred at 150 rpm. At each time point, dialysis cups were retrieved, and the content was centrifuged at 21,100 *g* for 8 min. The pellet was dissolved in 80% ACN overnight and processed as described above for HPLC analysis.

2.2.8 *In Vitro* Activity of DEX

The biological activity of DEX was evaluated *in vitro* using a test system involving the LPS treatment of DC2.4 dendritic cells. To validate the system, DC2.4 cells were first plated onto a 24-well tissue culture plate at 5×10^4 cells per well and cultured overnight with or without LPS at a concentration of 1 μg/mL. Then, supernatant was collected and the concentration of IL-6 was measured using a mouse IL-6 ELISA kit (Biolegend) according to manufacturer's protocol. To compare free DEX and VLA-DEX-NP, the two formulations were first added to the culture medium at final drug concentrations of 0.01, 0.1, and 1 μM, followed by 2 h incubation. For free DEX, 1000× stock solutions were prepared at 0.01, 0.1, and 1 mM in dimethyl sulfoxide. Then, the cells were treated with LPS overnight before measuring the concentration of IL-6 in the supernatant. To test the effect of empty nanoparticles, either PLGA cores or VLA-NP at a final concentration of 1 μg/mL were first incubated with the cells for 2 h, followed by an overnight incubation either with or without LPS before measuring IL-6 levels.

2.2.9 *In Vivo* Inflammation Targeting and Biodistribution

All animal experiments were performed in accordance with NIH guidelines and approved by the Institutional Animal Care and Use Committee (IACUC) of the University of California San Diego. In order to induce lung inflammation in mice, 30 μL of 400 μg/mL LPS in PBS was injected intratracheally into male BALB/c mice (Charles River Laboratories). At 1 h after LPS injection, 100 μL of 10 mg/mL DiD-labeled WT-NP or VLA-NP was administered intravenously. After 6 h, the heart, lungs, liver, spleen, kidneys, and blood were collected. All solid tissues were washed with PBS and suspended in 1 mL of PBS before being homogenized with Biospec Mini-

Beadbeater-16. The homogenates and blood were then diluted 4× with PBS, added to a 96-well plate, and fluorescence was measured using a BioTek Synergy Mx microplate reader. For each sample, the background signal measured from the corresponding organ or blood of control mice that did not receive any treatment was subtracted.

2.2.10 *In Vivo* Safety

Male BALB/c mice were intravenously injected with 100 µL of free DEX or VLA-DEX-NP, each at a drug concentration of 200 µg/mL, daily for the first 7 days. Then, for the next 2 days, the dosage was doubled by injecting 200 µL of each formulation at the same drug concentration. At 24 h after the last injection, blood was collected by submandibular puncture and collected into tubes containing sodium heparin (Sigma-Aldrich). Plasma samples were obtained by taking the supernatant of the blood after centrifuging at 800 *g* for 10 min. Creatinine levels were measured using a creatinine colorimetric assay kit (Cayman Chemical Company) according to manufacturer's protocol.

2.2.11 Inflammation Treatment Studies

To treat lung inflammation, male BALB/c mice were first intratracheally challenged with 30 µL of 400 µg/mL LPS in PBS. At 1 h after the challenge, 100 µL of free DEX, WT-DEX-NP, and VLA-DEX-NP, each at a drug concentration of 200 µg/mL, was injected intravenously. After 6 h, the lungs were collected and homogenized as described above. The homogenates were centrifuged at 10,000 *g*, and the supernatants were filtered through 0.22-µm PVDF syringe filters

(CellTreat). The concentration of IL-6 was measured using a mouse IL-6 ELISA kit according to manufacturer's protocol. For histology analysis, the lungs were collected after 6 h and fixed in 10% phosphate-buffered formalin (Fisher Chemical) for 24 h. The fixed lungs were sectioned, followed by staining with hematoxylin and eosin (Sakura Finetek) staining. Histology slides were prepared by the Moores Cancer Center Tissue Technology Shared Resource (Cancer Center Support Grant P30CA23100). Images were obtained using a Hamamatsu NanoZoomer 2.0-HT Slide Scanner and analyzed using the NanoZoomer Digital Pathology software.

2.3 Results and Discussion

VLA-4 is a heterodimer that is formed by the association of integrin α4 with integrin β1 [40]. In order to generate a cell line constitutively displaying the full complex, we elected to modify wild-type C1498 cells (C1498-WT), which were confirmed to express high levels of integrin β1 but lack integrin α4 (Figure 2.2A). Following viral transduction of C1498-WT to introduce the integrin α4 gene, a significant subpopulation of the resulting engineered cells (referred to as C1498-VLA) were found to express both VLA-4 components (Figure 2.2B). After successfully establishing C1498-VLA, the cells were harvested and their membrane was derived by a process involving cell lysis and differential centrifugation. The cell membrane was then coated onto poly(lactic-*co*-glycolic acid) (PLGA) nanoparticle cores that were prepared by a single emulsion method. Membrane-coated nanoparticles prepared with the membrane from C1498-WT and C1498-VLA (referred to as WT-NP and VLA-NP, respectively) both had an average diameter of approximately 175 nm, which was slightly larger than the uncoated PLGA cores (Figure 2.2C). In terms of zeta potential, the membrane-coated nanoparticles exhibited a

surface charge of approximately -20 mV, which was less negative than the PLGA cores (Figure 2.2D). Both the size and zeta potential data suggested proper membrane coating, which was further verified for VLA-NP by transmission electron microscopy, which clearly showed a membrane layer surrounding the core (Figure 2.2E). Western blotting analysis was used to probe for the two components of VLA-4 on the nanoformulations (Figure 2.2F). As expected, both integrins α4 and β1 were found on VLA-NP, whereas only integrin β1 was present on WT-NP. In order to evaluate long-term stability of the membrane-coated nanoparticles, they were suspended in 10% sucrose solution at 4 ℃ and their size was monitored over the course of 8 weeks (Figure 2.2G). Neither nanoparticle sample exhibited a significant increase in size during this period.

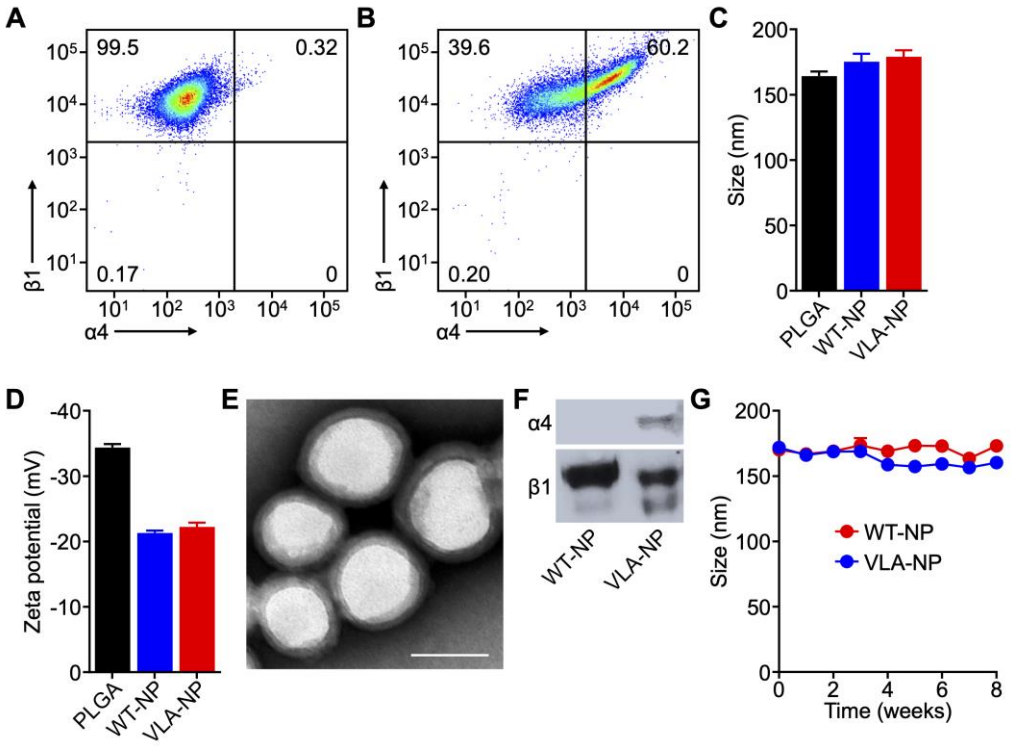

Figure 2.2: Development and characterization of inflammation-targeting nanoparticles. (**A** and **B**) Expression of integrins α4 and β1 on C1498-WT (A) and C1498-VLA (B) cells was confirmed by flow cytometry. (**C** and **D**) The average diameter (C) and surface zeta potential (D) of PLGA cores, WT-NP, and VLA-NP were confirmed by dynamic light scattering (n = 3, mean + SD). (**E**) Representative transmission electron microscopy image of VLA-NP (scale bar = 100 nm). (**F**) Western blots for integrins α4 and β1 on WT-NP and VLA-NP. (**G**) Size of WT-NP and VLA-NP when stored in solution over a period of 8 weeks (n = 3, mean ± SD).

The binding of VLA-NP was assessed in two different *in vitro* experiments. First, C1498-WT transduced to constitutively express high amounts of VCAM-1 (referred to as C1498-VCAM) was used as a model target cell. The expression of VCAM-1 on C1498-VCAM was confirmed via flow cytometry (Figure 2.3A). Whereas the C1498-WT cells did not show any expression, the C1498-VCAM cells yielded a signal that was over an order of magnitude higher than the isotype control. To evaluate binding, fluorescent dye-labeled WT-NP or VLA-NP were incubated with either C1498-WT or C1498-VCAM (Figure 2.3, B and C). For each pairing, the incubation was performed either with or without anti-VCAM-1 to block the specific interaction

between VLA-4 and VCAM-1. For the samples with blocking, cells were first incubated with the antibody for 30 min prior to nanoparticle treatment. After incubating the cells with the nanoparticles for 30 min, cells were washed twice and were analyzed by flow cytometry. The data revealed that there was significant nanoparticle binding only when VLA-NP were paired with C1498-VCAM. The level of binding was reduced back to baseline levels in the presence of anti-VCAM-1, thus confirming the specificity of the interaction. In contrast, there was no evidence of specific binding when VLA-NP were paired with C1498-WT, which does not express the cognate receptor for VLA-4. The same held true for the WT-NP paired with either cell type, where antibody blocking had no impact on the relative nanoparticle binding.

Next, we elected to study the nanoparticle binding to endothelial cells, which represent a more biologically relevant target compared to the artificially engineered C1498-VCAM cells. For this purpose, we employed a murine brain endothelial cell line, bEnd.3, whose VCAM-1 expression can be upregulated in the presence of proinflammatory signals [41]. To induce an inflamed state, bEnd.3 cells were treated with bacterial lipopolysaccharide (LPS), and the level of VCAM-1 expression was evaluated using flow cytometry (Figure 2.3D). Whereas expression of VCAM-1 was near baseline levels for the untreated bEnd.3 cells, those that were treated with LPS exhibited a distinct population with elevated VCAM-1. As we observed in the previous experiment with C1498-VCAM cells, enhanced nanoparticle binding was only observed when VLA-NP were paired with inflamed bEnd.3 cells, and antibody blocking reduced the levels back to baseline (Fig 3, E and F). When incubated with non-inflamed bEnd.3 cells, there was no evidence of specific binding interactions, and the same held true for the control WT-NP paired with bEnd.3 cells regardless of their inflammatory status. The data in these two studies

confirmed the successful engineering of membrane-coated nanoparticles with the ability to target inflammation based on the interactions between VLA-4 and VCAM-1.

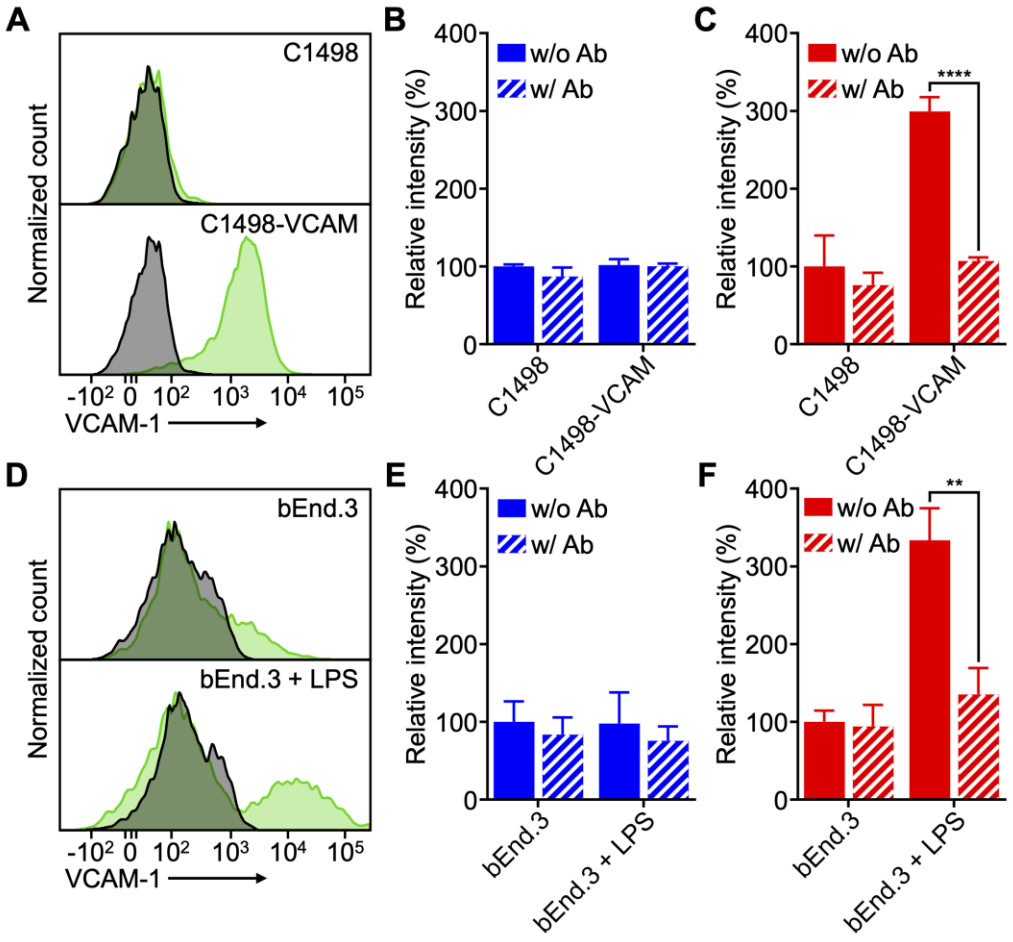

Figure 2.3: *In vitro* binding. (**A**) Expression of VCAM-1 on C1498-WT and C1498-VCAM cells (gray: isotype antibody, green: anti-VCAM-1). (**B** and **C**) Binding of WT-NP (B) or VLA-NP (C) to C1498-WT or C1498-VCAM cells; blocking was performed by preincubating cells with anti-VCAM-1 (n = 3, mean + SD). ****$p < 0.0001$, Student's *t*-test. (**D**) Expression of VCAM-1 on untreated or LPS-treated bEnd.3 cells (gray: isotype antibody, green: anti-VCAM-1). (**E** and **F**) Binding of WT-NP (E) or VLA-NP (F) to untreated or LPS-treated bEnd.3 cells; blocking was performed by preincubating cells with anti-VCAM-1 (n = 3, mean + SD). **$p < 0.01$, Student's *t*-test.

As a model anti-inflammatory payload, we selected DEX, which was loaded into the PLGA core by a single emulsion method prior to coating with either C1498-WT or C1498-VLA membrane to yield DEX-loaded WT-NP or VLA-NP (referred to as WT-DEX-NP or VLA-DEX-

NP, respectively). When the drug content was measured by high-performance liquid chromatography, it was determined that the encapsulation efficiency and drug loading yield were approximately 11 wt% and 2 wt%, respectively (Figure 2.4A). To evaluate drug release, VLA-DEX-NP was dialyzed against a large volume of phosphate-buffered saline, and the amount of drug retained within the nanoparticles was quantified over time (Figure 2.4B). The results revealed an initial burst of DEX, where approximately 80% of the drug payload was released in the first hour, followed by a sustained release. The release profile was in agreement with previous reports on DEX-loaded PLGA formulations [42, 43], and the data showed a good fit with the Peppas-Sahlin model with a regression coefficient of 0.978 [44]. In order to evaluate the biological activity of the DEX loaded within the nanoparticles, we employed an *in vitro* assay based on the LPS treatment of DC2.4 dendritic cells, which causes an elevation in the levels of proinflammatory cytokines such as IL-6 (Figure 2.4C). DC2.4 cells were first treated with either free DEX or VLA-DEX-NP for 2 h, followed by incubation with LPS overnight. The supernatant was then collected to measure the concentration of IL-6 by an enzyme-linked immunosorbent assay (ELISA). It was shown that both free DEX and VLA-DEX-NP were able to attenuate IL-6 secretion in a drug concentration-dependent manner (Figure 2.4D). Although free DEX more efficiently lowered IL-6 levels at drug concentrations of 0.01 μM and 0.1 μM, the level of inflammation was reduced to levels near baseline for both free DEX and VLA-DEX-NP at 1 μM of DEX. The data indicated that the activity of the drug payload was retained after being loaded inside of VLA-NP. It was confirmed that neither PLGA cores nor VLA-NP without DEX loading had an impact on the level of IL-6 production by the DC2.4 cells (Figure 2.4E).

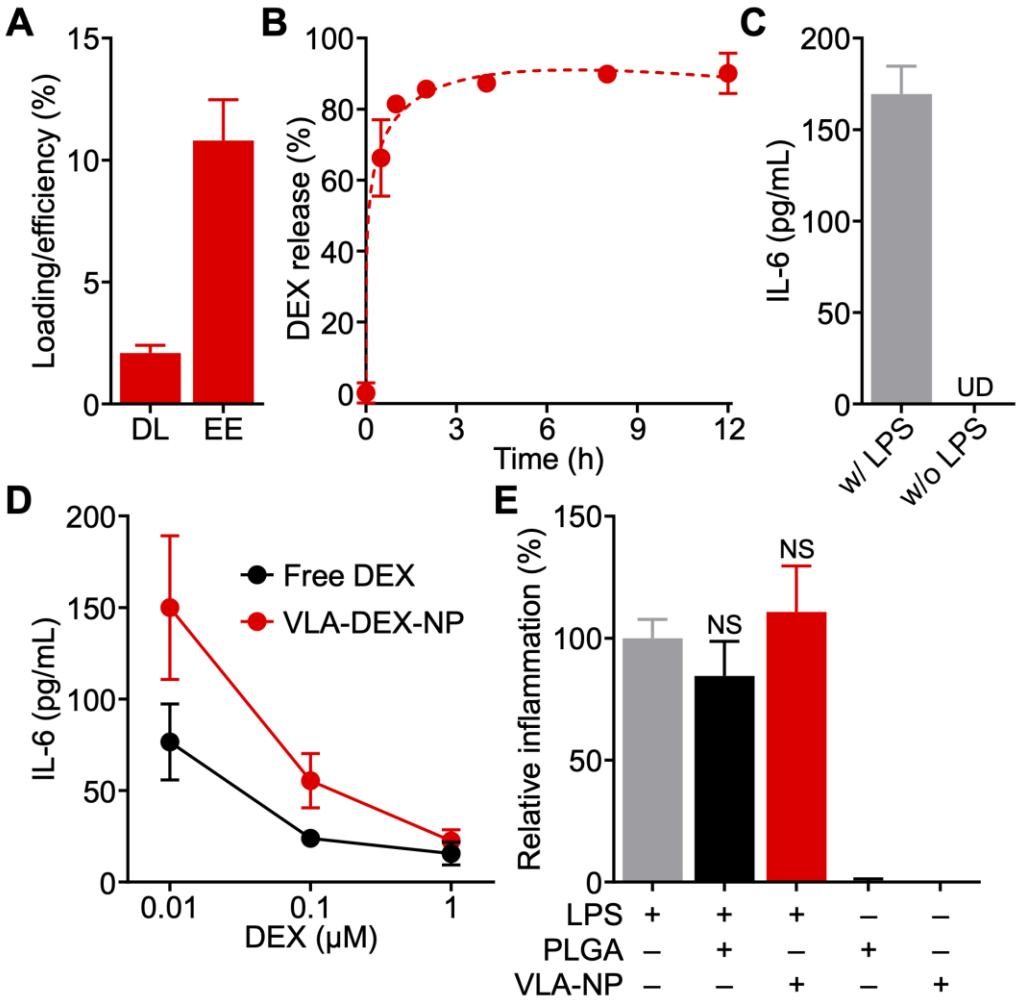

Figure 2.4: Drug loading and *in vitro* activity. (**A**) Drug loading (DL) and encapsulation efficiency (EE) of dexamethasone (DEX) into VLA-NP (n = 3, mean + SD). (**B**) Drug release profile of VLA-DEX-NP (n = 3, mean ± SD). The data was fitted using the Peppas-Sahlin equation. (**C**) Secretion of IL-6 by LPS-treated DC2.4 cells (n = 3, mean ± SD). UD = undetectable. (**D**) Secretion of IL-6 by LPS-treated DC2.4 cells preincubated with DEX in free form or loaded into VLA-NP (n = 3, mean ± SD). (**E**) Relative inflammatory response, as measured by IL-6 secretion, of DC2.4 cells treated with LPS only, LPS and PLGA nanoparticles, LPS and VLA-NP, PLGA nanoparticles only, or VLA-NP only; all of the nanoparticles were empty without DEX loading (n = 3, mean + SD). NS = not significant (compared to the LPS only group), one-way ANOVA.

After confirming the biological activity of the VLA-DEX-NP formulation *in vitro*, we next sought to evaluate the formulation *in vivo* using a murine model of lung inflammation. The model was established by intratracheal injection of LPS directly into the lungs of BALB/c mice. In order to evaluate targeting ability, fluorescently labeled WT-NP or VLA-NP were injected

intravenously immediately after the induction of lung inflammation. After 6 h, major organs, including the heart, lungs, liver, spleen, kidneys, skin, and blood, were collected to assess nanoparticle biodistribution (Figure 2.5A). The majority of the nanoparticles accumulated in the liver and spleen. Notably, a significant increase in accumulation of VLA-NP was observed in the lungs compared to WT-NP. This *in vivo* targeting result was in agreement with the *in vitro* findings where VLA-NP were able to specifically bind to inflamed cells. The safety of the formulation was assessed by monitoring the plasma levels of creatinine, a marker of kidney toxicity that has previously been studied in the context of DEX nanodelivery [45]. After 9 days of repeated daily administrations of free DEX or VLA-DEX-NP into healthy mice, it was shown that the creatinine concentration in mice receiving VLA-DEX-NP remained consistent with baseline levels, whereas it was significantly elevated in mice administered with free DEX (Figure 2.5B).

The therapeutic efficacy of VLA-DEX-NP was then evaluated following the same experimental design as the targeting study above. After 6 h, the lungs were collected and homogenized, and the homogenate was then clarified by centrifugation and filtered through a 0.22-µm porous membrane before measuring the concentration of IL-6 by ELISA. As shown in Fig. 5C, the VLA-DEX-NP formulation was able to completely abrogate lung inflammation, while both free DEX and WT-DEX-NP did not have any discernable effect. The fact that WT-DEX-NP was not able to significantly reduce lung IL-6 levels suggested that systemic exposure to DEX was not a major contributor to the efficacy observed with VLA-DEX-NP. The efficacy of the formulation against lung inflammation was further confirmed by analyzing lung sections stained with hematoxylin and eosin (Figure 2.5D). Leukocyte recruitment and peribronchial thickening, which are hallmarks of lung inflammation [46, 47], were prominent in the lungs of

mice receiving no treatment, free DEX, or WT-DEX-NP. In contrast, minimal leukocyte recruitment and no peribronchial thickening were observed for the group treated with VLA-DEX-NP, and there were no other signs of toxicity present in these lung sections. Overall, the results from the *in vivo* studies confirmed the benefit of targeted delivery to inflamed lungs using VLA-NP as a drug nanocarrier.

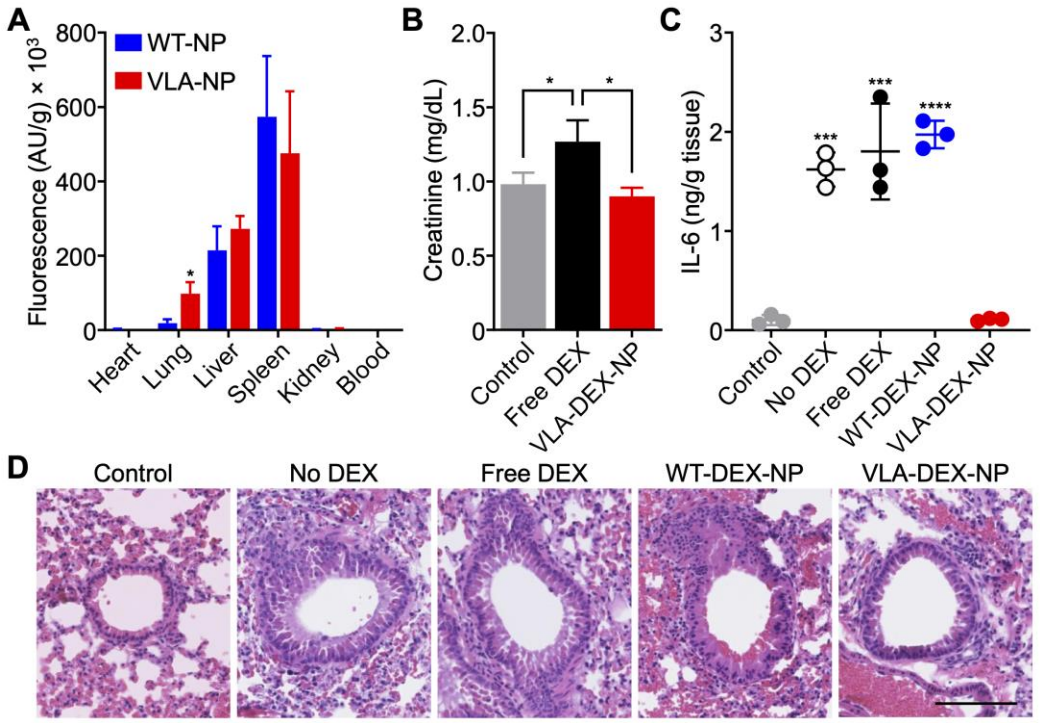

Figure 2.5: *In vivo* targeting, safety, and therapeutic efficacy. (**A**) Biodistribution of WT-NP or VLA-NP in a lung inflammation model 6 h after intravenous administration (n = 3, mean + SD). *p < 0.05, Student's *t*-test. (**B**) Creatinine levels in the plasma of mice after repeated daily administrations for 9 days with free DEX or VLA-DEX-NP (n = 3, mean + SD). *p < 0.05, one-way ANOVA. (**C**) IL-6 levels in the lung tissue of mice intratracheally challenged with LPS and then treated intravenously with vehicle solution, free DEX, WT-DEX-NP, or VLA-DEX-NP (n = 3, mean ± SD). ***p < 0.001, ****p < 0.0001 (compared to VLA-DEX-NP), one-way ANOVA. (**D**) Representative hematoxylin and eosin-stained lung histology sections of mice intratracheally challenged with LPS and then treated intravenously with vehicle solution, free DEX, WT-DEX-NP, or VLA-DEX-NP (scale bar = 100 μm).

2.4 Conclusions

In conclusion, we have engineered cell membrane-coated nanoparticles that can be used to specifically target and treat localized lung inflammation via systemic administration. A host cell positive for integrin β1 was modified to express integrin α4. Together, the two protein markers formed VLA-4, which specifically interacts with VCAM-1, a common marker for inflammation found on vascular endothelia. Nanoparticles fabricated using the membrane from these genetically engineered cells were able to leverage this natural affinity to target inflamed sites, including in a murine model of LPS-induced lung inflammation. When the nanoparticles were loaded with DEX, an anti-inflammatory drug, significant therapeutic efficacy was achieved both *in vitro* and *in vivo*. Future studies will comprehensively evaluate the safety profile of the VLA-DEX-NP formulation, obtain additional lung-specific efficacy readouts, elucidate the optimal time window for treatment, and assess clinical relevance using additional animal models of severe inflammatory disease. As pathological inflammation is heavily implicated in a number of important disease conditions [7, 48], the reported biomimetic platform could be leveraged to improve the *in vivo* activity of various therapeutic payloads through enhanced targeting. Notably, VCAM-1 upregulation has been observed in renal pathologies as well as in inflamed cerebral vasculature [49, 50]. Additionally, DEX has been shown to be effective at managing the inflammation associated with COVID-19 [51], and a targeted formulation capable of localizing the drug to the lungs may help to further boost its therapeutic profile. In this work, we specifically engineered the nanoparticles to display VLA-4, which is a complex, multicomponent membrane-bound ligand that would otherwise be infeasible to incorporate using traditional synthetic strategies. This highlights the advantages of employing genetic engineering techniques to expand the wide-ranging utility of cell membrane coating technology. In particular, the generalized application of this approach would enable researchers to streamline the development

of new targeted nanoformulations by utilizing target–ligand interactions that occur in nature. Combined with the biocompatibility and biointerfacing characteristics that are inherent to cell membrane coatings, the work presented here could initiate a new wave of biomimetic nanomedicine with finely crafted functionalities.

Chapter 2, in full, is a reprint of the material as it appears in *Science Advances*, 2021, Joon Ho Park, Yao Jiang, Jiarong Zhou, Hua Gong, Animesh Mohapatra, Jiyoung Heo, Weiwei Gao, Ronnie H. Fang and Liangfang Zhang. The dissertation author was a primary author of this paper.

2.5 References

1. Netea, M.G., F. Balkwill, M. Chonchol, F. Cominelli, M.Y. Donath, E.J. Giamarellos-Bourboulis, D. Golenbock, M.S. Gresnigt, M.T. Heneka, H.M. Hoffman, R. Hotchkiss, L.A.B. Joosten, D.L. Kastner, M. Korte, E. Latz, P. Libby, T. Mandrup-Poulsen, A. Mantovani, K.H.G. Mills, K.L. Nowak, L.A. O'Neill, P. Pickkers, T. van der Poll, P.M. Ridker, J. Schalkwijk, D.A. Schwartz, B. Siegmund, C.J. Steer, H. Tilg, J.W.M. van der Meer, F.L. van de Veerdonk, and C.A. Dinarello, *A guiding map for inflammation.* Nat. Immunol., 2017. **18**(8): p. 826-831.

2. Perlstein, R.S., M.H. Whitnall, J.S. Abrams, E.H. Mougey, and R. Neta, *Synergistic roles of interleukin-6, interleukin-1, and tumor necrosis factor in the adrenocorticotropin response to bacterial lipopolysaccharide in vivo.* Endocrinology, 1993. **132**(3): p. 946-952.

3. Naldini, A. and F. Carraro, *Role of inflammatory mediators in angiogenesis.* Curr. Drug Targets Inflamm. Allergy, 2005. **4**(1): p. 3-8.

4. Huang, A.L. and J.A. Vita, *Effects of systemic inflammation on endothelium-dependent vasodilation.* Trends Cardiovasc. Med., 2006. **16**(1): p. 15-20.

5. Meager, A., *Cytokine regulation of cellular adhesion molecule expression in inflammation.* Cytokine Growth Factor Rev., 1999. **10**(1): p. 27-39.

6. Kelly, M., J.M. Hwang, and P. Kubes, *Modulating leukocyte recruitment in inflammation.* J. Allergy Clin. Immunol., 2007. **120**(1): p. 3-10.

7. Kotas, M.E. and R. Medzhitov, *Homeostasis, inflammation, and disease susceptibility.* Cell, 2015. **160**(5): p. 816-827.

8. Pawelec, G., D. Goldeck, and E. Derhovanessian, *Inflammation, ageing and chronic disease.* Curr. Opin. Immunol., 2014. **29**: p. 23-28.

9. Cybulsky, M.I., K. Iiyama, H. Li, S. Zhu, M. Chen, M. Iiyama, V. Davis, J.C. Gutierrez-Ramos, P.W. Connelly, and D.S. Milstone, *A major role for VCAM-1, but not ICAM-1, in early atherosclerosis.* J. Clin. Invest., 2001. **107**(10): p. 1255-1262.

10. Chen, Q. and J. Massague, *Molecular pathways: VCAM-1 as a potential therapeutic target in metastasis.* Clin. Cancer Res., 2012. **18**(20): p. 5520-5525.

11. Jin, K., Z. Luo, B. Zhang, and Z. Pang, *Biomimetic nanoparticles for inflammation targeting.* Acta. Pharm. Sin. B, 2018. **8**(1): p. 23-33.

12. Howard, M.D., E.D. Hood, B. Zern, V.V. Shuvaev, T. Grosser, and V.R. Muzykantov, *Nanocarriers for vascular delivery of anti-inflammatory agents.* Annu. Rev. Pharmacol. Toxicol., 2014. **54**: p. 205-226.

13. Shuvaev, V.V., M.A. Ilies, E. Simone, S. Zaitsev, Y. Kim, S. Cai, A. Mahmud, T. Dziubla, S. Muro, D.E. Discher, and V.R. Muzykantov, *Endothelial targeting of antibody-decorated polymeric filomicelles.* ACS Nano, 2011. **5**(9): p. 6991-6999.

14. Garnacho, C., S.M. Albelda, V.R. Muzykantov, and S. Muro, *Differential intra-endothelial delivery of polymer nanocarriers targeted to distinct PECAM-1 epitopes.* J. Control. Release, 2008. **130**(3): p. 226-233.

15. Visweswaran, G.R., S. Gholizadeh, M.H. Ruiters, G. Molema, R.J. Kok, and J.A. Kamps, *Targeting rapamycin to podocytes using a vascular cell adhesion molecule-1 (VCAM-1)-harnessed SAINT-based lipid carrier system.* PLoS One, 2015. **10**(9): p. e0138870.

16. Li, R., P.S. Kowalski, H.W.M. Morselt, I. Schepel, R.M. Jongman, A. Aslan, M.H.J. Ruiters, J.G. Zijlstra, G. Molema, M. van Meurs, and J. Kamps, *Endothelium-targeted delivery of dexamethasone by anti-VCAM-1 SAINT-O-Somes in mouse endotoxemia.* PLoS One, 2018. **13**(5): p. e0196976.

17. Leus, N.G., H.W. Morselt, P.J. Zwiers, P.S. Kowalski, M.H. Ruiters, G. Molema, and J.A. Kamps, *VCAM-1 specific PEGylated SAINT-based lipoplexes deliver siRNA to activated endothelium in vivo but do not attenuate target gene expression.* Int. J. Pharm., 2014. **469**(1): p. 121-131.

18. Calderon, A.J., T. Bhowmick, J. Leferovich, B. Burman, B. Pichette, V. Muzykantov, D.M. Eckmann, and S. Muro, *Optimizing endothelial targeting by modulating the antibody density and particle concentration of anti-ICAM coated carriers.* J. Control. Release, 2011. **150**(1): p. 37-44.

19. Muro, S., C. Gajewski, M. Koval, and V.R. Muzykantov, *ICAM-1 recycling in endothelial cells: A novel pathway for sustained intracellular delivery and prolonged effects of drugs.* Blood, 2005. **105**(2): p. 650-658.

20. Muro, S., X. Cui, C. Gajewski, J.C. Murciano, V.R. Muzykantov, and M. Koval, *Slow intracellular trafficking of catalase nanoparticles targeted to ICAM-1 protects endothelial cells from oxidative stress.* Am. J. Physiol. Cell Physiol., 2003. **285**(5): p. C1339-C1347.

21. Mlinar, L.B., E.J. Chung, E.A. Wonder, and M. Tirrell, *Active targeting of early and mid-stage atherosclerotic plaques using self-assembled peptide amphiphile micelles.* Biomaterials, 2014. **35**(30): p. 8678-8686.

22. Rouleau, L., R. Berti, V.W. Ng, C. Matteau-Pelletier, T. Lam, P. Saboural, A.K. Kakkar, F. Lesage, E. Rheaume, and J.C. Tardif, *VCAM-1-targeting gold nanoshell probe for photoacoustic imaging of atherosclerotic plaque in mice.* Contrast Media Mol. Imaging, 2013. **8**(1): p. 27-39.

23. Pan, H., J.W. Myerson, L. Hu, J.N. Marsh, K. Hou, M.J. Scott, J.S. Allen, G. Hu, S. San Roman, G.M. Lanza, R.D. Schreiber, P.H. Schlesinger, and S.A. Wickline, *Programmable nanoparticle functionalization for in vivo targeting.* FASEB J., 2013. **27**(1): p. 255-264.

24. Fang, R.H., Y. Jiang, J.C. Fang, and L. Zhang, *Cell membrane-derived nanomaterials for biomedical applications.* Biomaterials, 2017. **128**: p. 69-83.

25. Fang, R.H., A.V. Kroll, W. Gao, and L. Zhang, *Cell membrane coating nanotechnology.* Adv. Mater., 2018. **30**(23): p. 1706759.

26. Fang, R.H., C.M. Hu, B.T. Luk, W. Gao, J.A. Copp, Y. Tai, D.E. O'Connor, and L. Zhang, *Cancer cell membrane-coated nanoparticles for anticancer vaccination and drug delivery.* Nano Lett., 2014. **14**(4): p. 2181-2188.

27. Hu, C.M., L. Zhang, S. Aryal, C. Cheung, R.H. Fang, and L. Zhang, *Erythrocyte membrane-camouflaged polymeric nanoparticles as a biomimetic delivery platform.* Proc. Natl. Acad. Sci. U.S.A., 2011. **108**(27): p. 10980-10985.

28. Dehaini, D., R.H. Fang, and L. Zhang, *Biomimetic strategies for targeted nanoparticle delivery.* Bioeng. Transl. Med., 2016. **1**(1): p. 30-46.

29. Hu, C.M., R.H. Fang, K.C. Wang, B.T. Luk, S. Thamphiwatana, D. Dehaini, P. Nguyen, P. Angsantikul, C.H. Wen, A.V. Kroll, C. Carpenter, M. Ramesh, V. Qu, S.H. Patel, J. Zhu, W. Shi, F.M. Hofman, T.C. Chen, W. Gao, K. Zhang, S. Chien, and L. Zhang, *Nanoparticle biointerfacing by platelet membrane cloaking.* Nature, 2015. **526**(7571): p. 118-121.

30. Li, J., Y. Ai, L. Wang, P. Bu, C.C. Sharkey, Q. Wu, B. Wun, S. Roy, X. Shen, and M.R. King, *Targeted drug delivery to circulating tumor cells via platelet membrane-functionalized particles.* Biomaterials, 2016. **76**: p. 52-65.

31. Fang, R.H., C.M. Hu, K.N. Chen, B.T. Luk, C.W. Carpenter, W. Gao, S. Li, D.E. Zhang, W. Lu, and L. Zhang, *Lipid-insertion enables targeting functionalization of erythrocyte membrane-cloaked nanoparticles.* Nanoscale, 2013. **5**(19): p. 8884-8888.

32. Wei, X., C. Zhan, Q. Shen, W. Fu, C. Xie, J. Gao, C. Peng, P. Zheng, and W. Lu, *A D-peptide ligand of nicotine acetylcholine receptors for brain-targeted drug delivery.* Angew. Chem. Int. Ed. Engl., 2015. **54**(10): p. 3023-3027.

33. Jiang, Y., N. Krishnan, J. Zhou, S. Chekuri, X. Wei, A.V. Kroll, C.L. Yu, Y. Duan, W. Gao, R.H. Fang, and L. Zhang, *Engineered cell-membrane-coated nanoparticles directly present tumor antigens to promote anticancer immunity.* Adv. Mater., 2020. **32**(30): p. 2001808.

34. Smith, H.O., D.B. Danner, and R.A. Deich, *Genetic transformation.* Annu. Rev. Biochem., 1981. **50**: p. 41-68.

35. Knott, G.J. and J.A. Doudna, *CRISPR-Cas guides the future of genetic engineering.* Science, 2018. **361**(6405): p. 866-869.

36. Lv, P., X. Liu, X. Chen, C. Liu, Y. Zhang, C. Chu, J. Wang, X. Wang, X. Chen, and G. Liu, *Genetically engineered cell membrane nanovesicles for oncolytic adenovirus delivery: A versatile platform for cancer virotherapy.* Nano Lett., 2019. **19**(5): p. 2993-3001.

37. Shi, X., Q. Cheng, T. Hou, M. Han, G. Smbatyan, J.E. Lang, A.L. Epstein, H.J. Lenz, and Y. Zhang, *Genetically engineered cell-derived nanoparticles for targeted breast cancer immunotherapy.* Mol. Ther., 2020. **28**(2): p. 536-547.

38. Nourshargh, S. and R. Alon, *Leukocyte migration into inflamed tissues.* Immunity, 2014. **41**(5): p. 694-707.

39. Kroll, A.V., R.H. Fang, Y. Jiang, J. Zhou, X. Wei, C.L. Yu, J. Gao, B.T. Luk, D. Dehaini, W. Gao, and L. Zhang, *Nanoparticulate delivery of cancer cell membrane elicits multiantigenic antitumor immunity.* Adv. Mater., 2017. **29**(47): p. 1703969.

40. Hemler, M.E., C. Huang, Y. Takada, L. Schwarz, J.L. Strominger, and M.L. Clabby, *Characterization of the cell surface heterodimer VLA-4 and related peptides.* J. Biol. Chem., 1987. **262**(24): p. 11478-11485.

41. Boggemeyer, E., T. Stehle, U.E. Schaible, M. Hahne, D. Vestweber, and M.M. Simon, *Borrelia burgdorferi upregulates the adhesion molecules E-selectin, P-selectin, ICAM-1 and VCAM-1 on mouse endothelioma cells in vitro.* Cell Adhes. Commun., 1994. **2**(2): p. 145-157.

42. Kim, D.H. and D.C. Martin, *Sustained release of dexamethasone from hydrophilic matrices using PLGA nanoparticles for neural drug delivery.* Biomaterials, 2006. **27**(15): p. 3031-3037.

43. Gomez-Gaete, C., N. Tsapis, M. Besnard, A. Bochot, and E. Fattal, *Encapsulation of dexamethasone into biodegradable polymeric nanoparticles.* Int. J. Pharm., 2007. **331**(2): p. 153-159.

44. Peppas, N.A. and J.J. Sahlin, *A simple equation for the description of solute release. III. Coupling of diffusion and relaxation.* Int. J. Pharm., 1989. **57**(2): p. 169-172.

45. Lorscheider, M., N. Tsapis, M. Ur-Rehman, F. Gaudin, I. Stolfa, S. Abreu, S. Mura, P. Chaminade, M. Espeli, and E. Fattal, *Dexamethasone palmitate nanoparticles: An efficient treatment for rheumatoid arthritis.* J. Control. Release, 2019. **296**: p. 179-189.

46. Ghosh, S., S.A. Hoselton, S.V. Asbach, B.N. Steffan, S.B. Wanjara, G.P. Dorsam, and J.M. Schuh, *B lymphocytes regulate airway granulocytic inflammation and cytokine production in a murine model of fungal allergic asthma.* Cell. Mol. Immunol., 2015. **12**(2): p. 202-212.

47. Ren, Y., X. Su, L. Kong, M. Li, X. Zhao, N. Yu, and J. Kang, *Therapeutic effects of histone deacetylase inhibitors in a murine asthma model.* Inflamm. Res., 2016. **65**(12): p. 995-1008.

48. Coussens, L.M. and Z. Werb, *Inflammation and cancer.* Nature, 2002. **420**(6917): p. 860-867.

49. Marcos-Contreras, O.A., C.F. Greineder, R.Y. Kiseleva, H. Parhiz, L.R. Walsh, V. Zuluaga-Ramirez, J.W. Myerson, E.D. Hood, C.H. Villa, I. Tombacz, N. Pardi, A. Seliga, B.L. Mui, Y.K. Tam, P.M. Glassman, V.V. Shuvaev, J. Nong, J.S. Brenner, M. Khoshnejad, T. Madden, D. Weissmann, Y. Persidsky, and V.R. Muzykantov, *Selective targeting of nanomedicine to inflamed cerebral vasculature to enhance the blood-brain barrier.* Proc. Natl. Acad. Sci. U.S.A., 2020. **117**(7): p. 3405-3414.

50. Kowalski, P.S., P.J. Zwiers, H.W. Morselt, J.M. Kuldo, N.G. Leus, M.H. Ruiters, G. Molema, and J.A. Kamps, *Anti-VCAM-1 SAINT-O-Somes enable endothelial-specific delivery of siRNA and downregulation of inflammatory genes in activated endothelium in vivo.* J. Control. Release, 2014. **176**: p. 64-75.

51. Group, R.C., P. Horby, W.S. Lim, J.R. Emberson, M. Mafham, J.L. Bell, L. Linsell, N. Staplin, C. Brightling, A. Ustianowski, E. Elmahi, B. Prudon, C. Green, T. Felton, D. Chadwick, K. Rege, C. Fegan, L.C. Chappell, S.N. Faust, T. Jaki, K. Jeffery, A. Montgomery, K. Rowan, E. Juszczak, J.K. Baillie, R. Haynes, and M.J. Landray, *Dexamethasone in hospitalized patients with Covid-19.* N. Engl. J. Med., 2021. **384**(8): p. 693-704.

Chapter 3

Engineered Cell Membrane-Coated Nanoparticles for Cytosolic Delivery of mRNA

3.1 Introduction

Achieving the proper subcellular localization of drug payloads is essential for maximizing their therapeutic potential. In the case of nanotherapeutics, delivery to the cytosol, which houses cellular machinery that is the target for a wide range of therapeutics [1-3]. has long presented a major challenge [4, 5]. Notably, nanodelivery vehicles must overcome the barrier posed by the endolysosomal pathway, which cells oftentimes use to sequester and degrade foreign objects [6, 7]. Endosomes transition from weakly acidic early endosomes to more acidic late endosomes, ultimately fusing with lysosomes, where nanoparticles can be destroyed by acids and enzymes [6, 8, 9]. One method to escape from this pathway is by the proton sponge approach, whereby nanoparticles are fabricated with buffering capabilities that enable them to rupture endosomes by osmotic swelling [10-12]. An alternate method is to destabilize the cell's exterior plasma membrane during endocytosis and prior to endosome formation, thus creating leaky endosomes [13, 14]. The endosomal pathway can also be avoided altogether by using nanoparticles whose shape and charge allow them to transport directly across the plasma membrane and into the cytosol [15, 16]. Unfortunately, many of these conventional strategies for cytosolic delivery are known to cause cytotoxicity [17, 18], making them difficult for clinical translation.

Most viruses require the delivery of their genetic material into the cytosol in order to replicate [19]. As such, many viruses have evolved methods that enable them to escape the endosomal compartment to avoid destruction [20]. In the case of the influenza virus, the hemagglutinin (HA) protein present on its surface helps to serve this purpose [21, 22]. After being expressed, HA is converted to its mature form through proteolytic cleavage, resulting in

the generation of two subunits [23]. The HA1 subunit allows the virus to attach to the plasma membrane of target cells in order to initiate endocytosis [24, 25]. After endocytic uptake, the HA2 subunit undergoes a conformational change triggered by lowered pH that facilitates the fusion of the viral envelope with endosomal membrane [26-28]. For the influenza A virus, different HA subtypes bind to different sialic acid receptors, which can significantly impact infectivity towards different host species [29, 30]. For example, the H1 subtype is found on strains such as H1N1, which is known to infect humans and was the cause of the 2009 flu pandemic [31]. Influenza A virus carrying the H5 or H7 subtype, commonly known as the bird flu, is known to mostly infect avian hosts, although some human infections have been reported [29].

Cell membrane coating is an emerging top-down approach for bestowing nanocarriers with enhanced biointerfacing capabilities [32, 33]. For example, erythrocyte membranes have been used to prolong nanoparticle circulation time [34], whereas cancer cell membranes [35] and platelet membranes [36] have been leveraged for targeted drug delivery. More recently, genetic engineering approaches have been employed to generate cell membrane enriched with a specific surface marker, thus enabling researchers to purposefully manipulate the functionality of cell membrane-coated nanoformulations [37, 38]. These engineered nanoparticles can be equipped with complex surface proteins that would otherwise be infeasible to incorporate using conventional synthetic approaches. In this work, we engineered a cell membrane-coated nanoparticle to display HA, thus enabling the resulting nanocarrier to exhibit virus-mimicking endosomal escape properties and enhanced cytosolic delivery (Figure 3.1). Given the recent interest in mRNA-based vaccines [39], we elected to evaluate the ability of our nanoformulation to deliver model mRNA payloads both *in vitro* and *in vivo*. Overall, the reported approach

represents a compelling strategy for further improving the utility of cell membrane-coated nanocarriers, particularly for the delivery drugs that require cytosolic localization.

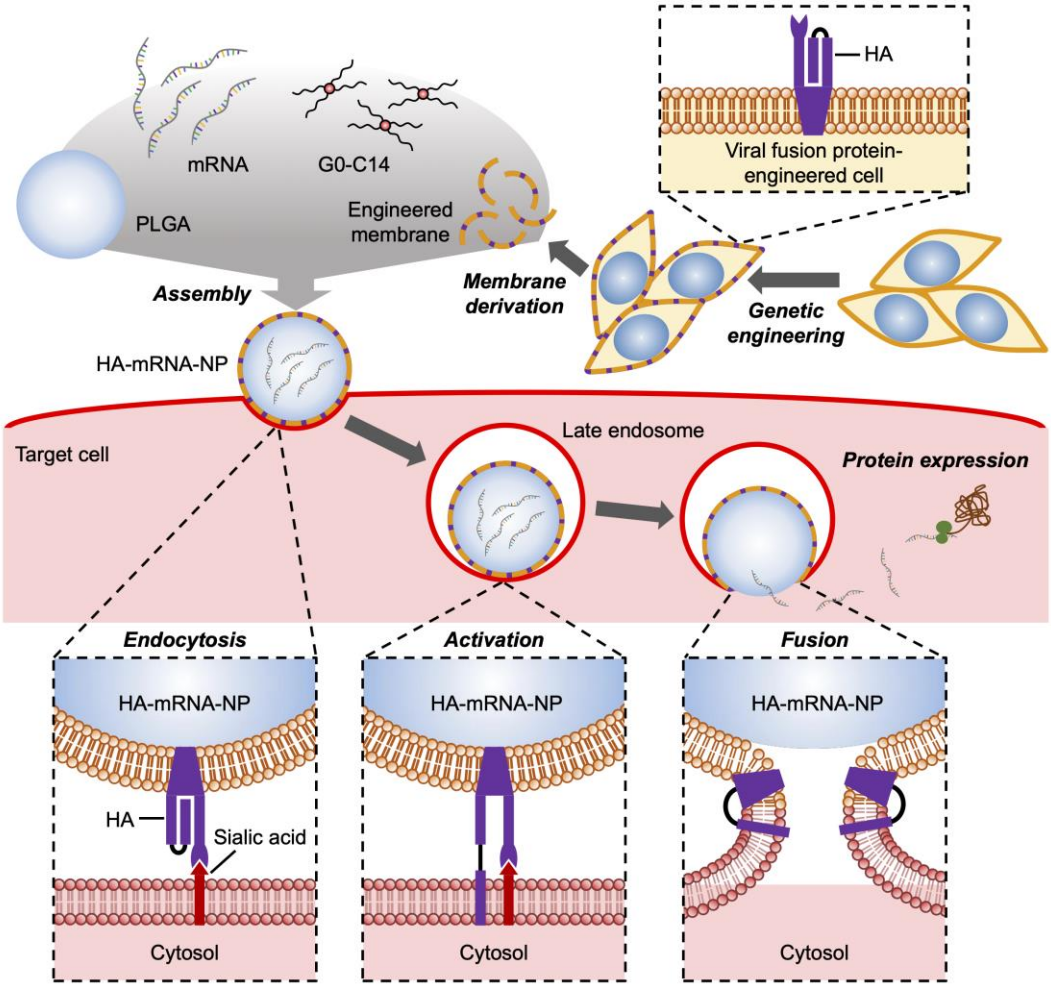

Figure 3.1: Schematic illustration of genetically engineered cell membrane-coated nanoparticles for the cytosolic delivery of mRNA. Cells are genetically engineered to express the influenza virus fusion protein hemagglutinin (HA). Then, the membrane from the engineered cells is isolated and coated onto poly(lactic-*co*-glycolic acid) (PLGA) nanoparticle cores that are loaded with mRNA with the help of the cationic lipid-like molecule G0-C14. After the final HA-mRNA-NP formulation is endocytosed by a target cell, the lowered pH in the late endosomes causes a conformation change in HA. The activated HA then triggers membrane fusion, enabling escape of the mRNA payload into the cytosol, where it can be translated into a protein product.

3.2 Experimental Methods

3.2.1 Cell Culture

B16-WT mouse melanoma cells (CRL-6475, American Type Culture Collection) were cultured using Dulbecco's modified Eagle medium with L-glutamine, 4.5 g/L glucose, and sodium pyruvate (DMEM; Corning) supplemented with 10% bovine growth serum (Hyclone) and 1% penicillin-streptomycin (Pen-Strep; Gibco) at 37 ℃ in 5% CO_2. Engineered B16-HA cells were cultured using DMEM supplemented with 10% USDA fetal bovine serum (Omega Scientific), 1% Pen-Strep, and 300 μg/mL hygromycin B (Invivogen) at 37 °C in 5% CO_2.

3.2.2 Genetic Engineering

Engineered B16-HA cells were generated by transfecting B16-WT with pNAHA plasmid (a gift from John Olsen; 44169, Addgene) encoding influenza A virus HA subtype H7 protein using Lipofectamine 2000 (Invitrogen) following the manufacturer's instructions. FITC-conjugated polyclonal rabbit anti-influenza A virus H7 (LS-C490688, LS Bio) was used to assess the expression level of HA. A Becton Dickinson FACSCanto-II flow cytometer was used for data collection and Flowjo software was used for analysis. A Becton Dickinson FACSAria-II flow cytometer was used to sort the engineered B16-HA cells to select for those expressing high levels of HA.

3.2.3 Cell-Cell Fusion Study

To assess the membrane fusion activity of HA expressed on the membrane of the engineered B16-HA cells, two separate cell–cell fusion studies were performed. In the first study, 6×10^5 cells, either B16-WT or B16-HA, were collected and divided into two equal groups each containing 3×10^5 cells. Each group was stained using either CellTrace Violet (Invitrogen) or CellTrace Far Red (Invitrogen) following the manufacturer's protocol. The stained cells were plated onto a 6-well tissue culture plate and incubated at 37 ℃ overnight. Then, the cells were detached, counted, and combined in a 12-well tissue culture plate such that each well contained a mixture of 1×10^5 cells stained with CellTrace Violet and 1×10^5 cells stained with CellTrace Far Red. The cell mixtures were incubated at 37 ℃ overnight, and the supernatant was removed from each well before incubating with 5 μg/mL TPCK-treated trypsin (Worthington Biochemical) in 500 μL of serum-free DMEM at 37 ℃ for 15 min. Then, the supernatant was removed from each well, 200 μL of phosphate buffered saline (PBS; Gibco) adjusted to pH 5.4 using citric acid (Sigma-Aldrich) was added, and the cells were incubated at 37 ℃ for another 15 min. The supernatant was removed from each well, 1 mL of DMEM containing 10% USDA FBS and 1% Pen-Strep was added, and the cells were incubated at 37 ℃ for 2 h. Finally, the cells were detached and analyzed using a Becton Dickinson FACSCanto-II flow cytometer. In the second study, B16-WT or B16-HA cells were plated onto a tissue culture-treated glass bottom dish (CellTreat) at 3×10^5 cells and incubated at 37 ℃ overnight. The supernatant was removed from each well and the cells were incubated with 5 μg/mL TPCK-treated trypsin in 1 mL of serum-free DMEM at 37 ℃ for 15 min. The supernatant was removed from each well, 1 mL of PBS adjusted to pH 5.4 using citric acid was added, and the cells were incubated at 37 ℃ for another 15 min. The supernatant was removed from each well, 3 mL of DMEM containing 10% USDA FBS and 1% Pen-Strep was added, and the cells were incubated at 37 ℃ for 2 h. Finally, the

cells were washed with PBS before being stained with Hoechst 33342 (Invitrogen), and imaging was done using a Keyence BZ-X710 fluorescence microscope.

3.2.4 Nanoparticle Synthesis

Cationic lipid-like molecule G0-C14 was synthesized as previously described [40, 41]. Briefly, poly(amidoamine) dendrimer G0 (Sigma-Aldrich) was mixed with 1,2-epoxytetradecane (TCI America) at a molar ratio of 1:7. The mixture was stirred at 1,100 rpm at 90 ℃ for 2 days to form G0-C14. All mRNAs were synthesized by *in vitro* transcription (IVT) except for Cy5-labeled EGFP mRNA (R1009, ApexBio). For IVT, pcDNA3-EGFP (a gift from Doug Golenbock; 13031, Addgene) and pCMV-CLuc2 (N0247, New England BioLabs) were used to generate the mRNA transcripts for EGFP and CLuc, respectively, using a HiScribe T7 ARCA mRNA kit (New England BioLabs) according to the manufacturer's protocol. Polymeric cores loaded with mRNA were synthesized by a double emulsion method using 0.66 dL/g carboxyl-terminated 50:50 PLGA (LACTEL Absorbable Polymers). A volume of 50 μL of 50 mg/mL PLGA in dichloromethane (DCM; Sigma-Aldrich) was initially mixed with 50 μg of G0-C14. Then, 5 μL of 1 mg/mL mRNA, 3 μL of UltraPure DNase/RNase-free distilled water (Invitrogen), and 2 μL of 1 M Tris-HCl pH 8 (Mediatech) were added to the solution. The resulting mixture was sonicated with a Fisher Scientific 150E Sonic Dismembrator at 70% power pulsed (2 s on/1 s off) for 1 min. After forming the first emulsion, a solution containing 500 μL of 10 mM Tris-HCl pH 8 and 10 μL of DCM was added, followed by sonication at the same settings for 2 min. Finally, the emulsion was added to 1 mL of 10 mM Tris-HCl pH 8 and magnetically stirred at 700 rpm for 2 h. Polymeric cores loaded with DiO dye (ex/em = 484/501

nm; Biotium) were synthesized by a single emulsion method. First, 500 μL of 50 mg/mL PLGA in DCM was mixed with 500 μL of 20 μg/mL DiO in DCM. This mixture was added to 5 mL of 10 mM Tris-HCl pH 8 and sonicated using a Fisher Scientific 150E Sonic Dismembrator at 70% power for 2 min. The sonicated mixture was added to 10 mL of 10 mM Tris-HCl pH 8 and magnetically stirred at 700 rpm overnight. To make cell membrane-coated nanoparticles, the polymeric cores were first centrifuged at 21,100 g for 8 min. The pellets were resuspended in solution containing either B16-WT or B16-HA membrane derived according to a previously reported procedure [42]. Note that B16-HA cells were incubated with 5 μg/mL TPCK-treated trypsin at 37 ℃ for 15 min prior to membrane derivation. The mixture of nanoparticle cores and cell membrane was sonicated using a Fisher Scientific FS30D bath sonicator at a frequency of 42 kHz and a power of 100 W for 2 min. Finally, the nanoparticles were suspended in 10% sucrose (Sigma-Aldrich) at a polymer concentration of 10 mg/mL.

3.2.5 Nanoparticle Characterization

Unless otherwise stated, all characterization was done using nanoparticles loaded with CLuc mRNA. Size and surface zeta potential were measured by dynamic light scattering using a Malvern ZEN 3600 Zetasizer. For electron microscopy visualization, an HA-mRNA-NP sample was negatively stained with 1 wt% uranyl acetate (Electron Microscopy Sciences) on a carbon-coated 400-mesh copper grid (Electron Microscopy Sciences) and visualized using a JEOL 1200 EX II transmission electron microscope. The presence of HA on B16-WT membrane, B16-HA membrane, WT-mRNA-NP, and HA-mRNA-NP was probed by western blotting. First, the samples were adjusted to 1 mg/mL protein content, followed by the addition of NuPAGE 4×

lithium dodecyl sulfate sample loading buffer (Novex) and heating at 70 ℃ for 10 min. Then, 25 µL of each sample was loaded into a 12-well Bolt 4–12% Bis-Tris gel (Invitrogen) and run at 165 V for 45 min in MOPS running buffer (Novex). The proteins were transferred for 60 min at a voltage of 10 V onto a 0.45-µm nitrocellulose membrane (Pierce) in Bolt transfer buffer (Novex). Nonspecific interactions were blocked using 5% milk (Genesee Scientific) in PBS with 0.05% Tween 20 (National Scientific). The blots were probed using polyclonal rabbit anti-influenza A virus H7 antibody, and secondary staining was done using the appropriate horseradish peroxidase-conjugated antibody (Biolegend). Membranes with stained samples were developed in a dark room using ECL western blotting substrate (Pierce) and an ImageWorks Mini-Medical/90 Developer. Long-term stability of WT-mRNA-NP and HA-mRNA-NP in 10% sucrose solution was tested by storing the particles at 4 ℃ for 2 months with weekly size measurements. To quantify loading and encapsulation efficiency, HA-mRNA-NP was loaded with Cy5-labeled EGFP mRNA. After synthesis, the nanoparticles were centrifuged at 21,100 *g* for 8 min, and the pellets were dissolved in dimethyl sulfoxide (Fisher Scientific). Fluorescence was measured using a BioTek Synergy Mx microplate reader.

3.2.6 *In Vitro* Endosomal Escape Study

In order to visualize the endosomal escape of the engineered membrane-coated nanoparticles, 2×10^4 B16-WT cells were first plated onto a tissue culture-treated glass bottom dish and incubated at 37 ℃ overnight. Then, either WT-DiO-NP or HA-DiO-NP was added to the cultures at a final concentration of 50 µg/mL, followed by incubation at 37 °C for 1, 4, 8, or 24 h. To prepare for visualization, the cells were washed with PBS and then stained with Hoechst

33342 and LysoTracker Red DND-99 (Invitrogen). Imaging was performed on a Keyence BZ-X710 fluorescence microscope.

3.2.7 *In Vitro* Transfection Studies

In the first study, the ability of the engineered membrane-coated nanoparticles to deliver EGFP mRNA for protein translation was evaluated by transfecting B16-WT. In this case, CLuc mRNA was used as a control. First, B16-WT cells were plated onto a 12-well tissue culture plate at 5×10^4 cells per well and incubated overnight. Then, naked control or EGFP mRNA, control or EGFP mRNA-loaded WT-mRNA-NP, and control or EGFP mRNA-loaded HA-mRNA-NP were added to the cells at an mRNA concentration of 1 μg/mL. The cells were allowed to incubate at 37 ℃ for 48 h before being washed with PBS, and analysis was performed using a Becton Dickinson FACSCanto-II flow cytometer. In the second study, the ability of the engineered membrane-coated nanoparticles to deliver CLuc mRNA for protein translation was evaluated using the same approach as above. In this case, EGFP mRNA was used as the control, and a *Cypridina* luciferase glow assay kit (Pierce) was used to analyze the supernatant according to the manufacturer's instructions.

3.2.8 *In Vivo* Transfection Studies

All animal experiments were performed in accordance with National Institutes of Health guidelines and approved by the Institutional Animal Care and Use Committee of the University of California San Diego. For both *in vivo* studies, CLuc mRNA was used as the payload. In order

to evaluate the ability of the engineered membrane-coated nanoparticles to locally deliver mRNA *in vivo*, male CD-1 mice (Charles River Laboratories) were anesthetized using isoflurane and intranasally administered with 100 μL of either WT-mRNA-NP or HA-mRNA-NP given in 50 μL doses with 5 min of rest in between. After 24 h, mice were intraperitoneally injected with 100 μL of 2 mg/mL *Cypridina* luciferin (NanoLight Technology) in PBS. Then, the mice were anesthetized by isoflurane and imaged using a Xenogen IVIS 200 animal imaging system. In order to evaluate the ability of the engineered membrane-coated nanoparticles to systemically deliver mRNA *in vivo*, male CD-1 mice were intravenously administered with 150 μL of either WT-mRNA-NP or HA-mRNA-NP. At 12 and 24 h after the injection, blood was collected via submandibular bleeding and allowed to clot at room temperature. The serum was separated by centrifuging the blood at 3,000 *g* for 10 min. A 0 h baseline sample was collected in the same manner prior to nanoparticle administration. A *Cypridina* luciferase glow assay kit was used to analyze the serum according to the manufacturer's instructions.

3.2.9 *In Vivo* Anti-HA Antibody Titer Studies

In order to evaluate the immune response against HA when administered with the HA-engineered membrane-coated nanoparticles, male CD-1 mice were injected either intranasally or intravenously with the same dose as the *in vivo* transfection study at week 0, week 1, week 2. Blood and feces samples were collected every week for 4 weeks. Blood samples were collected via submandibular bleeding and allowed to clot at room temperature. The blood samples were centrifuged at 3,000 *g* for 10 min and the serum was collected to measure anti-HA IgG antibody titers by an enzyme-linked immunosorbent assay (ELISA). The collected feces samples were

suspended at 200 mg/mL in PBS containing a protease inhibitor cocktail (Sigma-Aldrich). After centrifugation at 10,000 *g* for 10 min, the supernatant was collected to measure anti-HA IgA antibody titers by ELISA. For ELISA, 96-well plates were coated overnight with 1 μg/mL HA protein (Sino Biological) using an ELISA coating buffer (Biolegend). The blocking was performed using 1% (w/v) bovine serum albumin (Sigma-Aldrich) in PBS containing 0.05% Tween 20 (National Scientific) for 1 h. Then, serially diluted samples were added as the primary antibody. HRP-conjugated goat anti-mouse IgG (BioLegend) or HRP-conjugated goat anti-mouse IgA (SouthernBiotech) was then used as the secondary antibody for serum samples and feces samples respectively. TMB substrate (Biolegend) was used to develop the wells and absorbance was measured using Tecan Infinite M200 multiplate reader.

3.3 Results and Discussion

HA subtype H7 was chosen as a model viral protein for expression due to its strong ability to promote fusion [43-45]. Additionally, the fact that H7 targets α2,3-linked sialic acid enabled us to evaluate our platform *in vivo* using murine models [30]. Wild-type B16F10 cells (denoted 'B16-WT') were transfected with an expression plasmid encoding for H7, yielding engineered cells (denoted 'B16-HA') with high levels of the viral fusion protein on their surface (Figure 3.2a). As B16-WT is known to express α2,3-linked sialic acid [46], a cell–cell fusion study was used to evaluate the functionality of the HA transgene *in vitro* (Figure 3.2b,c). B16-HA cells were divided into two aliquots, which were then stained with either CellTrace Violet or CellTrace Far Red. After combining the two dye-labeled aliquots together, the cell mixture was incubated with L-(tosylamido-2-phenyl) ethyl chloromethyl ketone (TPCK)-treated trypsin for

HA maturation before being subjected to endosomal pH to promote fusion activity. Following 2 h of incubation, the cells were analyzed by flow cytometry, which revealed a significant population of cells positive for both CellTrace Violet and CellTrace Far Red. This indicated that the HA on the surface of the engineered cells was active and could promote cell–cell fusion. In contrast, flow cytometric analysis of B16-WT cells subjected to an identical experimental protocol showed a negligible population of double-positive cells. It should be noted that our analysis could not identify fusion events between cells labeled with the same dye or distinguish events between only two cells versus those involving three or more cells. This suggests that the rate of fusion could be significantly higher than the double-positive percentage reported in our data, especially given that daughter cells resulting from the mitotic division of the same parent cell are more likely to fuse with each other as a result of their close proximity. Next, in order to visualize the cell fusion, either B16-WT or B16-HA cells were incubated with TPCK-treated trypsin and incubated under endosomal pH values (Figure 3.2d,e). Upon inspection under a fluorescence microscope, syncytia with multiple nuclei were observed among the B16-HA cells, providing a clear indication of cell–cell fusion. No signs of fusion were observed for the B16-WT cells.

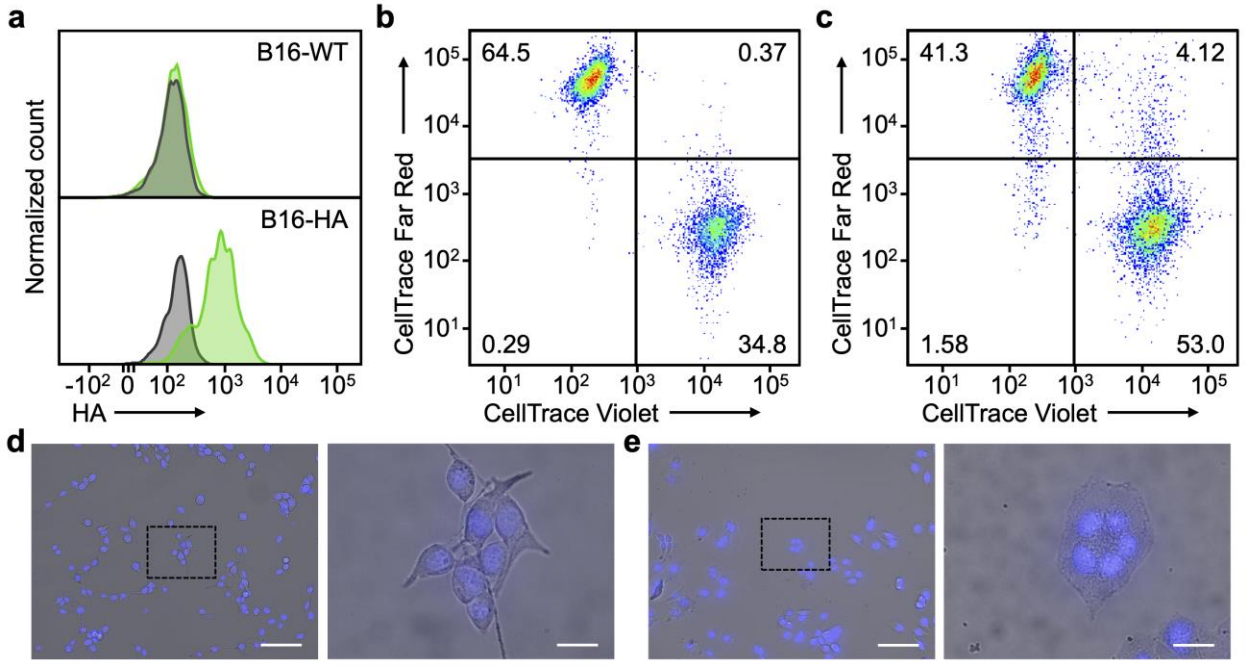

Figure 3.2: Fusion activity of HA on engineered cells. **a,** Flow cytometric analysis of HA expression on B16-WT and B16-HA cells (gray: isotype, green: anti-HA). **b,c,** Flow cytometric analysis of B16-WT (b) and B16-HA (c) cells co-incubated with themselves after half of the cell population was labeled with CellTrace Violet and the other half with CellTrace Far Red. **d,e,** Visualization of syncytia formation among B16-WT (d) and B16-HA (e) cells by optical microscopy (blue: nuclei). Scale bar = 100 μm (left) and 20 μm (right).

After confirming the successful expression of HA, the engineered B16-HA cells were harvested, and their membrane was derived as previously described [42]. The purified cell membrane was then coated onto preformed poly(lactic-*co*-glycolic acid) (PLGA) nanoparticle cores using a sonication process [47]. The PLGA nanoparticle cores were loaded with mRNA using a double emulsion method with the assistance of the cationic lipid-like molecule G0-C14 [40, 41]. The resulting mRNA-loaded nanoparticles coated with B16-WT membrane (denoted 'WT-mRNA-NP') and the engineered B16-HA membrane (denoted 'HA-mRNA-NP') both had an average diameter of approximately 185 nm and a zeta potential of approximately -20 mV (Figure 3.3a,b). Transmission electron microscopy of negatively stained HA-mRNA-NP verified

that the membrane was properly coated onto the polymeric cores (Figure 3.3c). In order to probe for the presence of HA on the purified cell membrane and on the nanoformulations, western blotting analysis was performed (Figure 3.3d). HA was clearly present on the membrane derived from B16-HA, as well as the final HA-mRNA-NP formulation. As expected, no signal was detected from the membrane of B16-WT or from WT-mRNA-NP. The long-term stability of WT-mRNA-NP and HA-mRNA-NP was evaluated by monitoring their size for 8 weeks when suspended in 10% sucrose solution at 4 ℃ (Figure 3.3e). No significant changes in size were detected during this period. Finally, mRNA loading was studied by measuring the fluorescent signal from a Cy5-labeled mRNA payload. It was determined that the encapsulation efficiency and drug loading yield were approximately 54% and 1 μg/mg of PLGA, respectively (Figure 3.3f).

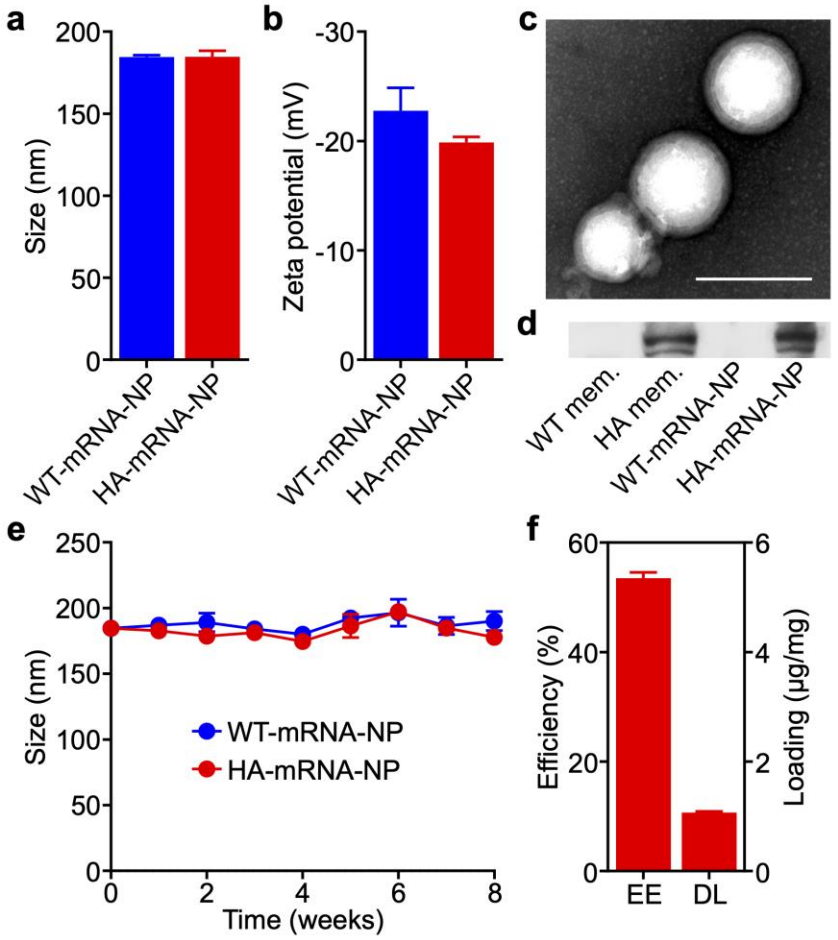

Figure 3.3: Nanoparticle characterization. **a,b,** Size (a) and surface zeta potential (b) of WT-mRNA-NP and HA-mRNA-NP as measured by dynamic light scattering (n = 3; mean + SD). **c,** Representative transmission electron microscopy image of HA-mRNA-NP negatively stained with uranyl acetate. Scale bar = 200 nm. **d,** Western blot probing for HA on B16-WT membrane (WT mem.), B16-HA membrane (HA mem.), WT-mRNA-NP, and HA-mRNA-NP. **e,** Size of WT-mRNA-NP and HA-mRNA-NP when stored in 10% sucrose over 8 weeks (n = 3; mean ± SD). **f,** Encapsulation efficiency (EE) and drug loading (DL) of mRNA into HA-mRNA-NP (n = 3; mean + SD).

In order to visualize endosomal escape, PLGA cores were loaded with the fluorescent dye benzoxazolium, 3-octadecyl-2-[3-(3-octadecyl-2(3H)-benzoxazolylidene)-1-propenyl]-, perchlorate (DiO) and coated with the membrane from either B16-WT or B16-HA (denoted ‘WT-DiO-NP’ or ‘HA-DiO-NP’, respectively). After 1, 4, 8, and 24 h of incubation with WT-DiO-NP or HA-DiO-NP, B16-WT cells were stained with Hoechst 33342 and LysoTracker Red

DND-99 prior to the imaging (Figure 3.4a). At the 1 h timepoint, nanoparticles could only be seen bound to the surface of the cells, while colocalization of the nanoparticles and the endosomes was observed at 4 h, indicating endocytosis for both formulations. After another 4 h, some nanoparticle signal was visualized outside of the endosomes for HA-DiO-NP, indicating endosomal escape, while intracellular WT-DiO-NP signal was still colocalized with the endosomes. At 24 h after starting the incubation, signal from HA-DiO-NP permeated the cytosol, and there was little to no evidence of cytosolic delivery for WT-DiO-NP.

Next, we evaluated the ability of HA-mRNA-NP to successfully deliver functional mRNA cargoes for protein translation. First, HA-mRNA-NP was formulated with mRNA encoding for enhanced green fluorescent protein (EGFP) as a model payload. Transfecting B16-WT cells with the resulting formulation led to a significant increase in detectable EGFP fluorescence compared to HA-mRNA-NP loaded with an irrelevant control mRNA (Figure 4b,c). The fluorescent signal increase was also significantly higher when compared to using EGFP mRNA either in free form or loaded within WT-mRNA-NP. As a secondary means of validating our platform *in vitro*, the experiment was repeated using *Cypridina* luciferase (CLuc) mRNA as the payload. Similar results were observed, where cells transfected with HA-mRNA-NP loaded with CLuc mRNA showed a significant increase in bioluminescent signal compared to cells treated with the same nanocarrier but loaded with irrelevant control mRNA (Figure 3.4d,e). As before, the CLuc signal increase for the HA-expressing formulation was higher than for its free CLuc mRNA and WT-mRNA-NP counterparts (Figure 3.4e).

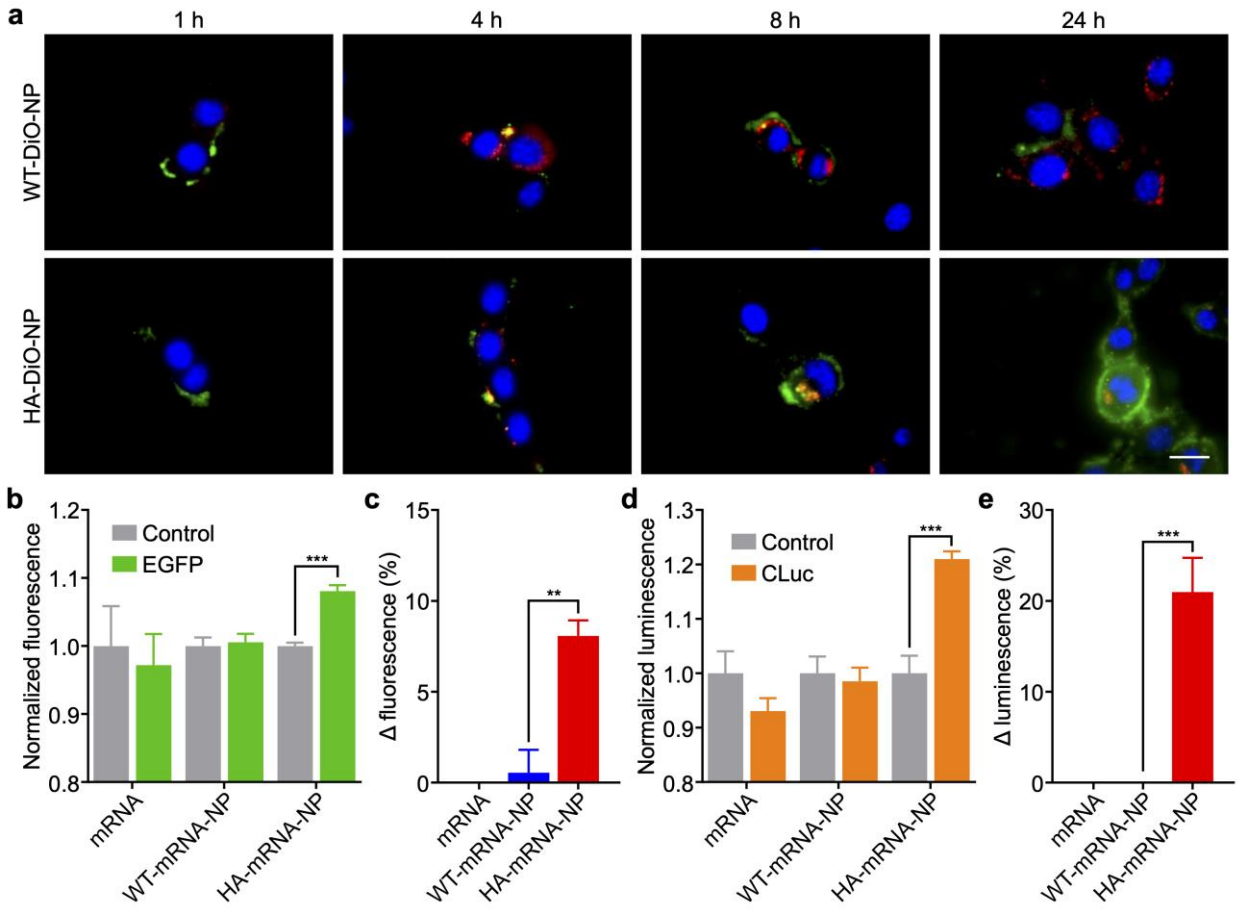

Figure 3.4: Endosomal escape and mRNA transfection *in vitro*. **a,** Fluorescent visualization of B16-WT cells incubated with WT-DiO-NP and HA-DiO-NP for 1, 4, 8, and 24 h (blue: nuclei, green: nanoparticles, red: endosomes). Scale bar = 20 μm. **b,c,** Normalized fluorescence (b) and change in fluorescence (c) of B16-WT cells after incubation with EGFP mRNA in free form, loaded within WT-mRNA-NP, and loaded within HA-mRNA-NP (n = 3; mean + SD). **d,e,** Normalized luminescence (d) and change in luminescence (e) of B16-WT cells after incubation with CLuc mRNA in free form, loaded within WT-mRNA-NP, and loaded within HA-mRNA-NP (n = 3; mean + SD). $^{**}p < 0.01$, $^{***}p < 0.001$; Student's *t*-test.

After confirming successful protein translation *in vitro*, we next assessed the ability of the engineered nanoformulation to achieve transfection *in vivo*. First, local delivery of CLuc mRNA was evaluated by administering WT-mRNA-NP or HA-mRNA-NP to mice via the intranasal route (Figure 3.5a,b). At 24 h after administration of the nanoparticles, the mice were injected with *Cypridina* luciferin, and bioluminescence activity was evaluated using a live animal

imaging system. Compared with the untreated controls, a small amount of signal was detected in mice treated with WT-mRNA-NP. Significantly stronger bioluminescence was detected for the mice treated with HA-mRNA-NP, demonstrating the ability of the engineered HA to promote efficient mRNA delivery *in vivo*. When the signals were quantified, it was determined that the total flux for the HA-mRNA-NP group was more than 2-fold higher than that of the WT-mRNA-NP group. The same nanoformulations were then evaluated for their ability to elevate the serum levels of a secreted payload after systemic delivery (Figure 3.5c,d). Mice were intravenously administered with each formulation, and their blood was sampled at 12 and 24 h after injection to monitor for CLuc activity. As expected, the untreated control group showed no changes in CLuc signal throughout the study. While there was a slight increase in bioluminescence for the WT-mRNA-NP group at 24 h, the signal for the HA-mRNA-NP group was significantly elevated at the same timepoint. Overall, the results demonstrated that the engineering of cell membrane-coated nanocarriers to express HA can lead to more efficient mRNA delivery *in vivo* after both local and systemic administration.

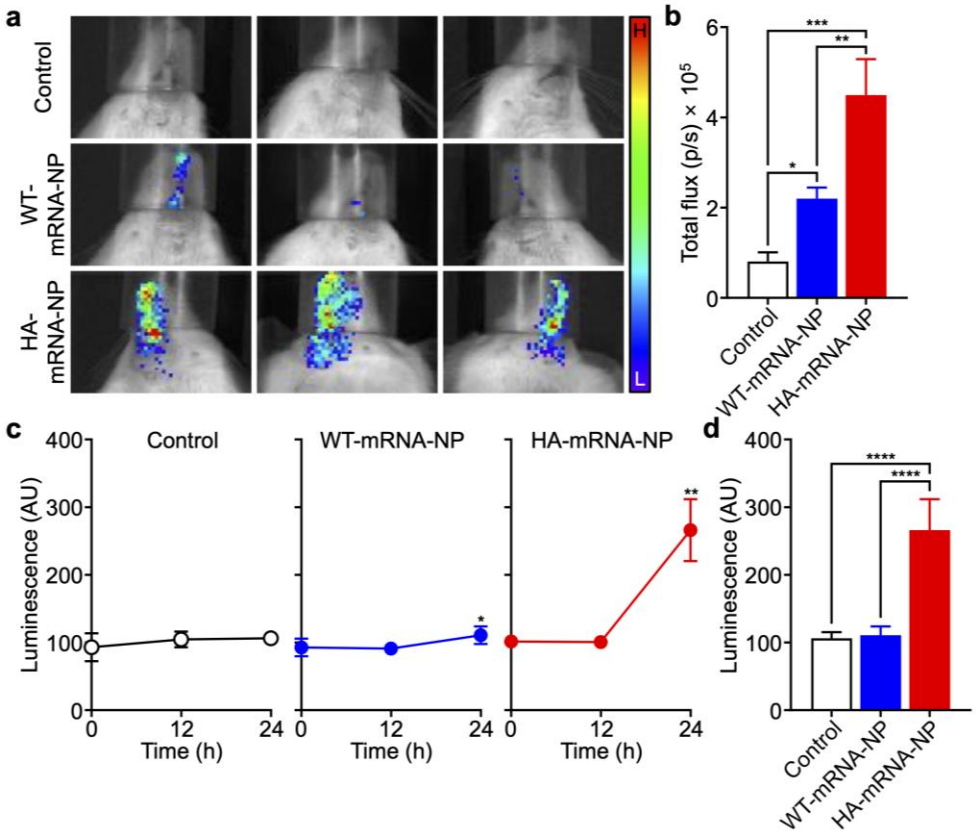

Figure 3.5: mRNA transfection *in vivo*. **a,** Visualization of bioluminescent signal from mice intranasally administered with WT-mRNA-NP and HA-mRNA-NP loaded with CLuc mRNA (H: high signal, L: low signal). **b,** Quantification of the total flux from the images in (a) (n = 3; mean + SD). *$p < 0.05$, **$p < 0.01$, ***$p < 0.001$; one-way ANOVA. **c,** Bioluminescence over time in the serum of mice intravenously administered with WT-mRNA-NP and HA-mRNA-NP loaded with CLuc mRNA (n = 5; mean ± SD). *$p < 0.05$, **$p < 0.01$ (compared to 0 h); Student's *t*-test. **d,** Bioluminescence in the serum of mice 24 h after intravenous administration with WT-mRNA-NP and HA-mRNA-NP loaded with CLuc mRNA (n = 5; mean + SD). ****$p < 0.0001$; one-way ANOVA.

3.4 Conclusions

In this work, cell membrane engineered to express a viral fusion protein was used to coat the surface of mRNA-loaded nanoparticle cores, enabling the resulting HA-mRNA-NP formulation to mimic the ability of some viruses to achieve endosomal escape. Influenza A virus HA subtype H7 bound to α2,3-linked sialic acid on the surface of murine cells, thus triggering

endocytic uptake. In the late endosomes, the lowered pH caused the HA to induce membrane fusion, thus allowing the nanoparticle contents to be unloaded into the cytosol. To prove our concept, we tested the ability of the engineered cell membrane-coated nanoparticles to escape the endosomal compartment and promote the expression of two model reporter genes *in vitro*. In both cases, the HA-expressing nanoparticles significantly outperformed a control formulation fabricated using the membrane of wild-type cells lacking the viral transgene. When tested *in vivo*, HA-mRNA-NP loaded with CLuc mRNA was able to significantly elevate levels of the encoded protein in both local and systemic administration scenarios.

Effective methods for mRNA delivery are highly desirable, particularly given the recent interest in mRNA vaccines driven by the COVID-19 pandemic [39]. Endosomal escape represents one of the key obstacles in mRNA nanodelivery since the payload needs to be present within the cytosol in order to carry out its biological function. As we have demonstrated here, utilizing naturally occurring viral fusion proteins such as influenza virus HA could provide an elegant solution to this challenge. By leveraging cell membrane coating technology in conjunction with genetic engineering, we were able to present HA in its natural context on the surface of nanoparticles, a task that would otherwise be difficult to achieve using conventional functionalization methods. Ultimately, continued research along these lines may yield novel strategies for controlling the subcellular localization of drug payloads, helping to further expand the utility of biomimetic nanomedicine.

Chapter 3, in full, is a reprint of the material being submitted. Joon Ho Park, Animesh Mohapatra, Jiarong Zhou, Maya Holay, Nishta Krishnan, Weiwei Gao, Ronnie H. Fang and Liangfang Zhang. The dissertation author was a primary author of this paper.

3.5 References

1. Li, Y., J. Wang, M.G. Wientjes, and J.L. Au, *Delivery of nanomedicines to extracellular and intracellular compartments of a solid tumor.* Adv. Drug Deliv. Rev., 2012. **64**(1): p. 29-39.

2. Mocan, L., C. Matea, F.A. Tabaran, O. Mosteanu, T. Pop, T. Mocan, and C. Iancu, *Photothermal treatment of liver cancer with albumin-conjugated gold nanoparticles initiates Golgi apparatus-ER dysfunction and caspase-3 apoptotic pathway activation by selective targeting of Gp60 receptor.* Int. J. Nanomedicine, 2015. **10**: p. 5435-5445.

3. Dam, D.H., J.H. Lee, P.N. Sisco, D.T. Co, M. Zhang, M.R. Wasielewski, and T.W. Odom, *Direct observation of nanoparticle-cancer cell nucleus interactions.* ACS Nano, 2012. **6**(4): p. 3318-3326.

4. Fu, A., R. Tang, J. Hardie, M.E. Farkas, and V.M. Rotello, *Promises and pitfalls of intracellular delivery of proteins.* Bioconjug. Chem., 2014. **25**(9): p. 1602-1608.

5. Field, L.D., J.B. Delehanty, Y. Chen, and I.L. Medintz, *Peptides for specifically targeting nanoparticles to cellular organelles: quo vadis?* Acc. Chem. Res., 2015. **48**(5): p. 1380-1390.

6. He, B., P. Lin, Z. Jia, W. Du, W. Qu, L. Yuan, W. Dai, H. Zhang, X. Wang, J. Wang, X. Zhang, and Q. Zhang, *The transport mechanisms of polymer nanoparticles in Caco-2 epithelial cells.* Biomaterials, 2013. **34**(25): p. 6082-6098.

7. Biswas, S. and V.P. Torchilin, *Nanopreparations for organelle-specific delivery in cancer.* Adv. Drug Deliv. Rev., 2014. **66**: p. 26-41.

8. Huotari, J. and A. Helenius, *Endosome maturation.* EMBO J., 2011. **30**(17): p. 3481-3500.

9. Scott, C.C., F. Vacca, and J. Gruenberg, *Endosome maturation, transport and functions.* Semin. Cell Dev. Biol., 2014. **31**: p. 2-10.

10. Zhang, C., T. An, D. Wang, G. Wan, M. Zhang, H. Wang, S. Zhang, R. Li, X. Yang, and Y. Wang, *Stepwise pH-responsive nanoparticles containing charge-reversible pullulan-based shells and poly(beta-amino ester)/poly(lactic-co-glycolic acid) cores as carriers of anticancer drugs for combination therapy on hepatocellular carcinoma.* J. Control. Release, 2016. **226**: p. 193-204.

11. Zhou, Z., A. Badkas, M. Stevenson, J.Y. Lee, and Y.K. Leung, *Herceptin conjugated PLGA-PHis-PEG pH sensitive nanoparticles for targeted and controlled drug delivery.* Int. J. Pharm., 2015. **487**(1-2): p. 81-90.

12. Smith, S.A., L.I. Selby, A.P.R. Johnston, and G.K. Such, *The endosomal escape of nanoparticles: toward more efficient cellular delivery.* Bioconjug. Chem., 2019. **30**(2): p. 263-272.

13. Convertine, A.J., D.S. Benoit, C.L. Duvall, A.S. Hoffman, and P.S. Stayton, *Development of a novel endosomolytic diblock copolymer for siRNA delivery.* J. Control. Release, 2009. **133**(3): p. 221-229.

14. Tran, K.K., X. Zhan, and H. Shen, *Polymer blend particles with defined compositions for targeting antigen to both class I and II antigen presentation pathways.* Adv. Healthc. Mater., 2014. **3**(5): p. 690-702.

15. Wu, X.A., C.H. Choi, C. Zhang, L. Hao, and C.A. Mirkin, *Intracellular fate of spherical nucleic acid nanoparticle conjugates.* J. Am. Chem. Soc., 2014. **136**(21): p. 7726-7733.

16. Hinde, E., K. Thammasiraphop, H.T. Duong, J. Yeow, B. Karagoz, C. Boyer, J.J. Gooding, and K. Gaus, *Pair correlation microscopy reveals the role of nanoparticle shape in intracellular transport and site of drug release.* Nat. Nanotechnol., 2017. **12**(1): p. 81-89.

17. Mukherjee, S.P. and H.J. Byrne, *Polyamidoamine dendrimer nanoparticle cytotoxicity, oxidative stress, caspase activation and inflammatory response: experimental observation and numerical simulation.* Nanomedicine, 2013. **9**(2): p. 202-211.

18. Lv, H., S. Zhang, B. Wang, S. Cui, and J. Yan, *Toxicity of cationic lipids and cationic polymers in gene delivery.* J. Control. Release, 2006. **114**(1): p. 100-109.

19. Staring, J., M. Raaben, and T.R. Brummelkamp, *Viral escape from endosomes and host detection at a glance.* J. Cell Sci., 2018. **131**(15): p. jcs216259.

20. Hamilton, B.S., G.R. Whittaker, and S. Daniel, *Influenza virus-mediated membrane fusion: determinants of hemagglutinin fusogenic activity and experimental approaches for assessing virus fusion.* Viruses, 2012. **4**(7): p. 1144-1168.

21. Russell, C.J., M. Hu, and F.A. Okda, *Influenza hemagglutinin protein stability, activation, and pandemic risk.* Trends Microbiol., 2018. **26**(10): p. 841-853.

22. Boonstra, S., J.S. Blijleven, W.H. Roos, P.R. Onck, E. van der Giessen, and A.M. van Oijen, *Hemagglutinin-mediated membrane fusion: a biophysical perspective.* Annu. Rev. Biophys., 2018. **47**: p. 153-173.

23. Lazarowitz, S.G. and P.W. Choppin, *Enhancement of the infectivity of influenza A and B viruses by proteolytic cleavage of the hemagglutinin polypeptide.* Virology, 1975. **68**(2): p. 440-454.

24. Tatulian, S.A. and L.K. Tamm, *Secondary structure, orientation, oligomerization, and lipid interactions of the transmembrane domain of influenza hemagglutinin.* Biochemistry, 2000. **39**(3): p. 496-507.

25. Thoennes, S., Z.N. Li, B.J. Lee, W.A. Langley, J.J. Skehel, R.J. Russell, and D.A. Steinhauer, *Analysis of residues near the fusion peptide in the influenza hemagglutinin structure for roles in triggering membrane fusion.* Virology, 2008. **370**(2): p. 403-414.

26. Xu, R. and I.A. Wilson, *Structural characterization of an early fusion intermediate of influenza virus hemagglutinin.* J. Virol., 2011. **85**(10): p. 5172-5182.

27. Kim, C.S., R.F. Epand, E. Leikina, R.M. Epand, and L.V. Chernomordik, *The final conformation of the complete ectodomain of the HA2 subunit of influenza hemagglutinin can by itself drive low pH-dependent fusion.* J. Biol. Chem., 2011. **286**(15): p. 13226-13234.

28. Han, X., J.H. Bushweller, D.S. Cafiso, and L.K. Tamm, *Membrane structure and fusion-triggering conformational change of the fusion domain from influenza hemagglutinin.* Nat. Struct. Biol., 2001. **8**(8): p. 715-720.

29. Matrosovich, M.N., T.Y. Matrosovich, T. Gray, N.A. Roberts, and H.D. Klenk, *Human and avian influenza viruses target different cell types in cultures of human airway epithelium.* Proc. Natl. Acad. Sci. U. S. A., 2004. **101**(13): p. 4620-4624.

30. Ibricevic, A., A. Pekosz, M.J. Walter, C. Newby, J.T. Battaile, E.G. Brown, M.J. Holtzman, and S.L. Brody, *Influenza virus receptor specificity and cell tropism in mouse and human airway epithelial cells.* J. Virol., 2006. **80**(15): p. 7469-7480.

31. Monsalvo, A.C., J.P. Batalle, M.F. Lopez, J.C. Krause, J. Klemenc, J.Z. Hernandez, B. Maskin, J. Bugna, C. Rubinstein, L. Aguilar, L. Dalurzo, R. Libster, V. Savy, E. Baumeister, L. Aguilar, G. Cabral, J. Font, L. Solari, K.P. Weller, J. Johnson, M. Echavarria, K.M. Edwards, J.D. Chappell, J.E. Crowe, Jr., J.V. Williams, G.A. Melendi, and F.P. Polack, *Severe pandemic 2009 H1N1 influenza disease due to pathogenic immune complexes.* Nat. Med., 2011. **17**(2): p. 195-199.

32. Fang, R.H., A.V. Kroll, W. Gao, and L. Zhang, *Cell membrane coating nanotechnology.* Adv. Mater., 2018. **30**(23): p. 1706759.

33. Fang, R.H., Y. Jiang, J.C. Fang, and L. Zhang, *Cell membrane-derived nanomaterials for biomedical applications.* Biomaterials, 2017. **128**: p. 69-83.

34. Hu, C.M., L. Zhang, S. Aryal, C. Cheung, R.H. Fang, and L. Zhang, *Erythrocyte membrane-camouflaged polymeric nanoparticles as a biomimetic delivery platform.* Proc. Natl. Acad. Sci. U. S. A., 2011. **108**(27): p. 10980-10985.

35. Fang, R.H., C.M. Hu, B.T. Luk, W. Gao, J.A. Copp, Y. Tai, D.E. O'Connor, and L. Zhang, *Cancer cell membrane-coated nanoparticles for anticancer vaccination and drug delivery.* Nano Lett., 2014. **14**(4): p. 2181-2188.

36. Wang, S., Y. Duan, Q. Zhang, A. Komarla, H. Gong, W. Gao, and L. Zhang, *Drug targeting via platelet membrane-coated nanoparticles.* Small Struct., 2020. **1**(1): p. 2000018.

37. Jiang, Y., N. Krishnan, J. Zhou, S. Chekuri, X. Wei, A.V. Kroll, C.L. Yu, Y. Duan, W. Gao, R.H. Fang, and L. Zhang, *Engineered cell-membrane-coated nanoparticles directly present tumor antigens to promote anticancer immunity.* Adv. Mater., 2020. **32**(30): p. 2001808.

38. Park, J.H., Y. Jiang, J. Zhou, H. Gong, A. Mohapatra, J. Heo, W. Gao, R.H. Fang, and L. Zhang, *Genetically engineered cell membrane-coated nanoparticles for targeted delivery of dexamethasone to inflamed lungs.* Sci. Adv., 2021. **7**(25): p. eabf7820.

39. Verbeke, R., I. Lentacker, S.C. De Smedt, and H. Dewitte, *The dawn of mRNA vaccines: the COVID-19 case.* J. Control. Release, 2021. **333**: p. 511-520.

40. Islam, M.A., Y. Xu, W. Tao, J.M. Ubellacker, M. Lim, D. Aum, G.Y. Lee, K. Zhou, H. Zope, M. Yu, W. Cao, J.T. Oswald, M. Dinarvand, M. Mahmoudi, R. Langer, P.W. Kantoff, O.C. Farokhzad, B.R. Zetter, and J. Shi, *Restoration of tumour-growth suppression in vivo via systemic nanoparticle-mediated delivery of PTEN mRNA.* Nat. Biomed. Eng., 2018. **2**(11): p. 850-864.

41. Xu, X., K. Xie, X.Q. Zhang, E.M. Pridgen, G.Y. Park, D.S. Cui, J. Shi, J. Wu, P.W. Kantoff, S.J. Lippard, R. Langer, G.C. Walker, and O.C. Farokhzad, *Enhancing tumor cell response to chemotherapy through nanoparticle-mediated codelivery of siRNA and cisplatin prodrug.* Proc. Natl. Acad. Sci. U. S. A., 2013. **110**(46): p. 18638-18643.

42. Kroll, A.V., R.H. Fang, Y. Jiang, J. Zhou, X. Wei, C.L. Yu, J. Gao, B.T. Luk, D. Dehaini, W. Gao, and L. Zhang, *Nanoparticulate delivery of cancer cell membrane elicits multiantigenic antitumor immunity.* Adv. Mater., 2017. **29**(47): p. 1703969.

43. Galloway, S.E., M.L. Reed, C.J. Russell, and D.A. Steinhauer, *Influenza HA subtypes demonstrate divergent phenotypes for cleavage activation and pH of fusion: implications for host range and adaptation.* PLoS Pathog., 2013. **9**(2): p. e1003151.

44. Su, B., S. Wurtzer, M.A. Rameix-Welti, D. Dwyer, S. van der Werf, N. Naffakh, F. Clavel, and B. Labrosse, *Enhancement of the influenza A hemagglutinin (HA)-mediated cell-cell fusion and virus entry by the viral neuraminidase (NA).* PLoS One, 2009. **4**(12): p. e8495.

45. Ma, M.J., Y. Yang, and L.Q. Fang, *Highly pathogenic avian H7N9 influenza viruses: recent challenges.* Trends Microbiol., 2019. **27**(2): p. 93-95.

46. Chang, W.W., C.Y. Yu, T.W. Lin, P.H. Wang, and Y.C. Tsai, *Soyasaponin I decreases the expression of α2,3-linked sialic acid on the cell surface and suppresses the metastatic potential of B16F10 melanoma cells.* Biochem. Biophys. Res. Commun., 2006. **341**(2): p. 614-619.

47. Copp, J.A., R.H. Fang, B.T. Luk, C.M. Hu, W. Gao, K. Zhang, and L. Zhang, *Clearance of pathological antibodies using biomimetic nanoparticles.* Proc. Natl. Acad. Sci. U. S. A., 2014. **111**(37): p. 13481-13486.

Chapter 4

Conclusions

4.1 Engineered Cell Membrane-Coated Nanoparticles for Lung Inflammation Targeted Delivery

This chapter reported on the genetically engineered cell membrane-coated nanoparticle that can target inflammation and specifically deliver anti-inflammatory drug to the inflamed lungs. This was made possible by engineering a host cell to constitutively express VLA-4 which can specifically bind to VCAM-1 that is being expressed on the surface of inflamed cells and using its membrane to coat the drug loaded nanoparticle. This nanoparticle platform enhanced the safety profile of the anti-inflammatory drug as well as preserving the efficacy of the drug. It is demonstrated that the engineered nanoparticle can specifically target inflamed cells and accumulate at the inflammation site both *in vitro* and *in vivo*. When lung inflammation was treated using this nanoparticle, the formulation was able to completely abrogate lung inflammation while free drug as well as non-engineered controls were not able to generate any efficacy. Overall, the work demonstrates that the engineering the membrane to express VLA-4 and harnessing the inflammation targeting capability can enhance the drug delivery. Although only lung inflammation targeting was demonstrated in this work, since the principle is the same throughout the inflamed tissue, we expect this platform to be able to be applied to other inflammations such as skin inflammation.

4.2 Engineered Cell Membrane-Coated Nanoparticles for Cytosolic Delivery of mRNA

The recent rise of interest in mRNA vaccines due to COVID-19 pandemic has brought cytosolic delivery of the payloads into the spotlight since mRNA can only function properly in the cytosol. However, the endosomal pathway presents a challenge in achieving cytosolic delivery.

This chapter demonstrated a biomimetic nanoparticle platform that harnesses the endosome escaping capability of an influenza virus. A host cell was engineered to constitutively express the fusogenic protein originated from the virus and its membrane was coated onto an mRNA loaded nanoparticle which grants the resulting nanoparticle to mimic the virus' endosome escaping capability. The cytosolic delivery of the payload was verified both *in vitro* and *in vivo*. Two different administration routes were explored *in vivo*: local and systemic. In both cases, the translated protein from the delivered mRNA was detected in significantly higher level than its non-engineered controls. This work presents a new and elegant way to escape endosome without disrupting it and deliver the payload to the cytosol which can be used with other drugs where cytosolic delivery is critical to their efficacy.

4.3 Future Outlook

In recent years, cell membrane-coated nanoparticle technology has revolutionized the field of drug delivery and using genetic engineering to further enhance its capability is still at its infancy. Considering the various ways the cells can be engineered, the possibility in application of the engineered cell membrane-coated nanoparticle technology is virtually endless. The versatility of this platform is demonstrated in the Chapter 2 and 3 of this dissertation which covered two of the key aspects of drug delivery: cytosolic delivery and targeted delivery. Further

development and optimization of the platform to be applied to other aspects of drug delivery such as prolonged circulation is expected.

Safety and scalability is something that needs to be closely examined and optimized if this platform is to be clinically translated. Genetic engineering can potentially improve the safety profile of the conventional cell membrane-coated nanoparticle technology. Furthermore, stable expression of the engineered protein on the surface of the host cell is a critical factor in maintaining and harvesting the membranes. Therefore, in order to scale up the production in order to meet the demand, generating and culturing stable cell lines is important. Once these concerns are addressed, this platform will be able to be applied in multiple clinical settings such as cancer therapy or vaccination.